University of Amsterdam

Masters Thesis

GerrySort: An Agent-Based Model for Simulating Gerrymandering and Geographical Partisan Sorting

Author:
River Vaudrin

Examiner:
Dr. Michael H. Lees
Supervisor:
Dr. Tanzhe Tang
Assessor:
Dr. Debraj Roy

A thesis submitted in partial fulfillment of the requirements for the degree of Master of Science in Computational Science

in the

Computational Science Lab
Informatics Institute

June 2025

Computational Science

Declaration of Authorship

I, River Vaudrin, declare that this thesis, entitled 'GerrySort: An Agent-Based Model for Simulating Gerrymandering and Geographical Partisan Sorting' and the work presented in it are my own. I confirm that:

- This work was done wholly or mainly while in candidature for a research degree at the University of Amsterdam.
- Where any part of this thesis has previously been submitted for a degree or any other qualification at this University or any other institution, this has been clearly stated.
- Where I have consulted the published work of others, this is always clearly attributed.
- Where I have quoted from the work of others, the source is always given. With the exception of such quotations, this thesis is entirely my own work.
- I have acknowledged all main sources of help.
- Where the thesis is based on work done by myself jointly with others, I have made clear exactly what was done by others and what I have contributed myself.

Signed:

Date: June 2025

"The gerrymander is an American name for a political abuse, which, though by no means exclusively American, has been most widely practiced and generally tolerated in this country."

C. O. Sauer, Geography and the Gerrymander, 1918 [1]

UNIVERSITY OF AMSTERDAM

Abstract

Faculty of Science
Informatics Institute

Master of Science in Computational Science

GerrySort: An Agent-Based Model for Simulating Gerrymandering and Geographical Partisan Sorting

by River VAUDRIN

This thesis investigates the relationship between *partisan gerrymandering* and *geographical partisan sorting* in the United States and evaluates the effectiveness of two redistricting reforms in mitigating their impact on the fairness of electoral maps used for congressional elections. To this end, a novel agent-based model—*GerrySort*—is developed to simulate these dynamics independently and in combination across multiple scenarios in four swing states: Georgia, Wisconsin, Michigan, and Pennsylvania. By incorporating high-resolution empirical data, including election results, demographic indicators, and geographical features, GerrySort is able to capture the unique political landscapes of each state.

The central research question investigates how gerrymandering and geographical partisan sorting influence the fairness of congressional district maps. Six sub-questions explore their individual and combined effects, the role of political geography, and the extent to which competitiveness and compactness reforms enhance fairness. Results show that both gerrymandering and partisan sorting can independently generate substantial partisan biases, while their combined effects lead to more variable and state-specific outcomes. The analysis highlights that the fairness of electoral maps is sensitive to spatial voter distributions: parties with geographically concentrated electorates are structurally disadvantaged in the redistricting process. Lastly, the findings demonstrate that competitiveness and compactness criteria can reduce partisan biases—particularly when implemented rigorously—but their effectiveness is contingent on a state's underlying political geography.

Acknowledgements

When I first began to synthesize some vague ideas for this project—sitting in a lecture during the second week of my master's program, while listening to Dr. Mike Lees speak about modeling school segregation—I had little idea that, nearly three years later, I would be writing the acknowledgments for a thesis that brought these thoughts to life.

I would first like to thank Dr. Mike Lees for his immediate enthusiasm and support when I nervously pitched my barely-formed proposal. Despite me accidentally calling him "Mike *van* Lees" during this interaction—even though I knew perfectly well what his name was—he responded with encouragement and a willingness to guide me through the project.

Throughout the project, both he and my other supervisor, Dr. Tanzhe Tang, consistently provided valuable feedback during meetings. Aware of how valuable their time was, I made a point of preparing thoroughly, aiming to make each meeting as productive and information-rich as possible. This approach to collaboration worked extremely well, after each meeting I felt like the path forward was crystal clear. I would also like to especially thank Tanzhe for his unwavering presence at every meeting and for his thorough feedback on my writing.

Finally, I would like to thank my friends and family for bringing color and joy to the moments when I wasn't immersed in this project. Most of all, I want to express my deepest gratitude to my partner, Manuka. Your constant encouragement, patience, and belief in me have mean more than I can put into words. You inspire me to grow every day and to keep striving, even when the road gets rocky. Thank you for being my anchor, my cheerleader, and my calm in the chaos.

Contents

Declaration of Authorship **i**

Abstract **iii**

Acknowledgements **iv**

Contents **v**

List of Figures **ix**

List of Tables **xi**

List of Algorithms **xii**

Abbreviations **xiii**

1 Introduction **1**
- 1.1 Background . . . 1
  - 1.1.1 Gerrymandering . . . 1
  - 1.1.2 Geographical Partisan Sorting . . . 2
- 1.2 Research Questions . . . 4
- 1.3 Research Approach . . . 6
- 1.4 Research Contributions . . . 7
- 1.5 Thesis Outline . . . 8

2 Literature Review **9**
- 2.1 Partisan Gerrymandering . . . 9
  - 2.1.1 Single-Member Districts . . . 9
  - 2.1.2 The Redistricting Cycle . . . 10
  - 2.1.3 History of Gerrymandering . . . 11
    - 2.1.3.1 Origins . . . 11
    - 2.1.3.2 The (Legal) History of Gerrymandering . . . 12
    - 2.1.3.3 Current State . . . 14
  - 2.1.4 Types of Gerrymanders and Strategies . . . 15
  - 2.1.5 Effects of Gerrymandering . . . 17

2.1.5.1 Representation . . . 18
2.1.5.2 Electoral Competitiveness . . . 18
2.1.5.3 District Compactness . . . 20
2.1.6 Quantifying Gerrymandering and its Effects . . . 21
2.1.6.1 Efficiency Gap . . . 22
2.1.6.2 Mean-Median Difference . . . 24
2.1.6.3 Declination . . . 25
2.1.6.4 Competitiveness . . . 27
2.1.6.5 Compactness . . . 27
2.1.7 Computational Redistricting . . . 28
2.2 Geographical Partisan Sorting . . . 30
2.2.1 “Unintentional Gerrymandering” . . . 32
2.2.2 Quantifying Segregation . . . 33
2.2.2.1 Global Moran’s I . . . 33
2.2.2.2 Anselin Local Moran’s I . . . 34

3 Model Description **36**
3.1 Overview . . . 36
3.1.1 Purpose . . . 36
3.1.2 Entities, State Variables, and Scales . . . 37
3.1.2.1 Entities and State Variables . . . 38
3.1.2.2 Spatial and Temporal Scales . . . 39
3.1.3 Process Overview and Scheduling . . . 39
3.1.3.1 Initialization Procedure . . . 40
Loading Input Data . . . 40
Entity Initialization . . . 40
Initial Elections . . . 42
Initial Utility Calculation . . . 43
Initial Redistricting Control . . . 43
Initial Model Statistics . . . 45
3.1.3.2 Main Processes . . . 46
Redistricting . . . 46
Partisan Sorting . . . 48
Elections . . . 48
3.2 Design Concepts . . . 49
3.2.1 Theoretical and Empirical Background . . . 49
3.2.2 Individual Decision-Making . . . 50
3.2.3 Individual Sensing . . . 53
3.2.4 Interaction . . . 53
3.2.5 Collectives . . . 54
3.2.6 Heterogeneity . . . 54
3.2.7 Stochasticity . . . 55
3.2.8 Observations . . . 56
3.3 Details . . . 56
3.3.1 Implementation Details . . . 56
3.3.2 Input Data . . . 57

4 Sensitivity Analysis **59**
4.1 Global Sensitivity Analysis 59
4.1.1 Sobol' Indices 60
4.1.2 Results 62
Partisan Fairness (Efficiency Gap) 62
Average Competitiveness 63
Average Compactness 65
4.2 Local Sensitivity Analysis 65
4.2.1 One-Factor-At-a-Time Method 65
4.2.2 Results 66
Partisan Fairness (Efficiency Gap) 66
Average Competitiveness 67
Average Compactness 67

5 Experiments and Results **69**
5.1 Baseline Experiments 69
5.1.1 Experimental Set-Up 69
5.1.2 Results 72
State-Specific Patterns 72
General Observations 79
5.2 Testing the Role of Democratic Strongholds 80
5.2.1 Experimental Set-Up 81
5.2.2 Results 84
MI 84
PA 85
5.3 Redistricting Reform Experiments 87
5.3.1 Experimental Set-Up 88
5.3.2 Results 89
Measuring the Effectiveness of Redistricting Reforms 90
State-Specific Patterns 91
General Observations 96

6 Discussion **97**
6.1 Main Contributions 97
6.2 Limitations 99
6.3 Future Work 100

7 Conclusion **101**

8 Ethics and Data Management **104**

A Additional Model Description **105**
A.1 Entity Attributes 105
A.1.1 Individual Agents 105
A.1.2 Congressional Districts 106
A.1.3 Precincts 106
A.1.4 Counties 107
A.2 Other Model Parameters 108

A.3 Process Overview and Scheduling . . . 109
A.4 Individual Decision-Making . . . 113
A.5 Other Observations . . . 113
A.6 Input Data . . . 116

B Supplementary SA **117**
B.1 GSA . . . 117
B.2 LSA . . . 121

C Supplementary Results **123**
C.1 Baseline Experiments . . . 123
C.2 Redistricting Reform Experiments . . . 136

Bibliography **143**

List of Figures

2.1 "The Gerry-Mander" from *The Boston Weekly Messenger.* 12
2.2 Examples of cracking and packing. 17
2.3 Illustration of the Declination metric. 26

3.1 Flowchart of processes in GerrySort. 40
3.2 RUCA codes in each state. 43
3.3 Partisan margins of victory after initialization in each state. 44
3.4 Simulated versus real-world congressional seat distributions after initialization. 45

4.1 S_1 and S_T indices for the efficiency gap output. 64
4.2 S_1 and S_T indices for the average competitiveness and average compactness outputs. 64
4.3 OFAT results. 68

5.1 Examples of generated congressional maps for the baseline experiments. . 71
5.2 Baseline results for efficiency gap output in GA. 73
5.3 Baseline results for efficiency gap output in WI. 75
5.4 Baseline results for efficiency gap output in MI. 76
5.5 Baseline results for efficiency gap output in PA. 77
5.6 Baseline results for initial versus final redistricting control for all states. . 78
5.7 Local Moran's I classification for MI and PA precincts. 82
5.8 Local Moran's I classification for MI and PA (Fabricated) precincts. . . . 83
5.9 Baseline results for efficiency gap output in MI (Fabricated). 85
5.10 Baseline results for efficiency gap output in PA (Fabricated). 86
5.11 Baseline results for initial versus final redistricting control for MI and PA (Fabricated). 87
5.12 Redistricting reform results for GA. 92
5.13 Redistricting reform results for WI. 93
5.14 Redistricting reform results for MI. 94
5.15 Redistricting reform results for PA. 95

A.1 Initial values of redistricting metrics. 109
A.2 Total number of agents and capacity per county. 110
A.3 Performance comparison of three redistricting algorithms. 111

B.1 Saltelli sample generated for GSA. 117
B.2 Output values per parameter setting obtained through GSA. 118
B.3 S_2 index for the efficiency gap output. 119

B.4 Additional GSA results for for average competitiveness and average compactness outputs in GA. . . . 120
B.5 Examples of output distributions obtained through OFAT. . . . 121
B.6 Additional OFAT results. . . . 122

C.1 Baseline results for declination and mean-median difference outputs in GA. 123
C.2 Baseline results for average district competitiveness and compactness outputs in GA. . . . 124
C.3 Baseline results for agent-based dynamics outputs in GA. . . . 125
C.4 Baseline results for declination and mean-median difference outputs in WI. 126
C.5 Baseline results for average district competitiveness and compactness outputs in WI. . . . 127
C.6 Baseline results for agent-based dynamics outputs in WI. . . . 128
C.7 Baseline results for declination and mean-median difference outputs in MI. 129
C.8 Baseline results for average district competitiveness and compactness outputs in MI. . . . 130
C.9 Baseline results for agent-based dynamics outputs in MI. . . . 131
C.10 Temporal evolution of the declination and mean-median difference in the baseline experiments for PA under both fixed control and model-determined control scenarios. . . . 132
C.11 Baseline results for average district competitiveness and compactness outputs in PA. . . . 133
C.12 Baseline results for agent-based dynamics outputs in PA. . . . 134
C.13 Local Moran's I classification for GA and WI precincts. . . . 135
C.14 Additional redistricting reform results for declination in GA and WI. . . . 136
C.14 Additional redistricting reform results for declination in MI and PA. . . . 137
C.15 Redistricting reform results for mean-median difference in GA and WI. . . 138
C.15 Redistricting reform results for mean-median difference in MI and PA. . . 139
C.16 Redistricting reform results for PA (Fabricated). . . . 140
C.17 Examples of generated congressional maps for each redistricting reform in GA and WI. . . . 141
C.17 Examples of generated congressional maps for each redistricting reform in MI and PA. . . . 142

List of Tables

3.1 Overview of main model parameters. 41

4.1 Parameter ranges and values used in GSA and LSA. 62

5.1 Global Moran's I before and after partisan sorting. 81

A.1 Overview of attributes for each individual agent. 105
A.2 Overview of attributes for each congressional district. 106
A.3 Overview of attributes for each precinct. 106
A.4 Overview of attributes for each county. 107
A.5 Overview of other model parameters. 108
A.6 Maximum relocation distances by state (in miles). 113
A.7 Overview of properties in the GeoJSON file. 116

List of Algorithms

1 Redistricting via GerryChain Optimization 112

Abbreviations

ABM	**A**gent-**b**ased **M**odel
US	**U**nited **S**tates
GA	**G**eorgia
WI	**W**isconsin
MI	**M**ichigan
PA	**P**ennsylvania
RUCA	**R**ural-**U**rban **C**ommuting **A**rea
SA	**S**ensitivity **A**nalysis
GSA	**G**lobal **S**ensitivity **A**nalysis
LSA	**L**ocal **S**ensitivity **A**nalysis
OFAT	**O**ne-**F**actor-**a**t-a-**T**ime

Chapter 1

Introduction

1.1 Background

This thesis is rooted in two core concepts: *gerrymandering* and *geographical partisan sorting* in the United States (U.S.). This section will briefly introduce these concepts. Note that these concepts will be discussed in more depth in the literature review (Chapter 2).

1.1.1 Gerrymandering

The U.S. functions as a federal republic made up of 50 states, where each state has its own constitution, government, laws, and state courts. At the federal level, each state is represented in the U.S. Congress (consisting of the House of Representatives and the Senate) by elected state representatives and senators. Members of the U.S. Congress and state legislatures are elected through statewide elections. In addition to federal representation, every state also has its own state legislature, typically composed of a State House of Representatives and a State Senate. These state-level legislative bodies are responsible for passing laws and shaping policy within their respective states. Members of both the U.S. Congress and state legislatures are elected from single-member electoral districts. That is, each district typically elects one representative to serve in a legislative body, whether it be a state house, state senate, or the U.S. House of Representatives. A crucial geographical component of these elections is the drawing of electoral district boundaries. To ensure representation aligns with population shifts, states are federally required to redraw their congressional and state legislative district boundaries every ten years, following the U.S. Census.

The authority to redraw these electoral districts is a crucial factor that can shape statewide and national election outcomes [2, 3]. In most states, the state legislature is responsible for proposing and enacting redistricting plans [4, 5]. The central problem with allowing state legislatures to control the redistricting process is that it enables the ruling party to manipulate district boundaries in its favor, a practice known as gerrymandering. This tactic, which has posed a persistent challenge to U.S. democracy since the nation's founding [1, 6, 7], allows the majority party to entrench its power by redrawing districts to dilute the influence of opposing voters, marginalize political competition, and secure future electoral dominance, often at the cost of fair representation [3, 8–11]. Extensive scholarly research has shown that gerrymandering reduces electoral competitiveness [12–15], entrenches partisan advantage [16, 17], contributes to rising political polarization [18–20] and suppresses voter turnout [21–25]. Together, these effects pose significant threats to the integrity and responsiveness of democratic governance.

However, federal and state officials have taken minimal action to combat partisan gerrymandering. In fact, a 2019 Supreme Court ruling[1] upheld the constitutionality of partisan gerrymandering, leaving it to individual states to decide whether to implement redistricting reforms. During the 2020 redistricting cycle, 33 state legislatures played a dominant role in congressional redistricting [5]. To address concerns of bias, some states have implemented independent or bipartisan commissions, or hybrid systems, to mitigate the risk of partisan interference [4, 5]. However, in practice, the effectiveness of these reforms varies, with instances where partisan bias continues to permeate the redistricting process [19, 26–30].

A more in-depth discussion of the history, mechanisms, consequences, and quantification of gerrymandering and its effects is presented in Section 2.1. This section also highlights the growing field of computational redistricting as a promising approach to analyzing and addressing gerrymandering.

1.1.2 Geographical Partisan Sorting

Another longstanding and deeply ingrained issue in the U.S. is the problem of residential segregation [31]. Historically, much attention has been given to segregation along racial [32–39] and economic [40–42] lines, but an emerging and politically significant form of segregation is partisan segregation.

In recent years, the American media has highlighted a trend where people moving to neighborhoods or states that align with their political beliefs, a phenomenon also known as geographical partisan sorting [43–51]. This phenomenon was popularized in John

[1] *Rucho v. Common Cause* 588 U.S. _ (2019)

Bishop's 2008 book "*The Big Sort: Why the Clustering of Like-Minded American is Tearing Us Apart*" [52]. Supported by a variety of data analyses, Bishop describes how Americans are increasingly moving to politically homogeneous neighborhoods while speculating about their causes and consequences. Whilst Bishop's methodologies have been questioned [53], it at least has sparked a lively debate among scholars about the phenomenon's existence and its potential implications.

In the past decade, scholars have found substantial evidence showing that the American electorate has segregated among party lines [54–58]. These studies show that partisan segregation has grown significantly since the 1990s. In broad terms, the phenomenon shows that Republican voters are more likely to spread out across rural areas, while Democratic voters tend to cluster in urban centers. This division creates distinct political landscapes across the country, with rural regions increasingly leaning conservative and urban areas solidifying as liberal strongholds.

Whether the driving forces behind geographical partisan sorting are intentional or inadvertent is contested. Skeptics of the "Big Sort Hypothesis" either fully negate the existence of the phenomenon or assert that partisanship isn't at the forefront of people's minds when moving to a new residential area [53, 59–62]. While, others argue that the American population might be inadvertently sorting into politically homogeneous areas because one's preference for residential environments and partisanship are correlated [63, 64]. However, set aside the reasons for migration, there is an observable trend of Americans sorting themselves along partisan lines.

The spatial distribution of Republican and Democratic voters has shown to significantly influence redistricting outcomes. In a 2013 study, Chen and Rodden introduced the concept of "unintentional gerrymandering" [65]. Using computational methods to generate large ensembles of redistricting plans, they demonstrated that geographic patterns of voter distribution alone can result in biased electoral maps. Specifically, they found that redistricting tends to favor parties whose supporters are more geographically dispersed, while disadvantaging those concentrated in dense urban centers. As a result, the typical clustering of Democratic voters in cities creates a structural bias that benefits Republicans, even in the absence of deliberate partisan manipulation. This concept of unintentional gerrymandering is particularly relevant to this thesis, as it captures the relationship between its two core concepts: gerrymandering and geographical partisan sorting.

In Section 2.2, a more in-depth discussion of the historical trends, scholarly debates, and driving forces behind geographical partisan sorting is provided. It also delves deeper into the concept of unintentional gerrymandering, presenting relevant studies and empirical findings that illustrate its causes and implications.

1.2 Research Questions

Scholars have been working to combat gerrymandering for decades, often playing crucial roles in landmark Supreme Court redistricting rulings [66–68]. With advancements in computational power and the availability of extensive datasets, computational science has become an increasingly valuable tool in the redistricting process [69]. These datasets provide detailed information about electorates and election outcomes, allowing for more accurate and sophisticated modeling of electoral systems. Since the 1960s, scholars have advocated for computational methods to make redistricting more transparent, objective, and fair, counteracting the widespread use of gerrymandering [70–73]. However, concerns have also been raised that algorithmic redistricting could empower state legislators to create even more precise and aggressive partisan gerrymanders [74]. Current research in computational redistricting primarily focuses on three central questions: how can fair electoral maps be designed?; how can partisan bias in existing maps be quantified?; and how does gerrymandering influence political outcomes such as voter competition, polarization, and electoral fairness? [14, 15, 75–86]. However, two key areas remain underexplored: (1) the relationship between geographical partisan sorting and redistricting [87–89] and (2) the effectiveness of redistricting reforms using computational methods [90]. This thesis addresses these gaps by developing the first agent-based model designed to simulate both the processes of gerrymandering and geographical partisan sorting.

The goal of this thesis is twofold. The first objective is to analyze how gerrymandering and partisan sorting influence the fairness, competitiveness and compactness of congressional electoral maps. While previous studies have examined these phenomena separately, their combined effects remain underexplored. Partisan sorting has the potential to amplify the partisan bias, even in the absence of intentional gerrymandering. Understanding this relationship helps determine whether partisan imbalances in congressional maps arise from deliberate manipulation, organic voter movement, or both. The findings from this research contribute to the broader debate on "unintentional gerrymandering" and its role in distorting representation. To deepen the understanding of this phenomenon of unintentional gerrymandering, experiments are conducted using different spatial voter distributions to identify which features of a state's political geography most strongly affect the partisan bias of electoral maps.

The second objective is to assess whether applying competitiveness and compactness criteria as redistricting reforms can effectively counteract distortions caused by gerrymandering and partisan sorting. Enforcing competitiveness helps ensure that elections remain contested, thereby reducing the risk of extreme partisan outcomes, while enforcing compactness limits the ability to draw irregular and strategically biased district boundaries. While 18 states impose compactness requirements for congressional redistricting, only two states mandate competitiveness, leaving the majority of the U.S. without formal safeguards against extreme gerrymandering—beyond the basic requirements of contiguity and equal population across districts [4, 5].

By simulating the both gerrymandering and partisan sorting, and evaluating the effects of competitiveness and compactness reforms across varied political geographic scenarios, this research offers empirical insights into these dynamics and assesses whether such reforms can improve electoral fairness, especially in states where they are not yet in place. The main research question is defined as follows:

- **(*M-RQ*):** How do **gerrymandering** and **geographical partisan sorting** combined affect the partisan bias of electoral maps?

This main question will be answered through six sub-questions, defined as follows:

- **(*S-RQ1*):** How does the presence of *geographical self-sorting* **alone** affect the fairness of electoral maps?
- **(*S-RQ2*):** How does the presence of *gerrymandering* **alone** affect the fairness of electoral maps?
- **(*S-RQ3*):** How does the **combination** between *partisan sorting* and *gerrymandering* affect the fairness of electoral maps?
- **(*S-RQ4*):** How do different spatial voter distributions influence the outcomes observed in *S-RQ1* through *S-RQ3*?
- **(*S-RQ5*):** How does promoting **competitive** districts affect the fairness of electoral maps?
- **(*S-RQ6*):** How does promoting **compact** districts affect the fairness of electoral maps?

The first three sub-questions are necessary to understand how the model behaves when either one or both phenomena are simulated. These simulations assume that mapmakers are always seeking to maximize partisan advantage when redistricting, and provide insights into the combined effects of gerrymandering and geographic partisan sorting. Additionally, these simulations function as the baseline used to compare with simulations where mapmakers are forced to draw competitive and compact districts. S-RQ4 aims to explore the influence of different initial spatial voter distributions on the fairness of congressional maps under different simulation scenarios, and provide insight into the concept of unintentional gerrymandering. The final two sub-questions are there to address the efficacy of competitive and compact redistricting criteria as potential countermeasures to partisan distortions. These simulations allow for an empirical evaluation of whether enforcing these criteria leads to fairer electoral outcomes.

1.3 Research Approach

To address the research questions, this thesis presents **GerrySort**, an agent-based model (ABM) specifically designed to simulate the redistricting process in tandem with geographic partisan sorting across multiple redistricting cycles. Agent-based modeling is particularly well-suited for this research because it enables the independent and combined simulation of gerrymandering and partisan sorting, allowing for the observation of emergent behaviors resulting from both their isolated and combined effects. Furthermore, modeling the dynamic feedback loop between redistricting rules and voter movement makes it possible to examine how these phenomena affect the effectiveness of the two redistricting reforms—competitiveness and compactness.

To ensure realism, the model integrates a diverse set of empirical data sources, including precinct-level presidential election results, county-level demographic indicators (such as population counts, housing units, and households), rural-urban commuting area classifications, and official county and congressional district boundaries. This data enables the model to accurately represent the spatial distribution of Republican and Democratic voters, the demographic and geographic characteristics of each state, and the initial configuration of congressional district maps. By grounding the simulation in high-resolution real-world data, the model can better capture the political and geographic complexity unique to each state, ultimately enhancing the credibility, interpretability, and policy relevance of its outcomes.

By adjusting a range of input parameters and recording various model statistics related to partisan fairness, electoral competitiveness, and district compactness, the model facilitates an exploration of potential behaviors and outcomes. To evaluate the reliability and robustness of the model, both global and local sensitivity analyses will be performed. These analyses serve two purposes: first, to verify that the model behaves as expected under a range of parameter settings; and second, to identify which parameters have the greatest influence on the simulation outcomes. Following the sensitivity analysis, a series of experiments will be conducted to investigate the combined effects of gerrymandering and geographical partisan sorting, and to assess how these dynamics influence the effectiveness of two mentioned redistricting reforms. These experiments are designed to systematically address each of the sub-research questions.

All analyses will be conducted across four politically important U.S. states: Georgia (GA), Wisconsin (WI), Michigan (MI), and Pennsylvania (PA). These states are commonly referred to as "swing states" due to their historically competitive elections and frequent shifts in partisan control. Swing states are particularly relevant to this study because their near-even partisan balance makes them more sensitive to changes in redistricting practices, making them ideal testbeds for evaluating the impacts of gerrymandering, partisan sorting, and redistricting reforms. Moreover, modeling multiple states allows for comparative analysis, helping to uncover how state-specific demographic, geographic, or political factors influence the fairness of congressional maps and/or the effectiveness of the redistricting reforms.

1.4 Research Contributions

This thesis provides new insights into the individual and combined effects of gerrymandering and geographical partisan sorting on the electoral fairness of congressional maps. By varying the initial spatial distribution of voters—either by concentrating partisan voters into clusters or dispersing them across the map—this study contributes to the broader discussion on "unintentional gerrymandering", a phenomenon where electoral bias emerges not from deliberate manipulation but from the natural political geography of a state. In addition, this work advances the discourse on redistricting reform by quantifying the impact of two reform criteria—competitiveness and compactness—and by assessing their potential to improve fair representation and electoral competitiveness despite the challenges posed by gerrymandering and partisan sorting. Specifically, the following research contributions have been made:

- A novel ABM—informed by high-resolution empirical data—has been developed capable of simulating both gerrymandering and geographical partisan sorting at the state level, enabling the analysis of their isolated and combined effects. Moreover, the model is capable of assessing the effectiveness of redistricting reforms across a diverse set of political-geographic scenarios.
- This thesis contributes to the existing literature on unintentional gerrymandering by demonstrating what political geographic features can lead to systematic representational biases, even in the absence of deliberate manipulation.
- This thesis contributes to the understanding of redistricting reform by showing that competitiveness and compactness criteria only lead to significant improvements in electoral fairness when implemented with strong enforcement and minimal partisan

interference. However, their effectiveness is contingent on the political geography of a state.

- A flexible simulation framework has been developed that can be adapted to investigate the effects of various forms of voter segregation and redistricting reforms on the partisan fairness of congressional maps, offering a valuable tool for future academic research and policy experimentation in the context of gerrymandering and voter migration patterns.

1.5 Thesis Outline

This thesis is structured as follows:

- Chapter 2 provides a comprehensive literature review, focusing on the two core concepts of this thesis: *partisan gerrymandering* (Section 2.1) and *geographical partisan sorting* (Section 2.2). This chapter establishes the theoretical framework and context for the research.
- Chapter 3 presents GerrySort following the ODD+D protocol. Here the ABM is described in detail and the design choices are substantiated.
- Chapter 4 presents the methodology and experimental set-up for both global and local sensitivity analyses. The results of these analyses are presented and discussed.
- Chapter 5 describes the experimental set-up used to address the sub-research questions. The findings from these experiments are analyzed and interpreted.
- Chapter 6 critically examines the main findings, situating them within the existing literature. This chapter also highlights the model's limitations and suggests possible avenues for future research.
- Chapter 7 provides the answers to all sub-research questions and the main research question. It also provides a summary of the main findings and offers concluding reflections.
- Chapter 8 discusses the ethical considerations and data management practices followed to throughout the research, providing a reflective closing to the thesis.

Chapter 2

Literature Review

This chapter establishes the theoretical framework necessary for understanding the two modeled phenomena: *partisan gerrymandering* (Section 2.1) and *geographical partisan sorting* (Section 2.2). It reviews definitions, scholarly debates, historical contexts, trends, and the effects of said concepts. The goal of the review is to equip you, the reader, with a thorough understanding for interpreting and contextualizing the design choices and results of GerrySort.

2.1 Partisan Gerrymandering

This section consists of seven subsections, each addressing an important aspect of redistricting and gerrymandering. Together, they establish a foundation for understanding gerrymandering's role within the model.

2.1.1 Single-Member Districts

As mentioned in the introduction, members of the U.S. Congress and state legislatures are elected through geographically defined electoral districts. These districts serve as the fundamental units through which representatives are chosen to serve in legislative bodies. In most cases, each electoral district is designed to elect a single representative, a structure known as a single-member district[1]. Reflecting the federalist structure of the U.S., each state maintains two primary types of electoral districts: *congressional districts*, which determine representation in the U.S. House of Representatives, and *state legislative districts*, which determine representation in the state legislature. These

[1] A few states, such as Arizona, New Jersey, and South Dakota, use multi-member districts for their state legislative elections, where more than one representative is elected per district.

two levels of districts operate independently and are redrawn separately, typically every ten years following the decennial U.S. Census to reflect population changes.

Congressional districts are the geographic units used to elect state representatives to the U.S. House of Representatives. The number of congressional districts, or representatives, allocated to each state is based on its share of the national population, as determined by the decennial U.S. Census [91]. However, every state is guaranteed at least one district, regardless of population size[2]. In contrast, U.S. Senate elections do not involve districts, as each state receives two senators regardless of population, and they are elected through statewide votes. As a result, congressional districts are the only type of federal electoral districts subject to redistricting, and thus, vulnerable to gerrymandering.

State legislative districts serve as the electoral units for electing representatives to each state's legislature, which is typically bicameral, comprising a state House of Representatives (or Assembly) and a state Senate[3]. In states with a bicameral system, two distinct sets of state legislative districts exist: one for electing members to the state House and another for the state Senate. Most states use single-member districts for both chambers, meaning each district elects one representative to the corresponding legislative body. Like congressional districts, state legislative districts must be redrawn every ten years, making them equally susceptible to gerrymandering, though at the state rather than federal level.

2.1.2 The Redistricting Cycle

The redistricting cycle in the U.S. is a foundational process in the maintenance of representative democracy. Every ten years, following the completion of the U.S. Census[4], states are constitutionally and federally obligated to redraw the boundaries of both their congressional and state legislative districts. This redistricting ensures that each district maintains roughly equal population size, thereby upholding the principle of "one person, one vote"[5]. The process begins with reapportionment, during which the 435 seats in the U.S. House of Representatives are redistributed among the states in proportion to their updated population counts from the decennial Census [91]. While each state is

[2] This applies to the six so-called single-member states, where congressional redistricting is not conducted.

[3] Nebraska is the only exception, operating with a unicameral, nonpartisan legislature.

[4] The U.S. Census is a constitutionally mandated survey conducted every ten years by the federal government, aiming to collect essential demographic, social, and economic information about the entire population within the country.

[5] This principle was established in landmark Supreme Court cases such as Reynolds v. Sims (1964) and Wesberry v. Sanders (1964), which mandated that legislative districts be equally populated to ensure fair representation.

guaranteed at least one congressional seat, shifts in population can cause states to gain or lose seats, thereby influencing their political weight at the federal level.

Following reapportionment, the redistricting phase commences. During this phase, each state redraws its internal district boundaries—both congressional and state legislative—to reflect internal demographic changes and population movements. The responsibility for drawing these new maps varies by state and may fall to the state legislature, an independent redistricting commission, or a bipartisan advisory body [4, 5]. The specific rules guiding the redistricting process also differ by state, but common criteria include contiguity, compactness, equal population, and respect for existing political or natural boundaries and communities of interest [4, 5]. Some states additionally require consideration of competitiveness or partisan fairness, though these criteria are less commonly enforced [4, 5].

Redistricting wields significant influence over the political landscape. At the federal level, congressional redistricting can affect the balance of power in the U.S. House of Representatives, while at the state level, redistricting shapes the composition of both state legislative chambers. To safeguard against abuse, redistricting plans are subject to legal oversight. Courts—often beginning with state courts and potentially escalating to the U.S. Supreme Court—may intervene to assess whether district maps violate constitutional or statutory protections. In cases of unlawful or discriminatory redistricting, courts have the authority to strike down maps and mandate revisions.

2.1.3 History of Gerrymandering

This subsection will provide a brief exploration of the historical evolution of gerrymandering in the U.S. It will delve into the origins of gerrymandering and underscore significant redistricting laws and pivotal Supreme Court decisions that have played a defining role in shaping the contemporary rule book of gerrymandering.

2.1.3.1 Origins

The term "gerrymandering" originated in 1812 when Massachusetts Governor Elbridge Gerry oversaw the redistricting of the state's senate districts, favoring his Democratic-Republican Party over the Federalist Party [6, 7]. In response to the redistricting, *The Boston Weekly Messenger* featured a cartoon of an oddly shaped district, resembling a prehistoric monster (Fig. 2.1). The district's peculiar shape, resembling a salamander, led to the suggestion of the name "salamander", to which another quipped, "gerrymander is what you mean". And so, a new term entered the U.S. political lexicon.

FIGURE 2.1: "The Gerry-Mander" from *The Boston Weekly Messenger* (March 26, 1812). Image is in the public domain. Source: https://commons.wikimedia.org/wiki/File:The_Gerry-Mander_Edit.png.

2.1.3.2 The (Legal) History of Gerrymandering

In his compelling argument, legal scholar Kang asserts that hyperpartisanship has consistently shaped the trajectory of U.S. political history, with gerrymandering serving as an enduring element [92]. Kang contends that the present era of hyperpartisanship, though perceived as historically extreme, shares parallels with earlier periods. This perspective emerges when contrasting it with the preceding Cold War era, which notably featured lower partisanship, reduced ideological polarization, and fewer instances of gerrymandering. Kang posits that the Cold War era stands as an anomaly in U.S. hyperpartisan history, showcasing an unprecedented level of bipartisanship. Notably, this period marked the first significant involvement of the Federal government and the Supreme Court in redistricting and election law.

The initial foray of the Supreme Court into redistricting occurred with the case of Baker v. Carr[6], establishing the federal courts' right to review redistricting issues. Before

[6] *Baker v. Carr*, 369 U.S. 186 (1962)

this case, the Court had refrained from intervening in partisan redistricting, fearing politicization. In Colegrove v. Green[7], Justice Frankfurter deemed redistricting issues "beyond [the Court's] competence" and "of a peculiarly political nature." However, in 1964, the Court, compelled by the surge in cases addressing malapportionment, ruled in Reynolds v. Sims[8]. This case challenged Alabama's state legislature apportionment, revealing a district with forty-one times as many eligible voters as another. The Court, viewing this through the lens of equal protection rather than a political question, held that neglecting redistricting for sixty years discriminated against voters in densely populated areas. This landmark decision introduced the "one person, one vote" principle, requiring roughly equal population sizes in districts. The Court acknowledged that the ruling would benefit the African American population by empowering urban areas, particularly in the American South. However, while empowering urban areas, the requirement for equal population alone failed to prevent partisan manipulation of district boundaries.

Another pivotal moment occurred in 1965 when President Lyndon B. Johnson signed the Voting Rights Act into law, responding to systematic exclusion of African American voters in the South under one-party Democratic rule during the Jim Crow era. The Voting Rights Act incorporated various provisions aimed at prohibiting racial discrimination in voting, including the prohibition of poll taxes and literacy tests. The impact of the act was profound, successfully dismantling the mechanisms of Jim Crow and empowering African Americans to exercise their voting rights [93]. This legislation was a response to peaceful demonstrations organized by Civil Rights leaders in 1964. The violent events encountered by protesters-including the murder of voting-rights activists in Mississippi and the assault by white state troopers on peaceful marchers in Selma, Alabama-garnered national attention, and renewed attention to the issue of voting rights. In White v. Regester[9], the Court, addressing a vote dilution claim, upheld that Texas's targeted use of multi-member districts—to diminish the voting strength of African-American and Latino voters—violated the equal protection clause. This decision, similarly to Reynolds v. Sims, focused on discrimination unrelated to partisan considerations, and required the use of majority-minority districts[10] for effective minority participation. While the remedy significantly increased minority representation as intended, it had virtually no impact on the partisan balance of power.

The 1990s witnessed the resurgence of hyperpartisanship in U.S. politics, marking the end of the Cold War era bipartisanship. Both the Democratic and Republican parties

[7] *Colegrove v. Green*, 328 U.S. 549 (1946)
[8] *Reynolds v. Sims*, 377 US 533 (1964)
[9] *White v. Regester, 412 U.S. 755 (1973)*
[10] A district where a racial minority group comprises a majority of the population.

underwent ideological realignment, transforming from heterogeneous coalitions into cohesive units with clear positions on a broader spectrum of issues. With the demise of Cold War bipartisanship, partisan redistricting re-entered the political arena. Notably, contemporary gerrymandering, aided by computational methods and rich datasets, is argued to be more severe than its 19^{th} century counterpart [69]. Kang argues that redistricting laws from the Cold War period, were ill-prepared for the magnitude of hyperpartisan gerrymandering seen today, and failed to acknowledge the potential dangers of partisan redistricting.

2.1.3.3 Current State

The redistricting cycle of 2010 witnessed unprecedented levels of partisan gerrymandering, surpassing anything seen between 1972 and 2012, as measured by the efficiency gap [3]. This gerrymandering was characterized by heightened one-sidedness, increased durability, and more aggression than ever before. The Republican Party, strategically prioritizing and allocating resources to gerrymandering during the 2000 and 2010 redistricting cycle, achieved significant success by securing numerous state legislatures for the decade and overturning the Democratic majority in the U.S. House in 2012. In response to this defeat, Democrats decided to actively participate in redistricting by matching Republican efforts and investments. Consequently, the 2020 redistricting cycle saw both major parties engaging in partisan gerrymandering, particularly in states where either party had majority control of state legislatures and authority over the redistricting process. Republicans, with dominance in more states, including major ones like Georgia, Texas, Florida, North Carolina, engaged in gerrymandering, while Democrats did so in states like Illinois, Maryland, Massachusetts, and New York. This ensured that the 2020 redistricting cycle was not as one-sided as the 2010 cycle, with the net effect of partisan gerrymandering mostly canceling nationally [15]. However, electoral competitiveness decreased due to an increase in safe districts.

The gerrymanders in the 2020 cycle are more aggressive for several reasons. Firstly, the Supreme Court's 2019 decision in Rucho v. Common Cause[11] eliminated the possibility of federal court intervention to block partisan gerrymanders. Unlike in the past, where federal courts could potentially invalidate partisan gerrymanders, the fear of judicial invalidation is now absent. It's worth noting that the Court left intact parts of the Voting Rights Act prohibiting racial or ethnic gerrymandering, but mapmakers could argue that a racial gerrymander was merely a partisan gerrymander if the racial group in question voted predominantly for one party. Secondly, technological advancements allow the algorithmic mass production of district maps, enabling mapmakers to generate

[11] *Rucho v. Common Cause* 588 U.S. _ (2019)

thousands or millions of maps with specific criteria, including partisan advantage. Lastly, voter behavior is now more predictable, with fewer swing voters and smaller shifts from election to election. This predictability allows gerrymanders to have more confidence in the longevity of their maps' tilted direction throughout the decade.

The reemergence of hyperpartisanship in the U.S., compelling both major parties to actively practice gerrymandering, combined with the Supreme Court's reluctance to intervene, indicates that partisan gerrymandering is likely here to stay and may even intensify in the coming years. The availability of sophisticated computational methods and the increased predictability of voting behavior suggest that gerrymanders will become more aggressive and successful [69]. Without Supreme Court intervention, it falls upon state legislatures to propose redistricting reforms to counteract gerrymandering. Michigan serves as a recent example, where an independent commission has been responsible for drawing congressional and state legislative districts since 2018 [4, 5]. However, even in Michigan, challenges persist, as Democratic state lawmakers have sued the commission, alleging racial gerrymandering. The Supreme Court's review of this case will determine if the maps are unconstitutional, highlighting the complexities of redistricting reform. Nationwide, bipartisan or independent commissions, theoretically designed to draw electoral boundaries fairly, have faced challenges in practice, making it difficult to counteract gerrymandering effectively. This further solidifies the notion that gerrymandering is likely to persist in U.S. politics.

2.1.4 Types of Gerrymanders and Strategies

Gerrymandering manifests in various forms [94]. While *partisan gerrymanders* and *incumbent protection gerrymanders* have generally been allowed to persist in the current political landscape, others like *malapportionment gerrymanders* and *racial gerrymanders*, have been prohibited through the establishment of the one person, one vote principle and the enactment of the Voting Rights Act. This study focuses exclusively on partisan gerrymandering, the most prevalent form and the one that continues to be permitted by the Supreme Court.

There are various gerrymandering strategies mapmakers employ to gain a partisan advantage, with *cracking* and *packing* standing out as the most renowned and impactful techniques. In addition to cracking and packing, legislators can resort to *hijacking* and *kidnapping*, although these strategies tend to operate on a more localized scale, contributing less significantly to the overall partisan bias of a district map. Recognizing cracking and packing is essential, as these strategies may emerge in the model's simulations. Additionally, cracking and packing play a fundamental role in the efficiency gap, a metric designed to assess the partisan fairness of electoral maps (Section 2.1.6.1).

Cracking involves strategically dispersing the voting power of a specific political group across multiple districts, preventing them from achieving a majority in any single district. By dispersing and diluting the influence of a cohesive voting bloc, the cracking strategy aims to weaken the overall electoral impact of the targeted group [95]. Historically, cracking has been employed as a discriminatory tactic, notably to prevent African-Americans from electing representatives who reflect their interests. While the Voting Rights Act successfully prohibited racially motivated cracking to a certain extent, the practice remains prevalent, often under the guise of partisan considerations—which are permitted by the Supreme Court. An illustrative case of cracking unfolded in Texas during the 2010 redistricting cycle. The Republican-controlled state legislature crafted a congressional map that conspicuously cracked the traditionally liberal city of Austin into six districts sprawling across hundreds of miles of conservative suburban and rural territory (Fig. 2.2a). This intentional cracking aimed to dilute the voting strength of Austin Democrats by incorporating conservative territories into their districts. The strategic inclusion of conservative areas increased the competitiveness of these districts—benefiting the Republicans—thus minimizing the overall impact of Austin Democrats on the state's congressional representation. The 2010 redistricting cycle in Texas was marked by turbulence, with proposed maps facing regular legal challenges. However, these legal battles predominantly revolved around concerns related to the dilution of Hispanic voting power, rather than the cracking of Austin [96, 97].

Packing involves strategically concentrating the voting power of a specific political group into a limited number of districts, aiming to ensure overwhelming victories in those areas while minimizing their impact in other districts. The primary objective of packing is to confine the targeted group to a small number of districts. The rationale behind this strategy lies in preventing the targeted group from having significant influence on multiple congressional elections by concentrating their voting strength [95]. An illustrative case of packing occurred in Alabama's 7^{th} Congressional District during the 2010 redistricting cycle [98]. The district, which was already 62 percent African-American and considered a safe majority-minority district, witnessed deliberate packing by the Republican-controlled state legislature. In their redrawing efforts, the legislature extended the district's boundaries further into Birmingham and Montgomery, carving out African-American neighborhoods and ultimately creating a district with a 64 percent African-American majority (Fig. 2.2b). This deliberate packing ensured that the surrounding districts, which were previously competitive, now had significantly reduced

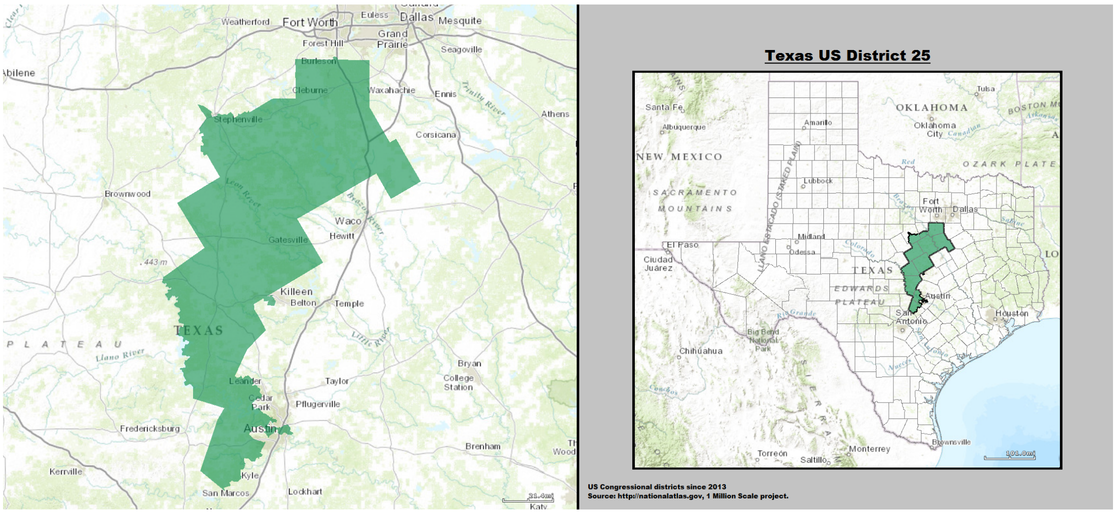

(A) Texas' 25^{th} District, this is one of six districts that cracked Austin.

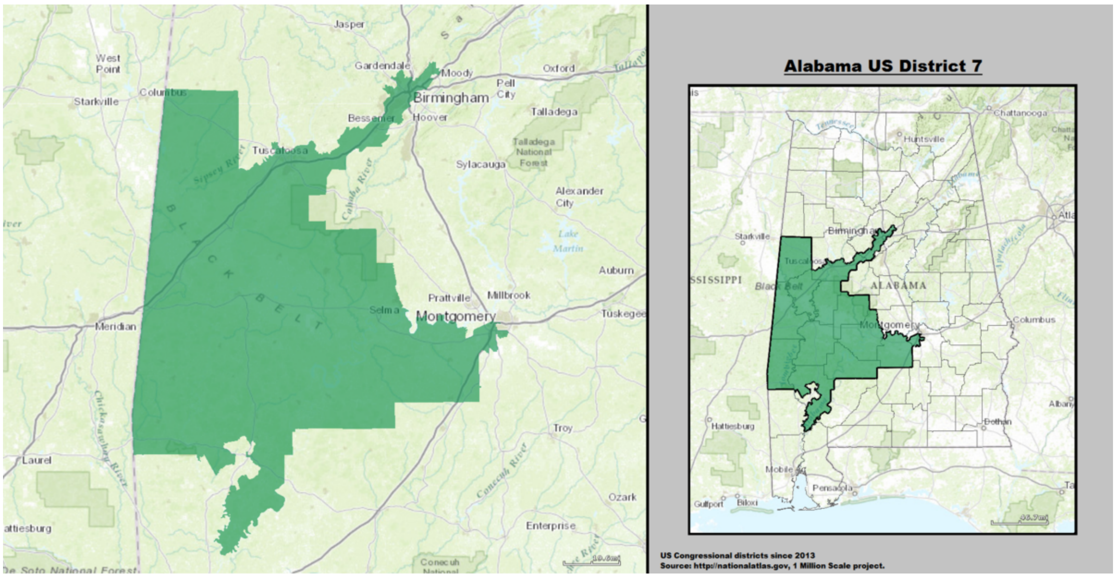

(B) Alabama's 7^{th} District that was subject to packing.

FIGURE 2.2: Examples of two gerrymandering strategies employed in 2010s redistricting cycle: cracking and packing.

African-American voter presence, rendering them safely Republican. While, Democratic voters and advocates challenged the constitutionality of the proposed legislative and congressional maps, as they allegedly illegally packed African-American voters, the state Courts upheld the district maps.

2.1.5 Effects of Gerrymandering

In recent decades, scholars have extensively explored the adverse effects of gerrymandering on U.S. democracy. This thesis is focused on analyzing gerrymandering's impact *representation*, *electoral competitiveness*, and *district compactness*. The following sections provide an overview of the ongoing debates surrounding these effects, as these can be measured by the model.

2.1.5.1 Representation

When a single party controls the redistricting process, it often draws maps designed to entrench its power, allowing it to secure a disproportionate share of legislative seats relative to its share of the popular vote. This partisan bias undermines the principle of equal representation, as a majority in the popular vote may not translate into a majority in a state legislature or a state's congressional seats. Despite legal advances, namely the prohibition of malapportionment and racial gerrymandering, partisan gerrymandering remains a persistent obstacle to equitable representation, especially in the wake of a recent Supreme Court ruling[12], which declared partisan gerrymandering claims to be nonjusticiable in federal courts, leaving its regulation primarily to the states.

Scholars have sought to quantify the extent of the distortion caused by partisan gerrymandering. An important contribution was the introduction of the efficiency gap by Stephanopoulos and McGhee in 2015, providing a method to measure the partisan bias of electoral maps [3]. Building on this, a 2018 study by Stephanopoulos analyzed a comprehensive dataset of state house and congressional plans from 1972 to 2016, showing that single-party control of redistricting is the main driver of partisan bias [11]. While seemingly intuitive, this finding underscores the intentional nature of partisan gerrymandering, when one party controls the process, it tends to prioritize its own advantage over fair representation. Additionally, the study noted that states with higher Black populations and greater urbanization were more susceptible to partisan bias favoring Republicans when they controlled redistricting.

Importantly, other research has underscored that not all partisan bias stems from partisan gerrymandering. Chen and Rodden demonstrated that natural political geography, specifically, the concentration of Democratic voters in urban areas, can itself lead to unintentional representational biases, complicating the distinction between partisan strategy and geographic inevitability [65].

2.1.5.2 Electoral Competitiveness

The relationship between gerrymandering and electoral competitiveness has sparked an ongoing and often contradictory scholarly debate. Intuitively, one might assume that

[12] *Rucho v. Common Cause* 588 U.S. _ (2019)

gerrymandering, particularly under the control of a single party, dampens competitiveness by maximizing the number of safe districts, fortifying the incumbency advantage, and reducing overall competition. However, paradoxically, gerrymandering can also yield more competitive races. Parties aiming to maximize their seat share often reallocate safe voters from secure districts into neighboring districts where they are less competitive. This strategy boosts their chances of winning in those adjacent districts. However, it comes at a cost: their own incumbents become more vulnerable. As a result, both the original and the targeted districts become more competitive. This tension, the delicate balance between incumbent protection and maximizing their party's electoral potential, renders the overall impact of gerrymandering on competitiveness far from straightforward.

Early scholarly debates reflect this dichotomy. One study attributed the decline in competitive districts during the 1960s to redistricting efforts [16], while another found that incumbents particularly benefited from reduced competition in 1992, especially in bipartisan redistricting contexts [17]. Meanwhile, others argued that redistricting either had a neutral or even positive effect on competition [99, 100]. One study further supported this notion, showing how partisan gerrymandering can inadvertently reduce incumbent safety by reallocating dependable voters to swing districts [101].

Despite improved computational tools and access to richer datasets in the 2000s, more recent studies did not converge on a consensus. One study argued that partisan and racial gerrymandering decreased the share of competitive state house seats [12], whereas another concluded that redistricting played only a limited role in the declining competitiveness of U.S. House elections during the 1980s through early 2000s [13]. Other studies, emphasized the multifactorial nature of declining competitiveness and deemed the precise impact of redistricting inconclusive [102]. Another argued that gerrymandering can actually increase competitiveness, as maximizing seats often requires reducing margins in otherwise safe districts [103].

In the past decade, the field has pivoted toward computational approaches that simulate thousands of neutral redistricting plans to quantify the effects of partisan gerrymandering [104, 105]. These simulation-based studies offer a clearer counterfactual: what a fair or neutral map might look like. For example, one study found that gerrymandering often produces more safe seats, particularly when a single party dominates the redistricting process [14]. Similarly, another study showed that while partisan gerrymandering tends to cancel out at the national level, it consistently reduces electoral competition, making the partisan composition of the U.S. House less responsive to shifts in the national vote [15].

In sum, although individual studies diverge in their findings, a broader pattern emerges: gerrymandering's effect on competitiveness is highly context-dependent. It can either entrench incumbents or destabilize them, depending on how aggressively the redistricting party pursues marginal gains. The move toward simulation-based analyses has helped clarify these dynamics by providing more precise benchmarks, yet the inherent trade-offs in partisan redistricting continue to defy simple conclusions.

2.1.5.3 District Compactness

The relationship between gerrymandering and district compactness has long been recognized, tracing back to the original "Gerry-mander" of 1812, whose irregular shape evoked comparisons to a salamander [6]. Compactness is often seen as a desirable criterion in redistricting, reflecting districts that are regular in shape and minimizing the manipulation of boundaries for political gain. Intuitively, gerrymandering tends to reduce compactness, as partisan actors seek to draw convoluted boundaries to achieve strategic advantages, such as concentrating or diluting particular voting blocs. Non-compact districts can serve as visual evidence of gerrymandering, making compactness an appealing procedural safeguard against partisan manipulation [106].

However, the effects of gerrymandering on compactness are more nuanced than a simple degradation of shape. In some cases, partisan mapmakers deliberately maintain relatively compact-looking districts to disguise gerrymandering, using subtle boundary shifts to secure electoral advantages without producing obviously irregular shapes [107]. Additionally, efforts to comply with other redistricting criteria, such as preserving communities of interest or satisfying the Voting Rights Act's requirements for minority representation, can lead to less compact districts even in the absence of partisan intent [108]. Thus, not all irregular shapes are products of gerrymandering, and not all gerrymanders are grotesquely shaped.

Early scholarly work emphasized compactness as a primary defense against gerrymandering. The influential Polsby-Popper measure, based on the ratio of a district's area to the area of a circle with the same perimeter, was proposed as an objective standard to detect irregularities [106]. Other measures, such as the Schwartzberg ratio [109], the Reock score [110], and the convex hull ratio [111], were developed to capture different aspects of geometric regularity. More recently, newer methods have emerged that leverage machine learning and large datasets to predict the likelihood of a district being non-compact [112]. Scholars have recognized that single-value compactness measures are sensitive to natural geographic features and the spatial distribution of voters [26, 107, 113].

In response to the realization that compactness alone is insufficient to diagnose gerrymandering, many states have adopted explicit compactness requirements in their redistricting laws, though their rigor and enforcement vary considerably [4, 5]. Some states define compactness qualitatively, while others mandate the use of specific mathematical tests. Despite these legal frameworks, the effectiveness of compactness standards in constraining partisan gerrymandering remains limited. Strategic actors often balance compactness with other criteria, crafting districts that technically meet legal definitions while still achieving partisan goals [107].

Recent advances in computational redistricting have further complicated the understanding of compactness. Simulation-based studies generate large ensembles of redistricting plans under non-partisan criteria, providing a statistical baseline against which enacted plans can be evaluated. These studies reveal that extreme deviations from compactness are often correlated with partisan intent but not exclusively so [65, 114]. Consequently, while compactness remains a valuable indicator, modern scholarship increasingly treats it as one piece of a broader toolkit for detecting and understanding gerrymandering.

2.1.6 Quantifying Gerrymandering and its Effects

The quantification of gerrymandering is a research topic that has interested scholars for decades. For several decades, scholars widely accepted that the *partisan bias* served as a suitable metric for gauging partisan gerrymandering [115, 116]. These early measures of partisan bias were grounded in the partisan symmetry principle [16, 115]. Partisan symmetry posits that a specific share of total votes received by a party should result in a predetermined number of legislative seats, irrespective of which party garnered that share of total votes. While many scholars acknowledged this principle, there was no universally accepted method for measuring partisan bias at that time [117]. The concept of measuring partisan bias involved predicting the relationship between the statewide average district vote for Democratic candidates (equivalent to 100% minus the fraction for Republican candidates) and the expected statewide fraction of seats for the Democratic Party. This relationship, commonly known as the seats-votes curve, formed the basis for partisan bias measurement. Various methods were employed to estimate the seats-votes curve, with early versions utilizing linear or nonlinear regression techniques. Once the seats-votes curve was established, partisan bias could be computed by analyzing how each party would perform in securing seats for any given vote share.

In a 2006 case[13], where a private citizen group challenged Texas's proposed redistricting plans, Supreme Court Justice Kennedy offered a critique of the partisan bias metric

[13] *League of United Latin American Citizens (LULAC) v. Perry*, 548 U.S. 399 (2006) (opinion of Kennedy, J.)

in his opinion statement. He argued that its reliance on predictions about seat shares, assuming an equal vote share, made it impractical as a judicial standard for measuring gerrymandering. This opinion sparked the scholarly debate on the subject of gerrymandering quantification, as scholars were eager to develop a measure that would satisfy the Court's requirements for a judicial standard.

The following sections introduce three recently developed metrics of partisan bias, or measures to quantify gerrymandering: *efficiency gap*, *mean-median difference*, and *declination*. These metrics will be used in GerrySort simulations to measure the partisan bias of electoral maps. Additionally, metrics for competitiveness and compactness will be presented, as both will be measured during the simulation to assess the overall competitiveness and shape of the districts.

2.1.6.1 Efficiency Gap

The *efficiency gap* measures partisan bias of a district plan by assessing the disparity in wasted votes between parties [3]. It is based on the premise that the goal of gerrymandering is to maximize seat gains relative to votes received. "Inefficiency" arises from votes that do not directly contribute to victory. This includes votes for a losing candidate and votes beyond the 50% threshold needed to secure a seat in a two-candidate race. A gerrymandering party does not seek to eliminate all wasted votes but aims to waste fewer votes than the opposition, typically by winning seats with smaller margins while forcing the opposing party to waste votes in landslide victories. This is achieved through packing (concentrating opposition voters into a few districts) and cracking (splitting them across multiple districts) (Section 2.1.4). The efficiency gap quantifies this imbalance across an entire district plan. It ranges from -1 to 1, where a negative score indicates a pro-Democrats bias, and a positive score indicates a pro-Republicans bias, and is defined as:

$$\text{Efficiency Gap} = \frac{W_D - W_R}{V_D + V_R} \tag{2.1}$$

where:

- W_D = the total amount of wasted votes for the Democratic Party across all districts,
- W_R = the total amount of wasted votes for the Republican Party across all districts,
- V_D = the total votes received by the Democratic Party across all districts,

- V_R = the total votes received by the Republican Party across all districts.

Wasted votes are computed as follows:

- For the winning party in a district:

$$W = V - \frac{S}{2} \tag{2.2}$$

  where V is the total votes received, and S is the total votes cast in that district.

- For the losing party in a district:

$$W = V \tag{2.3}$$

  since all votes for the losing party are wasted.

The efficiency gap was introduced by Stephanopoulos and McGee to address the Supreme Court's concerns about the partisan bias metric, as it doesn't rely on on predictive electoral outcomes. It gained prominence in the 2017 Supreme Court case[14] [66, 67], where Wisconsin's 2011 redistricting plan was challenged on the basis of an excessively high Efficiency Gap. However, despite its central role in the case, the Supreme Court ruled that Wisconsin's maps did not violate the Voting Rights Act and rejected the Efficiency Gap as a judicial standard

Scholarly scrutiny of the efficiency gap has extended well beyond the Supreme Court, with researchers subjecting the metric to extensive analysis. Legal scholars have raised several key critiques, arguing that the efficiency gap favors uncompetitive elections, discourages proportional representation, and may even create incentives for voter suppression [118]. Methodological concerns include the definition and weighting of wasted votes, imputations for uncontested races, and the handling of district-level turnout variations [119]. Additionally, critics highlight that the metric varies significantly across different elections, raising questions about its stability and reliability [120]. In response to these limitations, researchers have developed alternative measures of partisan gerrymandering [121–126]. Two measures that have gained particular traction are the *mean-median difference* and the *declination*, both of which emerged following the Supreme Court's 2018 ruling on the efficiency gap in the Wisconsin case.

Stephanopoulos and McGee, however, defend the efficiency gap by comparing it to other metrics—early measures of partisan bias, mean-median difference, and declination—across four criteria [116]. They conclude that the efficiency gap is the only metric

[14] *Gill v. Whitford*, 585 U.S. _ (2018) (opinion of Roberts, J.)

that consistently meets all four criteria across various electoral scenarios. In contrast, they argue, other metrics often violate the efficiency principle[15], making them unreliable in certain contexts. Importantly, Stephanopoulos and McGee clarify that their defense of the efficiency gap is not an advocacy effort but an attempt to refocus the academic debate on what makes a gerrymandering measure effective. Rather than promoting the efficiency gap as the definitive standard, they encourage a broader discussion on the fundamental criteria a gerrymandering metric should satisfy. Their framework provides a structured approach for assessing different measures, fostering more comprehensive evaluations in the study of partisan redistricting.

2.1.6.2 Mean-Median Difference

The *mean-median difference* quantifies asymmetry in vote share distribution by comparing the mean and median Democratic vote share across all districts. A significant gap between these two values suggests that the district distribution is skewed in favor of one party. If, for example, the mean Democratic vote share is 50%, but the median is 45%, the mean-median difference is 5% against Democrats, indicating a pro-Republican bias. This metric ranges from -1 to 1, where a positive value suggests a pro-Republican bias, while a negative value indicates a pro-Democratic bias. A small or zero difference implies a more symmetric and balanced redistricting plan. The formula for the mean-median difference is:

$$\text{Mean-median Difference} = \bar{D} - \tilde{D} \tag{2.4}$$

where:

- $\bar{D}$ = the mean Democratic vote share across all districts,
- $\tilde{D}$ = the median Democratic vote share across all districts.

McDonald and Best applied the mean-median difference in six legal cases concerning disputed redistricting plans, aiming to develop criteria for identifying gerrymandering using this metric [121]. They proposed four criteria to determine gerrymandering based on the mean-median difference. According to their definition, a map is considered gerrymandered if all of the following criteria are met:

[15] The efficiency principle states that a partisan gerrymandering measure should reflect a greater advantage for a party when its seat share increases without a corresponding increase in vote share. A measure violates this principle if it fails to register a shift in a party's favor despite clear changes in vote and seat share.

1. The mean vote percentage for one party consistently exceeds its median vote percentage.

2. A party's majority status among voters should be based on its statewide two-party percentage, rather than its district mean percentage.

3. A party achieves a mean vote share above 50% yet fails to secure a majority in any district.

4. The difference between a party's mean and median is significantly larger or smaller than expected under neutral redistricting plans.

While courts have yet to adopt a definitive legal standard for detecting gerrymandering using the mean-median difference, McDonald and Best argued that this metric, when combined with their criteria, provides a compelling framework for identifying partisan bias in electoral maps.

2.1.6.3 Declination

The *declination* metric detects discontinuities in vote share distributions between districts won by different parties [123, 124]. By using geometric principles, it assesses whether Republican- and Democratic-leaning districts exhibit distinct patterns of partisan concentration. In a neutrally drawn map, district vote shares should increase smoothly when ordered from the most Democratic to the most Republican district (Fig. 2.3). However, when gerrymandering occurs, opposition voters are often packed into a small number of districts where their preferred party wins by overwhelming margins, while cracking dilutes their influence elsewhere.

Declination quantifies this asymmetry by measuring the angular difference between the average Democratic vote share in Democratic-leaning districts and the average Democratic vote share in Republican-leaning districts. If both segments have similar slopes, the electoral map exhibits little or no partisan bias. The greater the deviation between them, the stronger the asymmetry. The metric ranges from -1 (pro-Democratic bias) to 1 (pro-Republican bias) and is defined as:

$$\text{Declination} = 2 * \frac{(\Theta_D - \Theta_R)}{\pi} \tag{2.5}$$

where:

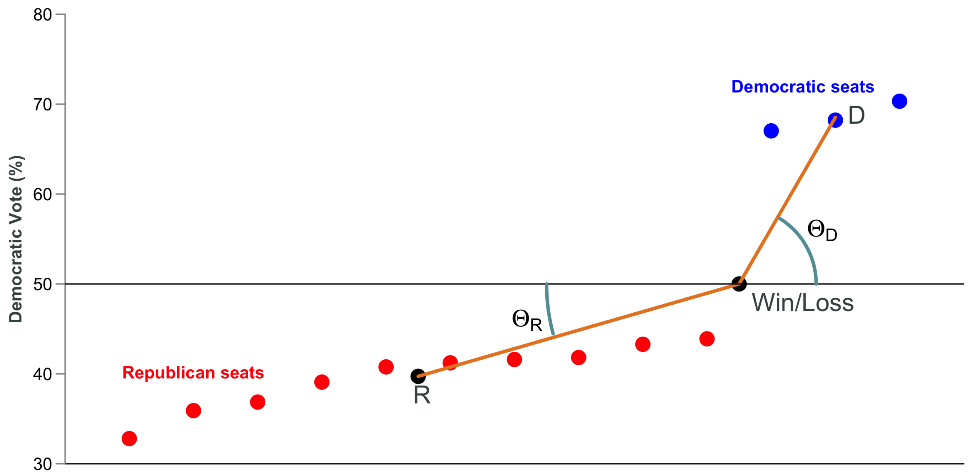

FIGURE 2.3: Illustration of the Declination metric: R and D denote the centers of mass for Republican and Democratic seats, respectively, with the 50-50 point marking the threshold between wins and losses. Source: https://planscore.org/metrics/declination/.

- Θ_D is the angle between the 50% vote share line and the average Democratic vote share in Democratic-leaning districts, given by:

$$\Theta_D = \arctan\left(\frac{2\bar{D}_D - 1}{\frac{N_D}{N}}\right) \tag{2.6}$$

- Θ_R is the angle between the 50% vote share line and the average Democratic vote share in Republican-leaning districts, given by:

$$\Theta_R = \arctan\left(\frac{1 - 2\bar{D}_R}{\frac{N_R}{N}}\right) \tag{2.7}$$

where:

- $\bar{D}_D$ = the mean Democratic vote share in Democratic-leaning districts,
- $\bar{D}_R$ = the mean Democratic vote share in Republican-leaning districts,
- N_D = the number of Democratic-leaning districts,
- N_R = the number of Republican-leaning districts,
- N = the total number of districts.

Warrington, who developed the declination metric, advocates for it due to its independence from district shapes, computational simplicity, and strong theoretical basis in cracking and packing [123, 124]. Unlike the efficiency gap, it avoids constitutional concerns related to vote weighting. However, he acknowledges its limitations and emphasizes that no single metric can fully capture gerrymandering. Consequently, a comprehensive approach—combining multiple measures—is necessary. For this reason, declination, efficiency gap, and mean-median difference are all calculated during GerrySort simulations to assess the partisan fairness of electoral maps.

2.1.6.4 Competitiveness

For this thesis, competitiveness is captured using a single score per district, due to two practical constraints: first, it is not feasible within the model to produce a large dataset of electoral outcomes for each district; and second, generating large ensembles of alternative maps would be computationally too expensive given the scope of the simulations. Therefore, a simple, intuitive measure is used:

$$\text{Competitiveness Score} = 1 - \frac{|D - R|}{N} \tag{2.8}$$

where:

- D = the number of Democratic voters in the district,
- R = the number of Republican voters in the district,
- N = the total number of voters in the district.

This formulation ensures that districts with an even balance between Democratic and Republican voters score highest on competitiveness, while districts dominated by one party score lower. By aggregating these scores across all districts in a map, the model can assess the overall competitiveness of the redistricting plan in a consistent and interpretable way.

2.1.6.5 Compactness

For this thesis, the compactness of districts is measured using the Polsby-Popper score. This choice is motivated by two considerations: first, the need for a computationally efficient metric that can be easily applied across many simulations, and second, the widespread recognition and interpretability of the Polsby-Popper score in both academic and legal settings. The Polsby-Popper score is defined as:

$$\text{Polsby-Popper} = \frac{4\pi A}{P^2} \tag{2.9}$$

where:

- A = the area of the district (in square miles),
- P = the length of the perimeter of the district (in miles).

This score ranges from 0 to 1, with 1 indicating a perfectly compact (circular) district, and values closer to 0 reflecting irregular shapes.

While the Polsby-Popper method is simple and scale-invariant, it is not without limitations. It tends to penalize districts with natural geographic boundaries (such as rivers, coastlines, or mountains), which may naturally produce irregular perimeters unrelated to partisan intent. It is also sensitive to small boundary variations, meaning that minor geographic or technical changes can cause notable shifts in the score [26]. Despite its limitations, the Polsby–Popper score remains a suitable choice for this study due to its simplicity, ease of interpretation, widespread use in redistricting research, and crucially, its continued use by mapmakers [27, 107, 112, 114].

2.1.7 Computational Redistricting

Computational redistricting is a research field dedicated to designing computer algorithms for drawing or optimizing political district boundaries. The primary objective is to create electoral districts that are fair, representative, and compliant with legal requirements. Typically, these algorithms consider factors such as population size, geographical contiguity, compactness, and community cohesion, whilst aiming to prevent boundary manipulation for political advantage. The overarching goal of computational redistricting is to diminish the influence of partisan bias in the creation of electoral maps, fostering transparency and fairness in the democratic process.

Since the 1960s, scholars have advocated for computational approaches to enhance the transparency, objectivity, and impartiality of redistricting [70–73]. However, critics have voiced concerns that automated redistricting might empower state legislators to create more precise and aggressive gerrymanders to achieve partisan goals [74]. Despite increased exploration and utilization of automated redistricting by legislators between 1980 and 2000, computational limitations and associated costs have limited its significant impact on redistricting during these cycles [127]. During this era, scholars not only focused on designing algorithms to eliminate unfairness but also designed algorithms to assess whether a map adhered to criteria aimed at mitigating gerrymandering [16, 75, 110, 128].

Recent advancements in computational capabilities, coupled with the increased availability of large datasets containing detailed information on the electorate and election outcomes, have sparked a renewed interest in computational approaches for addressing redistricting challenges. Present-day scholars seek to leverage the power of computation to address three key questions: How can fair electoral maps be created? How can partisan bias be quantified? And what is the impact of gerrymandering on factors such as electoral outcomes, competition, and polarization? The question of quantifying and detecting gerrymandering is particularly intriguing, given the absence of a judicial standard recognized by the Supreme Court. However, simulation-based methods have been presented to state courts in recent years, with varying degrees of success [68].

Contemporary computational techniques are designed to generate representative samples of redistricting plans that adhere to criteria, including contiguity, population parity, and compactness. These ensembles of generated maps can be employed to identify fair proposals by assessing them against specific quantification metrics. Alternatively, they can be used for outlier analysis, determining where an enacted or proposed plan ranks among the ensemble according to quantification metrics. Over the past couple of decades, scholars have proposed various methods and algorithms to generate plans, which can be categorized into three main groups: optimization, assembly, and random walks methods [129].

> **Optimization** approaches seek to find a single map that is the best according to user-defined criteria. Algorithms in this category maximize or minimize specific objective functions gauging plan properties while adhering to constraints. Typically, these objective functions include criteria such as maintaining contiguity and population balance across districts while seeking to enhance "compactness" [130, 131]. Common techniques include using Voronoi or power diagrams in tandem with some variation of k-means [132–136]. These methods combine the geometric proximity considerations from a diagram with the clustering capabilities of k-means to create district plans that balance population distribution and potentially other factors like contiguity or compactness criteria. Other scholars have explored integer programming [137] and partial differential equations [138] to find optimal district plans.
>
> **Assembly** algorithms create an ensemble of plans by generating each map through a randomized process from scratch [65, 78, 79, 139]. These algorithms use a greedy food-fill (agglomerative) strategy, iteratively adding geographic units to districts based on criteria and then merging adjacent districts. This approach starts from k random choices among geographical units as district seeds, growing outwards by adding neighboring units until the jurisdiction is filled up. If the plan is not

valid according to the user-defined criteria, the plan is discarded, and the algorithm restarts from scratch. Assembly algorithms aim to produce diversity, unlike optimization algorithms, which strive to find a single best example.

Random walks approaches use a step-by-step modification procedure, starting from an initial plan and incrementally transforming it to obtain an ensemble of maps. The most common random walk method include Markov chain Monte Carlo (MCMC) techniques [82, 84, 104, 114, 140–142]. MCMC methods generate a sequence of samples from a probability distribution to approximate its properties. In redistricting, MCMC can sample from the space of potential district plans based on specified criteria. Scholars have also proposed evolutionary [77, 143] and Sequential Monte Carlo [105] approaches.

As previously mentioned, these algorithms can be utilized to eliminate unfairness in the redistricting process by computationally generating a diverse set of proposals that adhere to specific criteria. Alternatively, scholars have undertaken outlier analyses of enacted plans in various states [75, 77–79, 81, 82, 84, 85]. Moreover, these ensemble generation techniques have been utilized by researchers to assess the impact of gerrymandering on electoral outcomes [80, 86], electoral competition [14, 15, 83], polarization [76], and gerrymandering reforms [90]. The resurgence of this field has prompted the development of open-source software tools [144–147]. These resources are designed to offer citizens and legislators redistricting tools that enable the easy generation of an ensemble of district plans based on demographic data. Additionally, users can assess proposed or enacted plans according to specific metrics and access rich datasets effortlessly.

To incorporate gerrymandering into GerrySort, the open-source Python library GerryChain [145] will be used to generate electoral maps throughout the simulation. GerryChain employs a MCMC method to produce district maps that satisfy the contiguity and population balance constraints. A key advantage of this library is its ability to guide the MCMC process using a customizable optimization function. In GerrySort, this function will be leveraged to generate gerrymandered maps or optimize redistricting criteria such as compactness or competitiveness.

2.2 Geographical Partisan Sorting

In the post-Cold War era, there has been a noticeable increase in Americans aligning their political loyalty with the party that reflects their ideological beliefs [148]. This phenomenon, known as ideological partisan sorting, has seen liberals gravitating toward the Democratic party and conservatives aligning more closely with the Republican party.

Currently, this alignment extends beyond individual preferences and is evident in the spatial distribution of partisans across all levels of American society [57]. One rationale for this shift is the growing polarization and the integration of party affiliation into personal identity, leading to the phenomenon known as geographical partisan sorting, wherein the American electorate is progressively becoming spatially segregated based on political affiliations [52].

Geographical partisan sorting (from here on referred to as partisan sorting) is characterized by individuals with similar political beliefs or partisan affiliations clustering together in specific geographic areas. This clustering often results in the formation of politically homogeneous communities or regions, where residents share similar ideologies and voting patterns. The concept of partisan sorting gained prominence through William Bishop's book *The Big Sort: Why the Clustering of Like-Minded Americans is Tearing Us Apart* [52, 54–56, 58]. Bishop argued, supported by data analyses, that Americans are increasingly sorting themselves into highly homogeneous communities, not just by region or state but down to the city and neighborhood level. The outcome is a polarized nation where people struggle to understand those living only a few miles away. While this sparked scholarly debate, no consensus has emerged. Some argue that residential partisan sorting has been ongoing for decades and is on the rise, while others dismiss it as a myth.

An early study suggested that migrants tend to move into congressional districts aligning with their ideological preferences [149]. However, this study had limitations, as it was based on a dataset with a short time frame. Subsequent studies, conducted with more extensive datasets spanning at least a couple of decades, have consistently found similar results [54–56, 58]. Interestingly, these studies indicate that geographical partisan sorting began to emerge around 1996. An examination of the increasing geographic divide proposed two mechanisms driving this phenomenon [64]: "inadvertent sorting", where people prefer residential environments correlated with partisanship, and "intentional sorting", where people consider partisanship directly.

The initial study, challenging the prevailing media narrative that suggested increasing political segregation in the U.S., argued that most Americans still reside in electorally competitive areas and maintain substantial exposure to members of the other party [59]. In response, Bishop critiqued this study's analyses and conclusions in the same journal [150]. A subsequent historical analysis contended that partisan segregation is one of the "myths of American political geography" [60]. However, this study lacked empirical data, making it potentially speculative. Stanford University scholars conducted subsequent studies explicitly countering Bishop's Big Sort hypothesis. One study emphatically concluded that there is no evidence of geographic partisan sorting, and if present, its effects are exaggerated by Bishop and his supporters [53]. Another study extensively analyzed the reasons for Americans' relocations, determining that partisanship or politics does not significantly influence these decisions [61]. A recent study proposed an alternative hypothesis, suggesting that Americans seem to be sorting based on non-political neighborhood attributes that correlate with partisan preferences, rather than actively seeking politically congruent neighbors [62]. In essence, one's partisanship may not be the primary driver of geographic partisan sorting.

The debate's core tension may lie in the interplay between inadvertent and intentional sorting. Supporters of the Big Sort hypothesis have noted a growing trend since 1996 but haven't delved into the reasons behind this phenomenon. Inadvertent and intentional sorting could be the underlying factors at play. Detractors have concentrated on the motivations behind migration, asserting that political factors have a negligible role. However, this doesn't negate the existence of the trend; rather, it emphasizes their belief that intentional sorting is not a significant driving force.

2.2.1 "Unintentional Gerrymandering"

The exploration of the connection between geographic partisan sorting and redistricting was initially undertaken by Chen and Rodden [65]. Their objective was to shed light on the impact of human geography on U.S. electoral bias, employing automated simulations. Using Florida as a case study, a state where Democrats are typically concentrated in urban areas while Republicans are more dispersed across rural areas, the authors simulated the outcome of state legislative and Congressional districts using precinct level data of the 2000 presidential election. They used equal population, contiguity and compactness as the criteria to generate an ensemble of Congressional and state legislative district plans, aiming for "fair" electoral maps. The results revealed that even these ostensibly fair maps could display partisan bias without intentional gerrymandering. The authors attribute this phenomenon to human geography, explaining that two-party winner-take-all district-based elections favor dispersed electorates across a specific territory. In the context of the U.S., they illustrate that pro-Republican bias can be significant even without intentional gerrymandering, particularly in states where Democratic voters are more concentrated geographically than their Republican counterparts. The term "unintentional gerrymandering" was introduced by the authors to characterize the impact of geographic patterns on redistricting. This type of gerrymandering underscores how political geography can reshape a party's fortunes, as seen in the case of Florida Democrats. Despite consistently leading in statewide registration and presidential voting, the party finds itself resembling a permanent minority in the legislative arena.

In the subsequent years, limited research has delved into unintentional gerrymandering. One undergraduate proposed potential solutions to alleviate the adverse effects of unintentional gerrymandering [87]. Another thesis, carried out by a postgraduate researcher, sought to measure population shifts by utilizing the efficiency gap to compare wasted votes in rural and urban districts [88]. A recent and noteworthy study employed an ensemble map generation technique, akin to Chen and Rodden's approach, to investigate whether geographical partisan sorting or intentional partisan gerrymandering is the cause of the discrepancies between the electorate's partisanship and the party distribution in the U.S. House [89]. Their findings revealed that while demographic clustering is significant, redistricting procedures play a much more substantial role in generating partisan bias in the House.

2.2.2 Quantifying Segregation

To evaluate the extent of partisan segregation and assess how it changes over time due to geographic sorting, it is necessary to quantify segregation using spatial statistical methods. These measures allow for a systematic comparison of segregation levels before and after voter movement occurs in the model. In this research, segregation is quantified using both a global and a local measure of spatial autocorrelation: Global Moran's I and Anselin Local Moran's I. These analyses were conducted using the software ArcGIS Pro, and the input variable used in both cases is the Democratic vote share at the precinct level.

2.2.2.1 Global Moran's I

Global Moran's I is a commonly used indicator of spatial autocorrelation, which captures the overall degree to which similar values cluster across space [151]. In the context of this research, it provides a summary statistic for the extent of partisan segregation across all precincts in a state. A high positive value of Moran's I suggests that precincts with similar Democratic vote shares tend to be spatially clustered, while a negative value would indicate a spatial pattern in which dissimilar precincts are adjacent to one another. The statistic is calculated as follows:

$$I = \frac{n}{W} \frac{\sum_{i=1}^{n} \sum_{j=1}^{n} w_{ij}(x_i - \hat{x})(x_j - \hat{x})}{\sum_{i=1}^{n}((x_i - \hat{x})^2} \tag{2.10}$$

where:

- n = the number of spatial units (precincts),

- x_i = the Democratic vote share in precinct i,
- $\hat{x}$ = the mean state-wide Democratic vote share,
- w_{ij} = a spatial weight between precincts i and j,
- W = the sum of all spatial weights[16].

A key strength of Moran's I is that it offers a single interpretable value to summarize overall spatial patterns, which is useful for comparing levels of segregation before and after sorting. However, it does not provide information about where in the state clustering occurs. Furthermore, the results of spatial autocorrelation analyses are sensitive to the choice of spatial weights matrix, which complicates comparisons across states. Differences in the shape, size, and density of spatial units mean that a uniform approach—such as using a k-nearest neighbors matrix (e.g., k = 8)—may yield inconsistent results. For example, what constitutes a close neighbor in a dense urban area may represent a much greater distance in a rural region. These structural differences can introduce bias or artifacts, undermining the validity of cross-state comparisons.

2.2.2.2 Anselin Local Moran's I

While Global Moran's I offers a summary measure of segregation, Anselin Local Moran's I provides a way to identify spatial clusters and outliers at the level of individual precincts [152]. It decomposes the global statistic into local contributions, allowing for the visualization of patterns of segregation across space. In this study, Local Moran's I is used to create cluster maps that identify specific spatial patterns of partisan preference. Four key cluster types are distinguished: high-high clusters represent Democratic enclaves, where precincts with high Democratic vote shares are surrounded by similar precincts; low-low clusters indicate Republican enclaves, where precincts with low Democratic vote shares (i.e., high Republican support) are adjacent to similar Republican-leaning areas. The measure also identifies low-high outliers, where a Republican precinct is surrounded by Democratic precincts, and high-low outliers, where a Democratic precinct is surrounded by Republican ones. This classification enables a more nuanced, spatially explicit understanding of how partisan sorting reshapes the political geography over time. The Local Moran's I for precinct i is computed as:

$$I_i = \frac{(x_i - \hat{x})}{m^2} \sum_{j=1}^{n} w_{ij}(x_j - \hat{x}) \tag{2.11}$$

[16]The spatial weights matrix defines which precincts are considered neighbors, typically based on contiguity or distance thresholds.

where:

- $m^2 = \frac{1}{n}\sum_{j=1}^{n}(x_j - \hat{x})$

To identify only statistically meaningful clusters, permutation testing is used to assess the significance of each precinct's Local Moran's I value. This involves comparing the observed I_i to a reference distribution generated under the null hypothesis of spatial randomness. Precincts that do not show significant spatial autocorrelation are excluded from the cluster map. Together, Global Moran's I and Anselin Local Moran's I offer complementary insights into partisan segregation: while the global measure captures the overall degree of spatial clustering, the local measure reveals where and how segregation manifests across the state, allowing for a detailed comparison of spatial dynamics before and after partisan sorting.

Chapter 3

Model Description

In this chapter, GerrySort, the model designed to answer the research questions outlined in Chapter 1 will be presented. This will be structured following the ODD+D protocol, which is commonly used to describe agent-based models [153–155].

3.1 Overview

3.1.1 Purpose

The main goal of this thesis is to explore the relationship between gerrymandering and partisan sorting. The model is based on the premise that both redistricting policies and partisan migration patterns contribute to the fairness, competitiveness, and compactness of electoral maps [12–15, 65]. Research has shown that partisan gerrymandering can significantly distort representation [8–11], while partisan segregation can cause partisan biases even in the absence of deliberate gerrymandering [65]. By developing a model that can simulate each process independently or in combination, it enables systematic analysis of how these dynamics interact under varying conditions. In particular, it allows for investigation into how patterns of partisan migration either amplify or mitigate partisan bias in congressional maps, both when mapmakers engage in partisan gerrymandering and when they follow neutral redistricting rules. Additionally, the model offers insights into which aspects of a state's political geography contribute to the structural biases introduced by partisan sorting.

A secondary goal is to evaluate the efficacy of two redistricting reforms—competitive and compactness criteria—by measuring their impact on the partisan fairness of electoral maps in both the presence and absence of partisan sorting. This analysis aims to understand whether such reforms can counteract the distortions caused by either partisan gerrymandering or partisan sorting, or whether their effectiveness is conditional on the political geography of a state.

To achieve these objectives, six experiments are designed to systematically address the sub-research questions. By adjusting the model's parameters, the simulations can represent a wide spectrum of electoral and demographic conditions, enabling the exploration of diverse redistricting scenarios. These experiments examine not only the isolated effects of gerrymandering and partisan sorting, but also their combined impact on electoral outcomes. By incorporating geographical partisan sorting, the model allows for the identification of conditions under which "unintentional gerrymandering" arises. Furthermore, the results will provide insights into whether implementing competitiveness and compactness criteria can meaningfully reduce partisan bias in redistricting, even as partisan residential segregation remains stable or intensifies. These findings contribute to the broader scholarly discourse on the concept of unintentional gerrymandering by offering empirical insight into how and when partisan residential patterns affect redistricting practices. Additionally, they provide valuable evidence for policymakers and reform advocates in assessing whether competitiveness and compactness criteria can serve as effective safeguards against the adverse effects of both partisan gerrymandering and geographically driven partisan bias.

3.1.2 Entities, State Variables, and Scales

The model contains four entities, each characterized by unique attributes that evolve during a simulation run. These entities represent core components of the U.S. electoral system and mimic their behavior and interactions. The components can be grouped into two categories: *individual agents* and *geographical units*. The individual agents represent the electorate of a given state. These agents are able to move around the state and affect the election results in their electoral district. The geographical units are spatial agents that represent the geographical components of the modeled state's electoral system (e.g. voting precincts, electoral districts). The boundaries of these units are initialized with the real-world boundaries of a given state as of 2020. Only in the case of the congressional districts, are the boundaries subject to redistricting, and thus evolve over simulation. The following sections will describe the actions and attributes of the four model entities, the individual agents, and the three geographical units, along with their function within the model.

3.1.2.1 Entities and State Variables

Individual agents represent the voting population within the modeled state. At each time step, they evaluate their living conditions and determine whether to relocate based on their personal utility score. An agent considers moving only if their utility falls below a user-defined threshold. Utility calculations incorporate both precinct-level and county-level factors (as detailed in Sections 3.1.3.2 and 3.2.2). A full description of all of the individual agent's attributes is provided in Appendix A.1.

Redistricting applies to multiple electoral maps, including congressional, state house, and state senate *districts*. However, in GerrySort, redistricting is only performed at the congressional level due to its national significance. Congressional elections receive greater attention and funding, as they influence the balance of power in the U.S. Congress. Additionally, limiting redistricting to congressional districts improves computational efficiency, as generating three separate maps—especially those with a larger number of precincts—would significantly increase computational costs. At each time step, district boundaries are redrawn either to benefit the party in control, defined as the party that won the majority of congressional districts in the previous election, or, in cases of divided legislative power, to produce "fair" maps (as detailed in Section 3.1.3.2). The attributes of congressional districts are described in Appendix A.2.

Precincts are the smallest geographical units in a state's electoral system, each containing a designated polling station where residents cast their votes. In the model, precincts play a crucial role in agent relocation. Their small size enables them to represent an agent's immediate neighborhood and exact living location, helping assess whether an agent's direct surroundings align with their political affiliation. When agents consider moving, a sample of precincts is drawn randomly, and they evaluate these potential new locations based on their associated utility scores (as detailed in Section 3.2.2). The attributes of precincts are described in Appendix A.3.

Counties are larger geographical units composed of multiple precincts, serving as administrative subdivisions of a state with defined boundaries and varying degrees of governmental authority. Like precincts, counties play a key role in the model's relocation process. When considering potential new locations, agents evaluate both precinct- and county-level attributes (as detailed in Section 3.2.2). Incorporating counties into the model was essential for integrating additional geographic and demographic data (e.g. Rural-Urban Commuting Area codes, number of households), as this was the smallest scale at which such data was available. Counties also represent the broader regional context of an agent's residence, helping determine whether their surrounding community aligns with their political affiliation. The attributes of counties are described in Appendix A.4.

3.1.2.2 Spatial and Temporal Scales

The model operates at three spatial levels: precincts, counties, and congressional districts. Precincts serve as the smallest spatial units, representing both the specific residential locations where agents can relocate and their immediate neighborhood, which influences whether their surroundings align with their political affiliation. Counties provide additional demographic data for agent utility calculations, such as Rural-Urban Commuting Area (RUCA) codes and capacity constraints, and represent a broader regional context that affects an agent's perception of neighborhood political alignment. Congressional districts define the electoral boundaries subject to redistricting, shaping the overall structure of the electoral map. The model's spatial extent includes four swing states—GA, WI, MI, and PA—with all calculations performed in the EPSG:5070 (NAD83 / Conus Albers) coordinate reference system. This Albers Equal Area projection is optimized for the contiguous U.S., minimizing area distortion, making it particularly well-suited for analyzing compactness in electoral maps.

Each time step in the model corresponds to one redistricting cycle, equivalent to 10 years. The model runs for a user-defined number of time steps, with all experiments conducted over four time steps to capture long-term trends in partisan sorting and redistricting effects. The model operates in discrete time, with redistricting, agent movement, and elections occurring sequentially within each step. Redistricting takes place at the beginning of each time step, immediately reshaping the congressional map. This is followed by agent relocation, where individuals adjust their residence based on political preferences, and finally, elections, which determine the party in control for the next redistricting cycle.

3.1.3 Process Overview and Scheduling

GerrySort models both the redistricting process and geographical partisan sorting, simulating their individual and combined effects on the partisan fairness of congressional maps over multiple time steps. This section outlines the model's scheduling, structured into two key phases: the initialization procedure and the model's main processes that occur at each timestep. A visual representation of the scheduling flow is provided in Figure 3.1.

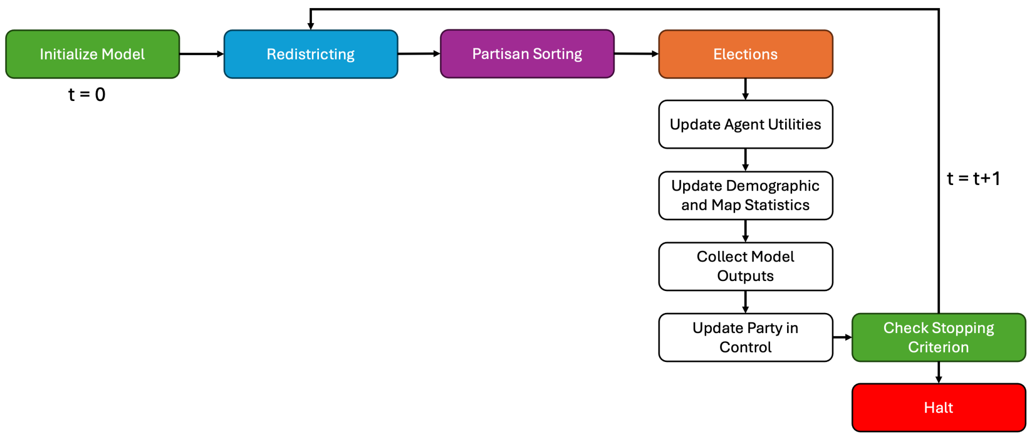

FIGURE 3.1: Flowchart of processes in GerrySort.

3.1.3.1 Initialization Procedure

The initialization phase sets up the model by establishing its geographical and demographic structure based on user-defined parameters, as detailed in Table 3.1[1]. The procedure involves the following steps:

Loading Input Data The model begins by loading a GeoJSON file containing precinct-level polygons along with geographic and demographic attributes used to initialize the congressional map of the selected U.S. state. This dataset combines information from multiple sources solely for initialization purposes. It includes, for instance, presidential election results per precinct to determine the Republican-to-Democrat ratio, as well as each precinct's corresponding county and congressional district. Additionally, county-level RUCA codes are used to simulate partisan residential preferences, reflecting Republicans' tendency toward rural areas and Democrats' preference for urban centers. Figure 3.2 illustrates the RUCA codes by county. A full description of the dataset and its construction is provided in Section 3.3.2.

Entity Initialization After loading the input data, the model initializes the three geographical entities: precincts, counties, and congressional districts. The attributes of these geographical units are derived from real-world data. For instance, county-level demographic data, such as total households and average persons per household, are used

[1]An overview of other model parameters is provided in Table A.5.

Parameter	**Symbol**	**Type**	**Range**	**Description**
`max_iters`	$T_{\max}$	Int	≥ 1	Maximum number of simulation steps.
`npop`	N	Int	≥ 100	Total number of agents.
`tolerance`	T	Float	$[0, 1]$	Happiness threshold of agents.
`beta`	β	Float	$[0.0, 100.0]$	Degree of randomness in agent decisions.
`ensemble_size`	E_S	Int	≥ 1	Number of redistricting maps generated.
`epsilon`	ϵ	Float	$[0.0, 1.0]$	Max population deviation from ideal district size (fraction).
`sigma`	σ	Float	$[0.0, 1.0]$	Std. dev. of noise added during redistricting optimization.
`n_moving_options`	M_O	Int	≥ 1	Number of alternative precincts considered for relocation.
`distance_decay`	D_D	Float	$[0.0, 1.0]$	Influence decay factor on utility of potential moving spot based on relocation distance.
`capacity_mul`	C_M	Float	$[0.9, 2.0]$	Multiplier adjusting county population capacity.

TABLE 3.1: Overview of main model parameters.

to estimate the county's capacity. Similarly, the population count per precinct is used to create a probability distribution for placing agents within a county. The boundaries of these geographical units are based on their real-world counterparts in 2020.

Once the geographical units are initialized, individual agents are placed in their initial living location—precincts—using real-world county population shares. The initial number of agents per county is calculated as follows:

$$N_C = C^{pop\_share} \times N \tag{3.1}$$

where:

- N_C = the initial number of agents in the county,
- C^{pop_share} = the real-world population share of the county relative to the total state population,

- N = the total number of agents.[2]

Once N_C is determined, the county capacity is estimated to ensure that counties cannot hold an infinite number of agents. The capacity is imposed at the county-level, rather than the precinct level, because the necessary demographic data to estimate capacity is not readily available at the precinct level. The capacity of each county is calculated as follows:

$$C_{capacity} = \frac{C^{housing\_units} \times C^{household\_size}}{C^{tot\_pop}} \times N_C \times C_M \tag{3.2}$$

where:

- $C^{housing\_units}$ = the real-world number of housing units in the county,
- $C^{household\_size}$ = the real-world average household size in the county,
- C^{tot_pop} = the real-world total population of the county,
- C_M = the model's capacity multiplier parameter (defaults to 1).

Once the total number of agents in a county and the county's capacity are defined, agents are assigned to precincts within the county based on a probability distribution that is proportional to the total population of each precinct. Each agent's political affiliation is determined by the 2020 presidential election results for the precinct they are assigned to. A random number, generated using `random.random()`, is compared to the precinct's Republican vote share. If the random number is less than or equal to the Republican vote share, the agent is assigned as a Republican voter; otherwise, the agent is assigned as a Democrat.

Initial Elections Once all entities are initialized, the model calculates the initial election outcomes for all geographical units. This involves setting the `color`[3] attribute of each geographical unit to the party that holds the majority of agents in that unit. Updating these majorities is crucial for calculating agents' utility and determining which party has control over the redistricting process in the first time step. The `color` attribute is subsequently updated at the end of each model step to reflect the evolving political landscape. Figure 3.3 shows the average initial election outcomes across the counties and congressional districts.

[2] The calculation of N_C is based on $N = \{\mathrm{GA} \mapsto 11000, \mathrm{WI} \mapsto 5900, \mathrm{MI} \mapsto 10000, \mathrm{PA} \mapsto 13000\}$, which represent their real-world population counts divided by 1000.

[3] "Red" indicates that the geographic unit has a Republican majority, while "Blue" signifies a Democratic majority.

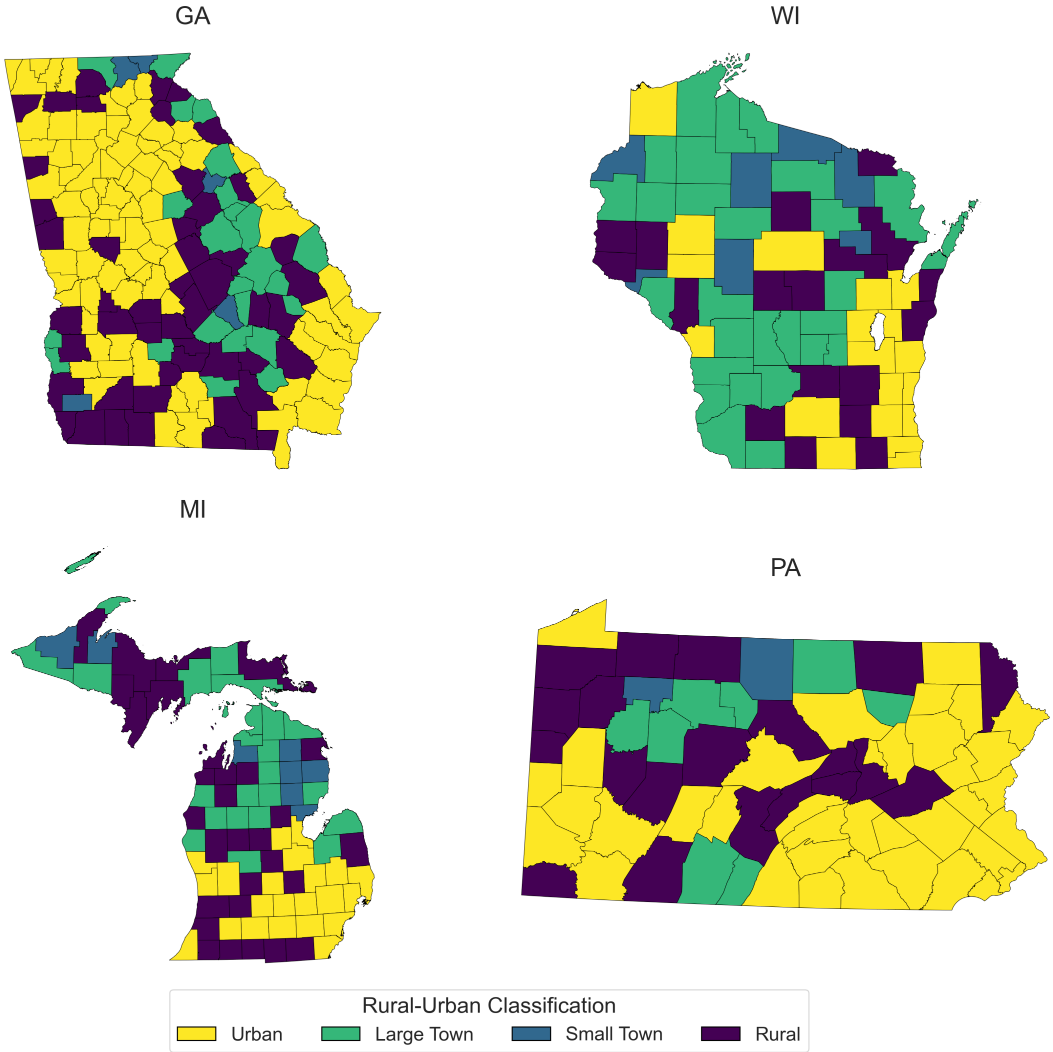

FIGURE 3.2: Rural–Urban Classification (RUCA) codes of counties in each state, based on four categories: Rural, Small Town, Large Town, and Urban.

Initial Utility Calculation After establishing the majorities in each geographical unit, the agents' utility scores are computed based on the political alignment of their surroundings (as formulated by Eq. 3.5 in Section 3.2.2). This score indicates how satisfied agents are with the political composition of their living area, with agents preferring to reside in areas where the majority of residents share their party affiliation, along with having preferences for either rural or urban neighborhoods. Agents with utility scores below a user-defined threshold (T) are flagged as dissatisfied and will consider relocating during the simulation.

Initial Redistricting Control The party in control of redistricting at $t = 0$ is determined by the congressional election results determined during initialization the model. The party with the majority of congressional seats assumes control of the redistricting process. It is important to note that this simplification does not mirror real-world

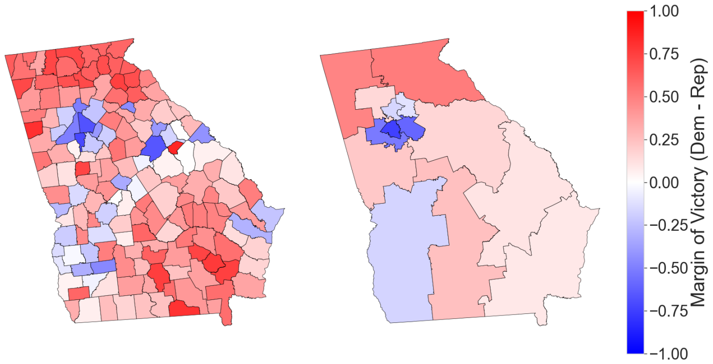

(A) GA

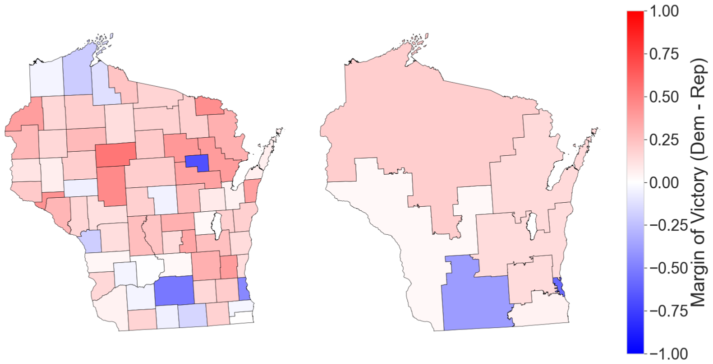

(B) WI

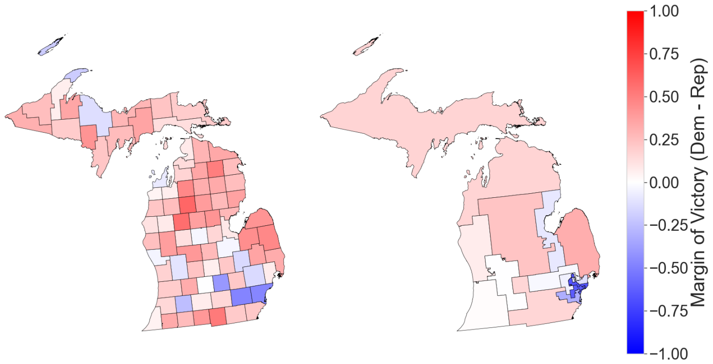

(C) MI

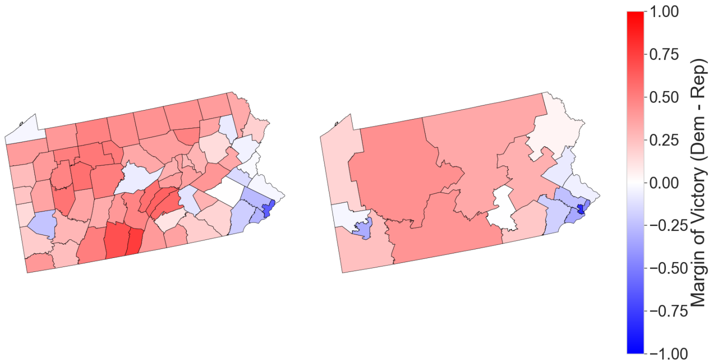

(D) PA

FIGURE 3.3: Partisan margins of victory after initialization in each state, shown at both the county and congressional district levels. Results are averaged over 100 simulation runs and reflect the initial spatial distribution of Democratic and Republican voters in the model.

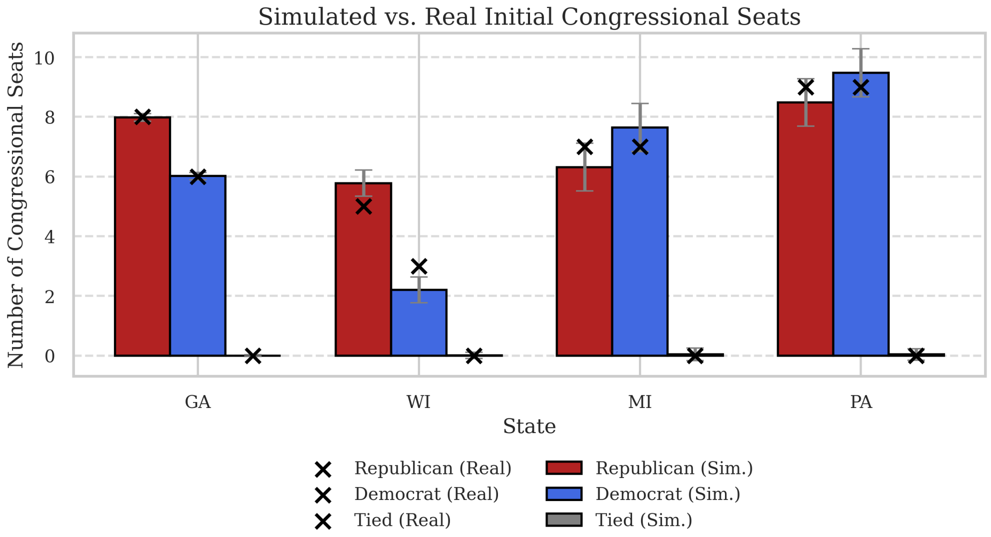

FIGURE 3.4: Simulated versus real-world congressional seat distributions after initialization for GA, WI, MI, PA. Colored bars represent the mean number of Republican, Democrat, and tied seats across 10,500 simulation runs per state, with standard deviations shown as gray error bars. Black × markers indicate the corresponding seat outcomes from the 2020 U.S. House elections.

processes, where the party controlling the state legislature typically holds redistricting power. The decision to model redistricting control based on congressional outcomes is made for computational efficiency, as incorporating state-level legislative control would require redistricting at those levels as well, introducing complexity that would make efficient simulation difficult. However, it is worth noting that a current congressional majority often correlates with the current state legislative majorities in the state house and state senate [156, 157]. In the four states modeled, MI and PA have seen relatively balanced partisan control in both their state House and Senate over the past five years, whereas in GA and WI, Republicans have maintained a consistently strong hold on both legislative chambers [157–159]. Figure 3.4 shows the modeled initial distribution of congressional seats per party. It illustrates which party typically has control over redistricting in the $t = 0$, as well as how the modeled seat allocation compares to the real-world 2020 seat distribution.

Initial Model Statistics Lastly, various model statistics, such as demographic statistics, partisan fairness measures, and average competitiveness and compactness, are calculated and collected at the end of the initialization phase and at each subsequent time step. These results are used for testing, understanding, and analyzing the behaviors of the model. A detailed description of these statistics and their purposes is provided in Section 3.2.8. Figure A.1 in Appendix A.3, presents the initial scores for the measures used to assess the partisan fairness, compactness, and competitiveness of the congressional electoral map (described in Section 2.1.6).

3.1.3.2 Main Processes

After initialization, the model advances through iterative time steps, each consisting of three main processes: *redistricting*, *partisan sorting*, and *elections* (Fig. 3.1). First, the congressional district boundaries are redrawn, either through partisan gerrymandering favoring the controlling party or through a neutral redistricting process in cases where congressional seat distribution is tied. Next, agents evaluate their surroundings and may choose to relocate to areas with a higher concentration of like-minded individuals, simulating geographical partisan sorting. Finally, elections are conducted to determine the distribution of political power, which in turn dictates which party will control redistricting in the next time step. Each of these processes is further detailed in the following sections:

Redistricting The first process in each model time step is redistricting. The party in control redraws the congressional districts to maximize its partisan advantage based on the spatial distribution of agents at that moment. This is done using the Python library GerryChain, which enables the generation of random redistricting plans or optimized maps based on specific criteria [145]. GerryChain provides three algorithms for this purpose: *short bursts*, *tilted runs*, and *simulated annealing* [129, 160].

To determine the most effective algorithm for GerrySort, an experiment was conducted comparing these built-in methods against a custom approach. The custom method generated a fully random ensemble of redistricting plans and then selected the map that yielded the maximum number of seats for the controlling party. In contrast, the built-in algorithms iteratively optimized redistricting plans based on a predefined metric. The experiment tested each method across different ensemble sizes in two states, with the Democratic Party fixed as the controlling party. The results, shown in Figure A.3 in Appendix A.3, indicate that all methods tend to improve with a larger ensemble size. In WI, the mean and standard deviation of the efficiency gap for all methods showed little variation. In GA, however, the random method performed the worst, while the short bursts and tilted runs methods yielded similar results. Ultimately, the tilted runs method was selected for GerrySort, with a default ensemble size of 250. This method was chosen because it required fewer parameters—only the number of runs—whereas short bursts required both the number of bursts and burst length. The ensemble size was set to 250 as a balance between computational efficiency and performance; while larger ensembles slightly improved the partisan advantage, the increase was marginal compared to the additional computational cost.

The selection of the tilted runs method requires defining an optimization function to generate redistricting plans that maximize partisan bias when either the Republican or Democratic Party controls redistricting. Additionally, a neutral function is needed in cases of a tie. The optimization function used to create the most gerrymandered map is defined as follows:

$$\mathcal{O}(x) = \begin{cases} \frac{1}{|\mathcal{D}(x)|} \sum_{i \in \mathcal{D}(x)} 1\left(N_R(i) > N_D(i)\right) + \varepsilon, & \text{if } P = R \\ \\ \frac{1}{|\mathcal{D}(x)|} \sum_{i \in \mathcal{D}(x)} 1\left(N_D(i) > N_R(i)\right) + \varepsilon, & \text{if } P = D \end{cases} \tag{3.3}$$

where:

- P = the party in control of redistricting, with R for Republicans and D for Democrats,
- $\mathcal{D}(x)$ = represents the set of all districts in the proposed redistricting plan x,
- $1(\cdot)$ = the indicator function, which equals 1 if the condition is true and 0 otherwise,
- $N_R(i)$ and $N_D(i)$ = denote the number of Republican and Democratic agents in district i,
- $\varepsilon \sim \mathcal{N}(0, \sigma)$ = a stochastic error term that introduces randomness into the redistricting process to reflect uncertainty and variability in decision-making.

In the case of a tie, the optimization function aims to find the "fairest" map, defined as one with a seat share closest to the state-wide presidential election results. The optimization metric that is minimized is given by:

$$\mathcal{O}(x) = \left| \frac{1}{|\mathcal{D}(x)|} \sum_{i \in \mathcal{D}(x)} 1\left(N_D(i) > N_R(i)\right) - \frac{N_D}{N_D + N_R} \right| \tag{3.4}$$

where:

- N_R and N_D = the total counts of Republicans and Democrats across the model, respectively.

Once a new map is generated, the boundaries of the congressional districts are updated for visualization. Additionally, any precincts reassigned to a new district are updated in the precinct-district map. This map facilitates the efficient calculation of election results across all districts by tracking the number of Republicans and Democrats in each precinct within a specific district. For an overview of the redistricting procedure, refer to the pseudocode in Appendix A.3, Algorithm 1.

Partisan Sorting After redistricting is complete, agents whose utility falls below the threshold T (i.e., the unhappy portion of the population) have the opportunity to relocate. Each unhappy agent considers a set number of options, determined by the user-defined parameter M_O. For each agent, M_O random counties that have not yet reached full capacity are selected. From these, a precinct is chosen using the same probability distribution that was used to assign the agent's initial location. Relocation decisions are made at the county level rather than the precinct level because capacity constraints are enforced per county. This approach is computationally more efficient: selecting counties that are not full avoids the need to repeatedly draw random precincts only to discard them if their county is at capacity. Note that the same county can be selected multiple times, with different precincts drawn from it. The agent evaluates each potential relocation precinct, including their current precinct, by calculating the utility score for each option. Further details on the utility calculation and the decision-making process are provided in Section 3.2.2. Once all unhappy agents have made their relocation decisions, the partisan sorting process concludes. These decisions are made sequentially, with the order of agents randomized at each time step to avoid systematic bias in movement patterns.

Elections The final step in each time cycle is the election process, which determines which party gains control over redistricting in the next step. This involves updating the majority party in each precinct, county, and congressional district based on the agents' current distribution. Precinct and county majorities are used to assess whether an agent's immediate and broader neighborhood aligns with their political affiliation, while congressional district majorities determine which party will control redistricting in the following cycle. After updating majorities, the model recalculates key statistics, including measures of partisan fairness, average competitiveness, and average compactness of the electoral map. A detailed description of all of the tracked statistics and their purpose is provided in Section 3.2.8. Finally, the model checks whether the maximum number of iterations ($t = T_{max}$) has been reached. If this condition is met, the simulation ends. If not, the time step is incremented ($t = t + 1$), and the main processes are repeated.

3.2 Design Concepts

3.2.1 Theoretical and Empirical Background

The design of the GerrySort model is grounded in two key concepts: gerrymandering and geographical partisan sorting. At the system level, the model captures the dynamic relationship between how voters are geographically distributed and how electoral districts are drawn. It builds on the understanding that gerrymandering manipulates district boundaries to favor a particular political party [1, 2, 6, 7], while geographical partisan sorting refers to the phenomenon where voters increasingly cluster into like-minded communities [52]. These intertwined processes ultimately undermine electoral fairness by reducing competition and skewing representation [2, 3, 14, 15, 57, 65].

The model's connection to complexity lies in its emphasis on feedback loops and emergent behavior. Voter movement patterns influence the partisan composition of districts, which in turn affect electoral outcomes and subsequent redistricting efforts. Redistricting shapes the future of legislative control within a state and contributes to control of the U.S. House of Representatives, creating a complex, adaptive system. The purpose of the model is to study the relationship between these two phenomena and to evaluate how redistricting reforms affect electoral fairness in the long term within this dynamic environment.

The agents' decision models are based on two main assumptions. First, voters exhibit a preference for living among politically like-minded individuals, reflecting tendencies documented in empirical studies of partisan sorting. Their movement decisions are probabilistic but biased towards areas where their preferred political party has a stronger presence. Second, the redistricting process reflects the goals of the political authority in control, favoring partisan advantage in the absence of reforms, or optimizing for competitiveness or compactness when reform policies are enforced.

These specific decision models were chosen because they allow the simulation to capture both bottom-up social processes and top-down institutional mechanisms. Voter relocation models partisan sorting and ideological clustering at the local level, while the redistricting model captures institutional responses that shape electoral opportunities. This dual approach makes it possible to study how redistricting reforms are affected by the underlying social dynamics, providing a richer understanding on the long-term effectiveness of said reforms than would be possible with static or purely top-down models.

The model is initialized using empirical data from various sources (see Section 3.3.2), providing a realistic foundation for the spatial distribution of voters, political preferences, demographics, and geographic characteristics within each modeled state. While the level of aggregation varies—electoral data and voter distributions are typically available at the precinct level, and demographic or geographic data at the county level—the finest available resolution was used for each dataset. This approach enables the simulation of voter movement and redistricting at a detailed scale, enhancing the realism and credibility of the model's outcomes.

3.2.2 Individual Decision-Making

During the simulation, agents have the option to relocate to another precinct within their state. At each time step, agents are classified as either *happy* or *unhappy*. An agent is considered *unhappy* if their utility score falls below a predefined threshold T. When this occurs, they will consider relocating. The decision-making process is modeled at the individual agent level, with each agent independently assessing potential relocation options based on a utility function that incorporates both precinct- and county-level factors. An agent's utility for a specific precinct is determined by three precinct- and county-level factors using the following equation:

$$U_{loc} = X_1 \cdot a_1 + X_2 \cdot a_2 + X_3 \cdot a_3 \tag{3.5}$$

where:

- X_1, X_2, and X_3 = the payoffs an agent receives when specific conditions are met.
- a_1, a_2, and a_3 = the weights assigned to each payoff, summing to 1[4].

The individual payoffs are defined as follows:

$$X_1 = \begin{cases} 1, & \text{if the precinct's majority party matches the agent's party affiliation} \\ 0, & \text{otherwise} \end{cases}$$

$$X_2 = \begin{cases} 1, & \text{if the county's majority party matches the agent's party affiliation} \\ 0, & \text{otherwise} \end{cases}$$

[4] In all experiments, the weights are set to $\frac{1}{3}$, meaning all payoffs contribute equally to the overall utility.

$$X_3 = \begin{cases} 1, & \text{if the agent is Republican and the county is rural or a small town} \\ 0.5, & \text{if the agent is Republican and the county is a large town} \\ 1, & \text{if the agent is Democrat and the county is urban or a large town} \\ 0.5, & \text{if the agent is Democrat and the county is a small town} \\ 0.25, & \text{otherwise} \end{cases}$$

where:

- **Precinct- and County-Level Partisan Alignment (X_1 and X_2)**: Agents prefer to live in areas where the majority of voters share their political affiliation [52, 54, 55]. This behavior reflects empirical trends in partisan sorting, where individuals increasingly cluster in ideologically homogeneous communities. Although some studies suggest partisan migration at the state level, incorporating such dynamics would significantly increase model complexity and is therefore left for future research. Furthermore, there is no strong empirical evidence to suggest that individuals consider Congressional district-level alignment when making residential decisions. As a result, the model focuses on precinct and county alignment, as these smaller geographic units better capture an agent's immediate social and political environment.

- **Urban-Rural Political Preferences (X_3)**: Residential utility is also influenced by the urban-rural character of a location, which has long been associated with partisan divides. Republicans tend to prefer rural and small-town areas, which have historically been conservative strongholds, while Democrats show a strong preference for urban and large-town environments, where their voter base is more concentrated [52, 57, 65]. In more mixed contexts, such as large towns for Republicans or small towns for Democrats, the partisan preference is weaker and is reflected in the model by a moderate payoff of 0.5. The lowest utility payoff (0.25) is assigned to locations that are least aligned with an agent's expected partisan preference. Figure 3.2 visualizes the RUCA codes used to define urban-rural typologies across the four modeled states.

When an agent is unhappy, they consider relocating. The relocation process follows these steps. First, the agents samples M_O counties that are not at full capacity. The specific precinct within these counties are selected randomly, using the same probability distribution that determines an agent's initial placement within a county. Hereafter, the agent calculates the utility U_{loc} for each candidate precinct and for their current precinct.

To incorporate a penalty for relocating, the parameter D_D is introduced to control the extent to which moving longer distances reduces an agent's utility. The adjusted utility function is defined as follows:

$$\hat{U}_{loc} = U_{loc} \times (1 - (D_D \times D_{norm})) \tag{3.6}$$

where:

- D_{norm} represents the normalized relocation distance:

$$D_{norm} = \frac{\text{relocation distance (in miles)}}{\text{max relocation distance in state (in miles)}} \tag{3.7}$$

This formulation ensures that moves over longer distances incur a greater penalty, with D_D acting as a tuning parameter to determine the strength of this effect. Table A.6 presents the maximum relocation distance for each state, defined as the greatest straight-line distance between the centroids of any two precincts within that state's borders.

To introduce an element of randomness in agent decision-making, a probabilistic choice model is implemented, parameterized β [161]. Instead of always selecting the highest-utility location, agents make relocation decisions based on a softmax function, where the probability of choosing a new precinct i is given by:

$$\Delta U_i = U_{\text{new},i} - U_{\text{current}} \tag{3.8}$$

$$P_i = \frac{\exp(\beta \cdot \Delta U_i)}{\sum_{j=1}^{n} \exp(\beta \cdot \Delta U_j)} \tag{3.9}$$

where:

- ΔU_i = the change in utility for moving to precinct i,
- P_i = the probability that an agent selects precinct i as their relocation destination,
- n = the total number of relocation options available to the agent,
- β = a control parameter that determines how strongly utility differences influence decision-making.

The β parameter ranges from 0 to 100:

- When $\beta = 0$, agents move completely at random, ignoring differences in utility,

- As β increases, agents become more deterministic, favoring higher-utility locations with greater probability,
- When $\beta \to 100$, agents always select the option with the highest utility, making purely rational decisions.

This probabilistic approach ensures that agent movement reflects both rational utility maximization and real-world uncertainty in decision-making.

3.2.3 Individual Sensing

Individual agents in the model perceive and process precinct- and county-level information when evaluating potential relocation options. These factors influence their utility calculation, as described in Section 3.2.2. Agents take into account the majority party affiliation at the precinct and county levels, as well as the rural-urban classification of the county. While the model assumes that agents have access to accurate information about these variables within their current location and set of potential relocation options, their decisions are influenced by a stochastic utility function that introduces randomness into the choice process. As such, even though agents are assumed to have perfect knowledge of the relevant attributes, the presence of noise in the utility function means their behavior may not always reflect fully rational or error-free decision-making. The model does not simulate the process of information gathering, nor does it assign explicit costs to obtaining or processing information. Agents are also assumed to only consider relocation options within the state they reside in.

3.2.4 Interaction

Agent interactions in the model are indirect, meaning agents do not communicate with one another directly but influence each other through changes in their environment. Specifically, agents interact through the partisan composition of precincts and counties, which affects relocation decisions via the utility function (as described in Section 3.2.2). Two factors in the utility function, X_1 and X_2, depend on the majority party affiliation in a given precinct or county. As agents relocate, they alter these local partisan majorities, which in turn affects the utility scores of other agents considering relocation. This dynamic creates a feedback loop where partisan sorting patterns emerge over time.

3.2.5 Collectives

During simulations, agents form spatial aggregations based on their relocation decisions, which in turn influence the utility of other agents (as described in Section 3.2.4). Over time, agents with similar party affiliations tend to cluster together, leading to an increasingly homogeneous partisan distribution in precincts and counties. These aggregations emerge endogenously as a result of agents optimizing their individual utility scores rather than being imposed by the model.

The parameters β and T shape the dynamics of partisan sorting in the model by influencing how agents make relocation decisions. The parameter β governs the degree of randomness in an agent's decision-making. When β is high, agents are more likely to choose the option that maximizes their utility, leading to more decisive and accelerated sorting into like-minded precincts. In contrast, lower values of β introduce greater randomness into decisions, which slows down the sorting process and results in more diverse precinct compositions. In the extreme case of very low β, agents effectively relocate at random, which prevents strong partisan clustering from forming.

The happiness threshold T determines how tolerant agents are of living in precincts that do not match their partisan preference. A high T value leads to a larger share of agents being classified as unhappy, prompting more frequent relocations and increasing partisan segregation. For example, when $T = 1$, nearly all agents are unsatisfied with mixed environments and seek out more homogenous areas, accelerating the emergence of partisan enclaves. Conversely, a low T value means fewer agents relocate, resulting in weaker sorting dynamics. If $T = 0$, agents are always content with their current environment, and no relocations occur, thereby halting any partisan clustering.

These collective patterns of partisan sorting have significant implications for the long-term spatial distribution of political affiliations, affecting electoral outcomes, the overall competitiveness of districts, and perhaps the fairness of electoral maps.

3.2.6 Heterogeneity

Agents in the model are heterogeneous in their attributes but share a uniform decision-making process. Each agent differs in variables such as political affiliation, location, and utility, which influence whether they are satisfied with their current precinct and where they might relocate. These differences emerge from initial and environmental conditions rather than agent-specific rules.

All agents evaluate relocation options using the same decision logic and utility function (see Section 3.2.2). However, partisan affiliation affects how agents value the rural-urban classification of counties: Republican agents tend to prefer rural environments, while Democrat agents favor urban ones. These preferences are built into the utility function and are the only source of variation in how agents assess relocation options.

3.2.7 Stochasticity

Several processes within the model incorporate randomness to reflect the inherent uncertainty and variability in real-world political and demographic dynamics. These stochastic elements are present in the initialization, redistricting, and partisan sorting processes, and they contribute to variation across simulation runs.

During initialization, randomness plays a role in assigning both the geographic location and party affiliation of agents. When agents are placed within the state, their specific precinct is selected based on the precinct's population size, and their exact position within the precinct is randomly chosen (as described in Section 3.1.3.2). Although these precise positions do not influence the simulation outcomes, they are used for visualization purposes. Each agent's party affiliation is also determined probabilistically, using the share of Republican votes in the precinct. This ensures that agent-level political affiliations reflect local partisan leanings while introducing slight variations across simulations due to the limited number of agents relative to the real population.

Redistricting introduces additional randomness through the use of a randomly generated starting map in the optimization process. While the objective of redistricting (e.g. gerrymandering, compactness or competitiveness) remains consistent, the specific starting point varies each time, allowing the process to explore different pathways toward a valid solution. This random initialization ensures population balance from the outset and accommodates the shifting agent distribution caused by partisan sorting.

Finally, the partisan sorting process includes stochasticity through the β parameter in the relocation decision model. This parameter controls the degree to which agents prioritize maximizing their utility versus choosing locations more randomly. When β is low, agents' choices are largely random, resulting in more diffuse and unpredictable settlement patterns. As β increases, agents are more likely to relocate to higher-utility areas, reinforcing partisan clustering and segregation. The inclusion of this probabilistic behavior allows the model to simulate a range of sorting dynamics, from entirely random to strongly preference-driven.

3.2.8 Observations

During the simulation, various statistics are calculated and collected at the end of each time step. These statistics are crucial for testing, understanding, and analyzing the model's behavior and performance. The primary outputs from the simulation focus on evaluating the core aspects of this research, specifically partisan fairness, competitiveness, and compactness of the electoral maps. These metrics provide a systematic approach to assessing the impact of the model's emergent characteristics, such as changes in district boundaries and the degree of partisan segregation, on the fairness and competitiveness of the congressional map. These results lay the groundwork for evaluating the effectiveness of redistricting reforms. Additional details on the calculation and formulation of these metrics are presented in Section 2.1.6. An overview of the additionally collected data, including definitions, descriptions, and their purposes, can be found in Appendix A.5.

3.3 Details

3.3.1 Implementation Details

The model for this research was implemented entirely in Python, leveraging a variety of libraries for (geo)data processing, agent-based modeling, and electoral map generation.

The input datasets used to initialize the model were constructed with GeoPandas[5]. This library extends the functionality of Pandas to allow for spatial operations on geospatial data. GeoPandas enables the manipulation of geographic data and is essential for handling and preparing the precinct and county-level geospatial data used in the model.

The core agent-based model was developed using MesaGeo[6], an extension of the Mesa framework designed for building agent-based models. MesaGeo enhances the standard Mesa framework by introducing a GeoSpace, a specialized space for hosting GIS-based GeoAgents. These GeoAgents differ from standard agents in that they possess a geometry attribute (represented as a Shapely object) and a CRS (Coordinate Reference System) attribute, making them suitable for spatial analysis in GIS contexts.

For the generation of congressional maps, the model utilizes GerryChain[7], a library designed to evaluate and optimize electoral maps according to various criteria, including population equality, contiguity and compactness [145]. GerryChain was instrumental

[5]https://github.com/geopandas/geopandas
[6]https://github.com/projectmesa/mesa-geo
[7]https://github.com/mggg/GerryChain

for modeling the redistricting process, providing the necessary functionality to generate electoral maps as part of the simulation.

Due to the high computational cost of running tens of thousands of simulations per state, the experiments were parallelized using MPI and executed on the DAS-5 supercomputer, allowing for efficient distribution of model runs across multiple computing nodes [162].

The full implementation of the model, including the code, documentation, and examples, can be accessed on GitHub at: `https://github.com/aMONKE/GerrySort-ABM`.

3.3.2 Input Data

To ensure that the initial conditions of the model accurately reflect the political landscape of the modeled state as of 2020, an extensive dataset was constructed. This dataset is stored in a GeoJSON file, which includes precinct-level polygons and various properties necessary to simulate the electoral system. These properties include:

- **County and Congressional District Codes**: Each precinct is associated with a county and congressional district code based on the 2010-2020 boundaries. These codes are used to define county and district boundaries, with the `dissolve()` function in GeoPandas merging multiple precinct geometries into unified county and district geometries.
- **Election Results**: The precinct-level election results for the 2012, 2016, and 2020 presidential elections are included. These results determine the initial distribution of Republican and Democratic agents within each precinct. For the model's experiments, the 2020 election data was used to define the party affiliation of agents.
- **Population Counts**: Each precinct includes population counts, which are essential for creating a probability distribution of agent residence within a county. These counts help determine where agents are most likely to live when the model is initialized.
- **County-Level Information**: Additional county-level data such as population counts, RUCA codes, and the number of housing units and households are provided. Population counts guide the distribution of agents across counties, while housing units and households estimate each county's capacity for agents. The RUCA codes are used to model the residential preferences of Republican and Democratic agents, reflecting their tendencies to prefer rural or urban areas.

This dataset was constructed using data from multiple sources:

- Districtr[8] for precinct polygons associated with county codes and congressional district numbers. The population count and election results per precinct could typically also be found in these datasets.
- Economic Research Service[9] for the county-level RUCA codes.
- Index Mundi[10] for county-level demographic information, such as the number of housing units and persons per household.

Table A.7 in Appendix A.6, describes all the properties that each precinct in the dataset contains. These input data enable the model to replicate the political, demographic, and geographical conditions of the state under study, ensuring that the simulation is grounded in realistic and up-to-date information.

[8] https://districtr.org
[9] https://www.ers.usda.gov/data-products/rural-urban-commuting-area-codes
[10] https://www.indexmundi.com/facts/united-states/quick-facts/all-states/

Chapter 4

Sensitivity Analysis

Sensitivity Analysis (SA) is a crucial tool in agent-based modeling, used to assess how variations in model parameters influence simulation outcomes. By systematically adjusting input parameters and analyzing their impact on model outputs, SA helps identify which parameters play the most significant role in shaping the partisan fairness, competitiveness, and compactness of congressional maps. Additionally, it serves as a validation check, ensuring that the model responds logically to changes in assumptions and aligns with theoretical expectations. This chapter explores two complementary approaches to sensitivity analysis: a global method using Sobol' indices [163, 164], which evaluates the overall influence of parameters and their interactions, and a local method using the One-Factor-At-a-Time approach[164], which isolates the effects of individual parameters to detect non-linearities and threshold behaviors.

4.1 Global Sensitivity Analysis

Global Sensitivity Analysis (GSA) is a robust method used to quantify the influence of input parameters on model outcomes across the entire parameter space. Unlike local sensitivity analysis, which examines the effect of changing one parameter at a time, GSA evaluates how variations in multiple parameters interact to shape the results. For this thesis, Sobol' indices are used to assess the relative importance of different model parameters in shaping outputs such as partisan fairness, competitiveness, and compactness. Sobol' analysis is a variance-based global sensitivity method that decomposes total output variance into contributions from individual parameters (first-order effects) and their interactions (higher-order effects). Alternative global sensitivity techniques—such as mutual information [165], distance correlation (dCor) [166], and Hilbert-Schmidt Independence Criterion (HSIC) [167]—capture general dependencies between inputs and outputs and are well-suited for detecting non-linear or non-monotonic relationships, especially with irregular or multimodal output distributions. However, they do not attribute variance and are less interpretable in terms of parameter contribution. While Sobol' indices assume square-integrable and smooth outputs, they have shown to be robust in bimodal settings [161] and provide a clear, quantitative breakdown of parameter influence. That said, output distributions that are approximately Gaussian can improve numerical stability and reduce the number of samples required to accurately estimate variance contributions. Results from the local sensitivity analysis revealed that the model output distributions vary significantly across parameters, states, and output metrics (Fig. B.5 in Appendix B.2). The average competitiveness and compactness metrics tend to resemble Gaussian distributions[1], while the efficiency gap outputs display multimodal patterns, with the number and prominence of peaks differing by state and parameter setting. Although not all output distributions are Gaussian, Sobol' analysis remains well-suited due to its robustness to non-Gaussianity under sufficient sampling, its clear interpretability, and its ability to quantify both main and interaction effects. These strengths make it a reliable and effective method for assessing the influence of model parameters.

4.1.1 Sobol' Indices

Sobol' sensitivity analysis is a variance-based method that decomposes the total variance of the model output into contributions from individual input parameters and their interactions [163, 164]. Given a model $Y = f(X_1, X_2, ..., X_k)$ where X_i represents the input parameters, the total variance of the output Y is given by:

$$V(Y) = Var(Y) = \int (f(X) - E(Y))^2 dX \tag{4.1}$$

where $E(Y)$ is the expected value of the model output. Sobol' indices are derived from this total variance decomposition to assess both individual effects and interaction effects among parameters. By analyzing Sobol' indices, we gain insights into which parameters drive model outputs, how they interact, and whether model behavior aligns with expected theoretical relationships.

- The **first-order Sobol' index** S_i measures the proportion of output variance that is explained by a single parameter X_i alone, independent of interactions with other

[1]The sole exception is the output distribution of the average competitiveness when the tolerance parameter is varied, these output distributions are multimodal.

parameters. It is computed as:

$$S_i = \frac{V_i}{V(Y)}, 0 \leq S_i \leq 1 \tag{4.2}$$

where $V_i = Var_{X_i}(E_{X\sim i}(Y|X_i))$ is the variance of the conditional expectation of Y given X_i. A higher S_i value indicates that the parameter has a significant direct influence on the model output.

- The **second-order Sobol' index** S_{ij} quantifies the contribution of interaction effects between two parameters, X_i and X_j to the output variance. It is computed as:

$$S_{ij} = \frac{V_{ij}}{V(Y)} \tag{4.3}$$

where $V_{ij} = Var_{X_{ij}}(E_{X\sim ij}(Y|X_i, X_j)) - V_i - Vj$. captures the variance due to joint effects of X_i and X_j that is not explained by their individual contributions. If S_{ij} is large, it indicates that the two parameters strongly interact, meaning their combined effect on the output is greater than the sum of their individual effects.

- The **total Sobol' index** S_{Ti} accounts for both the direct contribution of a parameter and all its interactions with other parameters. It is given by:

$$S_{Ti} = 1 - \frac{V_{\sim i}}{V(Y)} \tag{4.4}$$

where $V_{\sim i} = Var_{X\sim i}(E_{X_i}(Y|X_{\sim i}))$ represents the variance of the model output when all variations in $X_{\sim i}$ are removed. A parameter with a high S_T value has a significant impact on model output, either directly or through interactions with other parameters. Conversely, a parameter with a low S_{Ti} suggests that its role in shaping the model's behavior is minimal.

Thus, if $S_i \approx S_{Ti}$, the parameter acts mostly independently, meaning it influences the model outcome without significant interaction effects. Furthermore, if $S_{Ti} - S_i$ is large, the parameter exhibits strong interactions with others, indicating that its effect cannot be understood in isolation. Finally, if both S_i and S_{Ti} are close to zero, the parameter has little to no impact on the model outcome, suggesting that it can potentially be fixed at a nominal value without significantly altering the results.

To perform the Sobol' sensitivity analysis, the Python library SALib[2] is used. The parameter space is explored using Saltelli's sampling scheme [164], which generates a quasi-random distribution of samples based on the parameter ranges defined in Table 4.1. The total number of simulations is given by $N(k+2)$, where N is the base sample size and

[2] https://github.com/SALib/SALib

Parameter	Default Value	GSA Range	LSA Values
T	0.5	[0.0, 1.0]	[0.0, 0.25, 0.5, 0.75, 1.0]
β	100.0	[0.0, 100.0]	[0.0, 25.0, 50.0, 75.0, 100.0]
E_S	250	[10, 500]	[10, 50, 100, 250, 500]
σ	0.01	[0.0, 0.25]	[0.0, 0.01, 0.05, 0.1, 0.25]
M_O	10	[1, 20]	[1, 5, 10, 15, 20]
D_D	0.0	[0.0, 1.0]	[0.0, 0.25, 0.5, 0.75, 1.0]
C_M	1.0	[0.9, 1.25]	[0.9, 1.0, 1.1, 1.25]

Table 4.1: Parameter ranges and values used in the global (GSA) and local sensitivity analysis (LSA).

k is the number of parameters. For this analysis, $N = 4096$ and $k = 7$, resulting in a total of 65,536 model runs per state. Figure B.1 in Appendix B.1 visualizes the full parameter space covered by the Saltelli sample. Each parameter combination is passed to the model, which is executed to record outputs related to partisan fairness, competitiveness, and compactness. Upon completion of all simulations, the Sobol' analysis module in SALib is used to compute the first-order, second-order, and total-effect sensitivity indices. This analysis is carried out for four swing states—GA, WI, MI, PA—to identify potential differences in model sensitivity across distinct political and geographic contexts. The findings are summarized below.

4.1.2 Results

The Sobol' indices provide insights into how each input parameter individually (via first-order indices) and interactively (via second-order and total-effect indices) contributes to output variance. The results of the GSA are presented across three model output metrics: a measure of partisan fairness (efficiency gap), average district competitiveness, and average district compactness of congressional maps.

Partisan Fairness (Efficiency Gap) The Sobol' sensitivity analysis shows that three parameters consistently have the strongest individual influence on the efficiency gap across all four swing states: tolerance (T), ensemble size (E_S), and redistricting stochasticity (σ). These parameters exhibit the highest first-order Sobol' indices (S_i), indicating they each account for a notable share of the variance in partisan fairness outcomes (Fig. 4.1). However, in every state, the total Sobol' indices (S_{Ti}) far exceed the first-order indices, implying that interaction effects between parameters explain most of the observed variance (Fig. B.3 in Appendix B.1).

State-specific patterns emerge beyond this general trend. In *GA*, additional parameters, including the number of moving options (M_O), distance decay (D_D), and capacity multiplier (C_M), also contribute substantially to the variance. Model outputs reveal that increasing tolerance reduces the efficiency gap, improving Democrats' ability to gerrymander effectively (Fig. B.2a in Appendix B.1). Since higher tolerance drives segregation, Democrats appear to benefit from more homogeneous precincts and districts in GA.

In *WI*, tolerance alone dominates the sensitivity profile. As in GA, higher tolerance correlates with a reduced efficiency gap, again favoring Democratic gerrymandering under more segregated conditions (Fig B.2b in Appendix B.1).

MI stands out as the only state where redistricting noise (σ) has the highest first-order effect. Here, increasing σ tends to raise the efficiency gap, favoring Republican outcomes (Fig. B.2c in Appendix B.1). This suggests that increased randomness disrupts initial Democratic control, leading more frequently to Republican gains. Additionally, in contrast to GA and WI, higher tolerance in MI increases the efficiency gap, benefiting Republicans. This opposite effect hints at state-specific dynamics in how segregation affects partisan bias.

In *PA*, the analysis yielded negative Sobol' indices, which are theoretically invalid, as variance contributions cannot be negative. This issue commonly arises from numerical estimation errors in the Monte Carlo procedure used to compute Sobol' indices, especially when the true sensitivity of an input is close to zero. In such cases, random fluctuations due to finite sampling can cause estimates to dip below zero. Other contributing factors include uninformative inputs, model stochasticity, and rounding effects that amplify estimation noise. Additionally, the multimodal distribution of the efficiency gap outputs likely increased estimator variance, making it more difficult to reliably attribute variance to individual parameters. We initially assumed the problem was due to an insufficient sample size, as increasing the number of simulations had resolved similar issues in the other states. However, even after running 65,536 simulations, the issue persisted. Due to the high computational cost of further increasing the sample size, we opted to halt additional runs and interpret the negative indices as an indication of negligible sensitivity for the corresponding parameters.

Average Competitiveness Tolerance emerges as the primary driver of average competitiveness across all states with $S_i \approx S_{Ti}$ (Fig. 4.2a). Model outputs show a clear trend: as tolerance increases, average competitiveness declines (Fig. B.4a in Appendix B.1). This aligns with intuition, higher tolerance means agents require a greater proportion of like-minded neighbors to be satisfied, leading to increased partisan segregation.

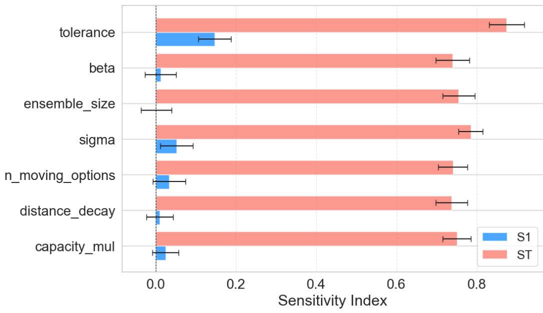

(A) GA

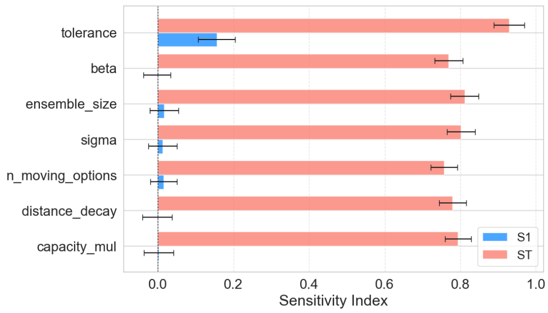

(B) WI

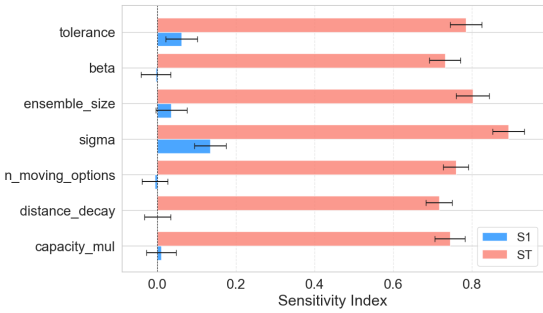

(C) MI

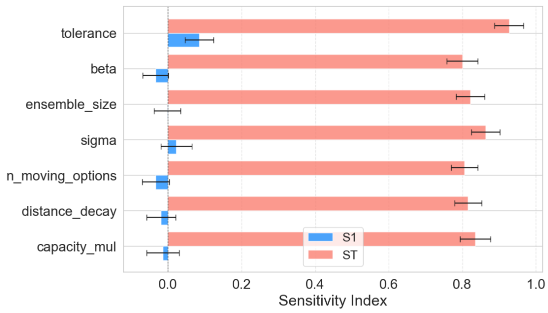

(D) PA

FIGURE 4.1: First-order (S_1) and total-effect (S_T) Sobol' sensitivity indices for the *efficiency gap*, a measure of partisan fairness, across four swing states. Each bar reflects the contribution of individual model parameters to the variance in the respective output metric, with 95% confidence intervals shown.

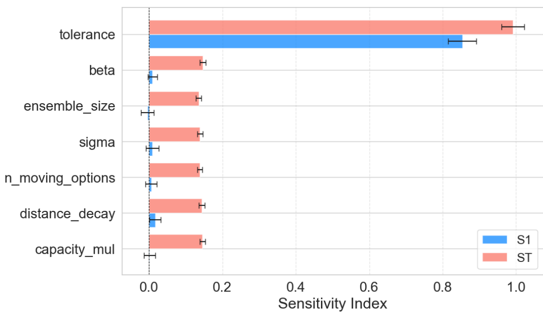

(A) Avg. Competitiveness

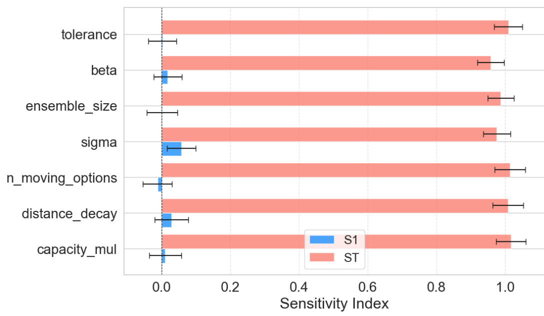

(B) Avg. Compactness

FIGURE 4.2: First-order (S_1) and total-effect (S_T) Sobol' sensitivity indices for *average competitiveness* and *average compactness* in GA. Each bar reflects the contribution of individual model parameters to the variance in the respective output metric, with 95% confidence intervals shown.

As a result, precincts, counties, and districts become more politically homogeneous, making it more difficult to draw competitive electoral maps.

Average Compactness No single parameter stands out as a strong driver of average compactness across all states (Fig. 4.2b). This suggests that compactness is less sensitive to the parameters explored in the model. Instead, compactness may be more heavily influenced by the underlying geography of each state and the spatial distribution of voters.

In conclusion, the GSA primarily serves to verify whether the model behaves as expected. Across all four swing states, the tolerance parameter consistently emerges as the most influential factor driving variation in partisan fairness outcomes. Redistricting-related parameters—such as redistricting noise and ensemble size—also frequently rank among the top three contributors to variance. However, no single parameter accounts for all variation, indicating that interaction effects between parameters play a substantial role (Fig B.3 in Appendix B.1). Notable differences between states were observed, though explaining these in-depth lies beyond the scope of this research. For average competitiveness, tolerance proves to be the dominant factor, with its first-order Sobol' indices closely matching the total indices, suggesting minimal interaction effects. In contrast, no parameter meaningfully explains the variance in average compactness. Overall, the sensitivity results align with expectations and confirm that the model behaves in a consistent and interpretable manner.

4.2 Local Sensitivity Analysis

To complement the GSA, a local sensitivity analysis (LSA) was conducted using the One-Factor-at-a-Time (OFAT) method. Whereas global methods assess how interactions between parameters contribute to output variability across the entire parameter space, LSA focuses on the effect of small, individual parameter changes around a fixed baseline. This allows for a more intuitive understanding of how each parameter influences the model's outputs in isolation and near the default configuration.

4.2.1 One-Factor-At-a-Time Method

The OFAT method involves varying one parameter at a time while keeping all other parameters constant at their default values [164]. For each parameter, a series of simulations is performed by incrementally increasing its value across a predefined local range.

This approach isolates the effect of each parameter and enables the measurement of its direct impact on model outputs.

The analysis was performed for the same four swing states used in the GSA: GA, WI, MI, and PA. Each parameter was varied across a locally defined range centered around its default value (see Table 4.1). All other parameters were kept fixed during each experiment. For each parameter setting, the model was executed 100 times to account for stochastic variation, and the results were averaged. Furthermore, to examine how the model behaves under different control scenarios, the LSA was conducted under three separate control conditions: (1) *model-determined control*, where party control of redistricting is determined by the model's electoral outcomes; (2) *fixed Democratic control*, where the Democratic party controls redistricting throughout the entire simulation; and (3) *fixed Republican control*. By fixing the redistricting control throughout the simulation, we can isolate and compare the effects of each parameter on redistricting outcomes for both the Democratic and Republican parties, allowing a clearer interpretation of how parameter changes benefit or disadvantage each party under stable control conditions. The findings are summarized below.

4.2.2 Results

The LSA explores how small, one-at-a-time changes in input parameters affect model outputs, offering insights into the immediate responsiveness of the system around a baseline scenario. Results are presented across the same three output metrics: the efficiency gap (partisan fairness), average competitiveness, and average compactness of congressional maps.

Partisan Fairness (Efficiency Gap) Among the tested parameters, those related to redistricting, namely, the ensemble size (E_S) and redistricting noise (σ), exerted the strongest influence on partisan fairness metrics (Fig. 4.3b and 4.3d). Increasing the ensemble size, which represents the resources available for gerrymandering, consistently enhanced a party's ability to produce favorable maps when that party held control. Conversely, higher levels of σ diluted the effectiveness of gerrymandering across all states and control scenarios. A notable exception to these trends was observed in PA. In the model-determined control scenario, increasing the ensemble size led to an efficiency gap that remained stable, suggesting a balance between the parties. This stability persisted even with higher randomness in redistricting decisions (σ). These results can be attributed to PA's unique dynamics: while Democrats initially tend to control redistricting, partisan sorting in the state strongly benefits the Republican Party. This often results in a transfer of control over time, effectively neutralizing early advantages—a dynamic confirmed by the results of the baseline experiments presented later.

In contrast, tolerance (T)—which determines the extent to which agents require like-minded neighbors to feel satisfied—showed a moderate influence on the efficiency gap (Fig. 4.3a). Higher T levels appeared to impede Republicans more than Democrats in their ability to gerrymander effectively, especially in states like GA and WI, where Republicans typically hold initial control. In MI and PA, where initial control is either Democratic or more contested, increases in tolerance produced more stable efficiency gap outcomes.

Overall, these findings mirror the trends in the GSA, where T, E_S, and σ all exhibited meaningful first-order Sobol' indices, albeit with some variation across states.

Average Competitiveness Tolerance exhibited the strongest influence on average competitiveness across all redistricting control scenarios and states (Fig. 4.3c). As the value of T increased, district competitiveness consistently declined. These findings align with the GSA, where tolerance similarly stood out as the most significant driver of changes in average competitiveness.

Average Compactness None of the tested parameters showed a strong individual effect on average compactness. This result is also consistent with the GSA, where no parameter yielded significant influence on compactness when assessed independently.

In conclusion, the LSA reinforces the insights from the GSA, with T, E_S, and σ consistently emerging as key parameters influencing the efficiency gap and average competitiveness. Notably, while tolerance demonstrated a strong and consistent impact on average competitiveness, no single parameter could explain the variation in average compactness. The observed state-specific differences, particularly in PA, highlight the complexity of redistricting dynamics, where multiple parameters and state-specific characteristics interact to shape outcomes. These results align with expectations, confirming that the model behaves predictably.

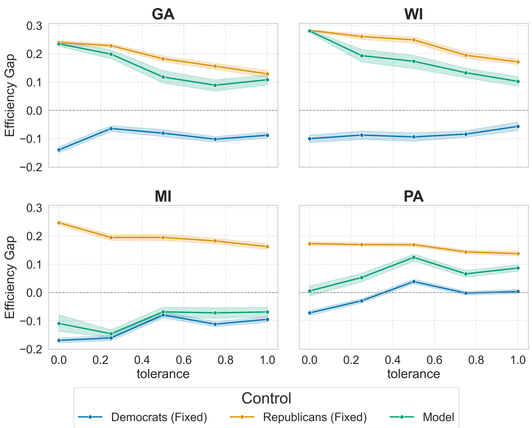

(A) Sensitivity of the *efficiency gap* to the tolerance parameter (T).

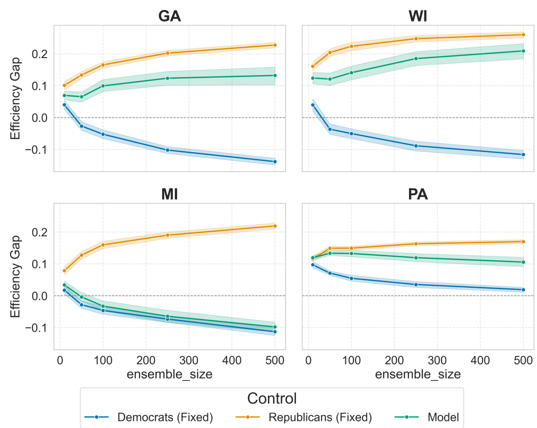

(B) Sensitivity of the *efficiency gap* to the ensemble size parameter (E_S).

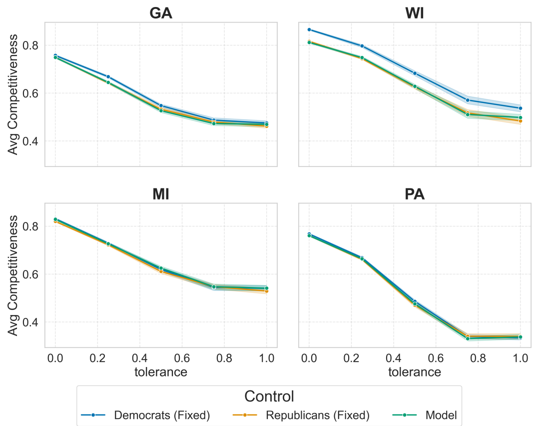

(C) Sensitivity of *average competitiveness* to the tolerance parameter (T).

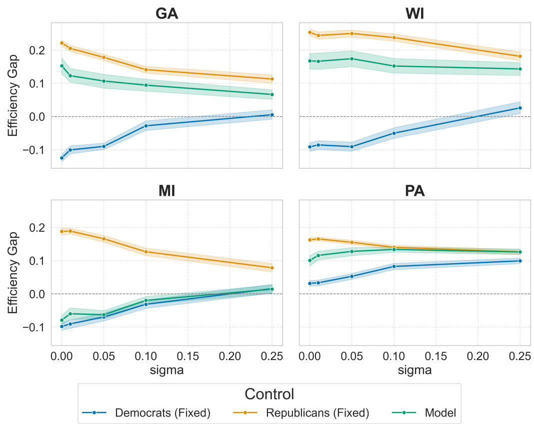

(D) Sensitivity of the *efficiency gap* to the random noise parameter (σ).

FIGURE 4.3: OFAT sensitivity analysis results for selected model parameters (tolerance (T), ensemble size (E_S), and redistricting noise (σ)). The plots show the effect of varying each parameter on outcome metrics (*efficiency gap* and *average competitiveness*) across four states and under different redistricting control regimes: fixed Democratic, fixed Republican, and model-determined control.

Chapter 5

Experiments and Results

5.1 Baseline Experiments

The baseline experiments are designed to address sub-research questions S-RQ1, S-RQ2, and S-RQ3 (See Section 1.2), which explore the effects of partisan sorting, gerrymandering, and their combined effects on the partisan fairness, competitiveness, and compactness of congressional maps. These experiments form the foundation for understanding how each phenomenon individually and jointly influences these redistricting outcomes.

5.1.1 Experimental Set-Up

To isolate the individual and combined effects of geographical partisan sorting and gerrymandering, three distinct experimental conditions are simulated:

1. **Geographical Partisan Sorting Only**: In this condition, partisan sorting is enabled, allowing individuals to relocate based on partisan preferences, while redistricting is disabled. This setup isolates the influence of self-sorting on the partisan fairness of electoral maps, showing how demographic shifts alone may lead to partisan biases, even in the absence of deliberate manipulation.

2. **Gerrymandering Only**: In this condition, redistricting is enabled to maximize the advantage of the controlling party (or to maximize fairness in tied states), while agents do not move. This isolates the impact of gerrymandering on electoral outcomes, independent of partisan sorting.

3. **Both Sorting and Gerrymandering**: In this condition, both partisan sorting and redistricting are enabled simultaneously. This configuration captures the full

> dynamics of the model, allowing for the exploration of how these two phenomena interact—whether they amplify, offset, or complicate each other's effects—and what emergent outcomes they produce in terms of partisan fairness, competitiveness, and compactness.

Each baseline experiment is run under four distinct redistricting control conditions: (1) *model-determined control*, where redistricting power shifts based on the electoral outcome after each cycle; (2) *fixed Democratic control*, where the Democratic Party retains redistricting authority throughout; (3) *fixed Republican control*, where the Republican Party consistently holds control; and (4) *fairness-maximizing control*, where maps are drawn to optimize partisan fairness. Fixing control to one party allows for evaluation of that party's ability to leverage the initial spatial distribution of voters—particularly in gerrymandering-only scenarios—or to assess the extent of partisan advantage when both sorting and gerrymandering are active. The fairness-maximizing condition serves as a benchmark, helping determine whether a fair map is achievable in a given state under different experimental conditions. Note that control conditions are not required for the partisan sorting experiment, as no redistricting takes place. Instead, the model-determined control is used to assess whether partisan sorting alone can shift the partisan control of a state under the initial congressional map.

All experiments are run using the model's default parameter settings (see Table 3.1) and are repeated across the four swing states to enable consistent cross-state comparisons. The tracked outputs include three measures of partisan fairness—efficiency gap, mean-median difference, and declination—alongside average district compactness and competitiveness, which together reflect how congressional map characteristics evolve under varying experimental conditions (see Section 2.1.6). To clearly present the results on partisan fairness, the efficiency gap is used as the primary metric to discuss the results of all of the experiments. The results of the additional metrics, including declination and mean–median difference, are provided in Appendix C.1. The results indicate that the efficiency gap and declination generally show similar trends, although the declination tends to exhibit more extreme values. In contrast, the mean–median difference consistently behaves differently from the other two measures and appears less sensitive to changes in congressional maps and levels of partisan segregation. However, together, these baseline experiments provide a foundation for analyzing the independent and combined effects of gerrymandering and partisan sorting, while serving as a reference point for evaluating the impact of redistricting reforms in later experiments.

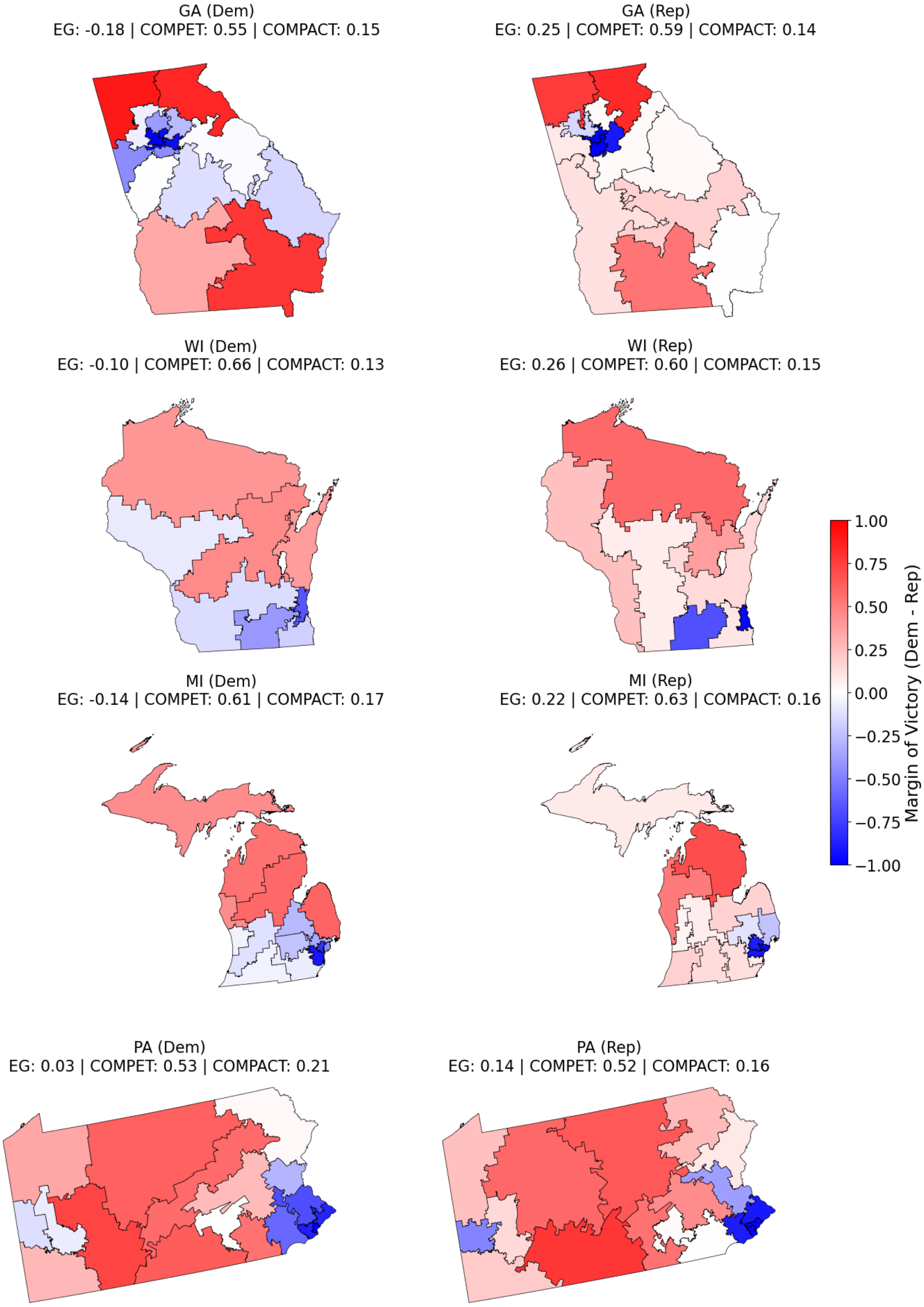

FIGURE 5.1: Examples of generated congressional maps after partisan sorting for the baseline experiments under fixed Democratic (left) and fixed Republican (right) control. District color and intensity reflect the winning party's margin of victory. Each map also displays its efficiency gap (EG), average competitiveness (COMPET), and average compactness (COMPACT).

5.1.2 Results

The baseline experiments reveal how gerrymandering and partisan sorting interact to shape redistricting outcomes under different redistricting control conditions. Each state displayed distinct dynamics, influenced by their initial conditions and state characteristics. The results are presented in two parts: first, state-specific findings that highlight the distinctive patterns and behaviors observed in each case; and second, general findings that capture consistent trends shared across all four states.

State-Specific Patterns In ***GA***, the gerrymandering-only scenario under fixed Democratic control shows that the party is capable of producing advantageous congressional maps (Fig. 5.2a). However, this advantage is somewhat diminished when partisan sorting is introduced. The Democrats' main strategy involves cracking their voter base in and around the Atlanta area by drawing districts that extend deep into rural regions, thereby diluting Republican votes across a wider area (Fig. 5.1). Under fixed Republican control, the gerrymandering-only scenario similarly results in favorable maps for the party, indicating that Georgia's political geography enables both parties to effectively exploit voter distributions when given control over redistricting (Fig. 5.2a). That said, Republicans consistently achieve slightly higher efficiency gaps than Democrats, regardless of whether sorting is modeled, indicating a structural advantage in the state's political geography. Their dominant strategy is to pack Democratic voters into a few heavily concentrated districts in the Atlanta metro area (Fig. 5.1). Interestingly, the introduction of partisan sorting appears to hinder the ability of both parties to fully capitalize on gerrymandering, suggesting that partisan migration patterns introduce a degree of unpredictability that may help counterbalance the effects of extreme partisan redistricting.

In the model-determined control experiment modeling only partisan sorting, the efficiency gap increases in favor of Republicans (Fig. 5.2b), suggesting that GA's initial congressional map structurally benefits the Republican Party when voters self-sort, since a positive efficiency gap indicates an advantage for Republicans. In the gerrymandering-only condition, Republicans, who are typically granted initial control, retain it throughout the simulation, allowing them to create even more advantageous maps (Fig. 5.2b and 5.6a). However, this advantage is less reliably achieved when both sorting and gerrymandering are simulated. The added unpredictability of sorting complicates attempts to anticipate and exploit population shifts, thus reducing the efficacy of gerrymandering. In some cases, this leads to a shift in redistricting control toward the Democratic Party, as shown in Figure 5.6a. Nevertheless, across all experimental scenarios, it remains possible to generate a relatively fair map, defined by an efficiency gap of $0 \leq 0.05$.

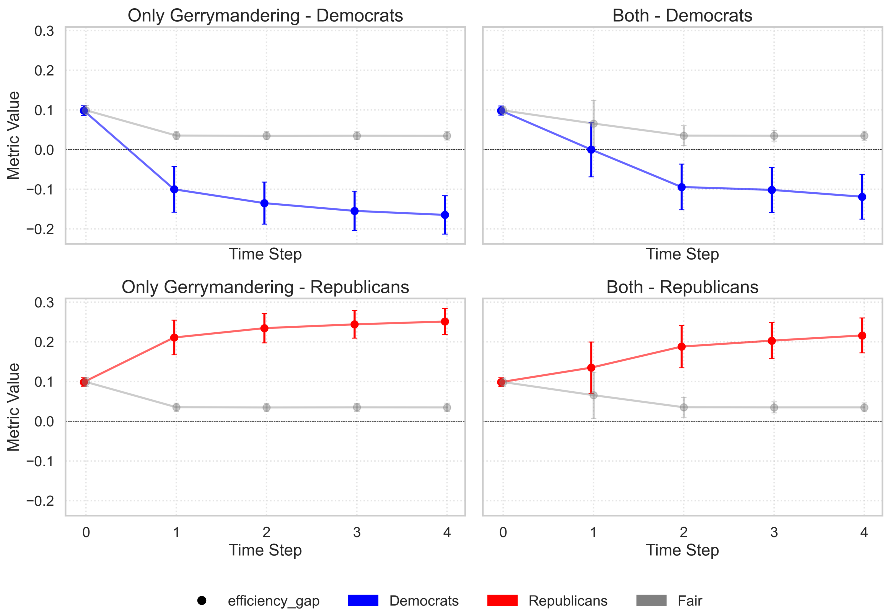

(A) Fixed Party Control

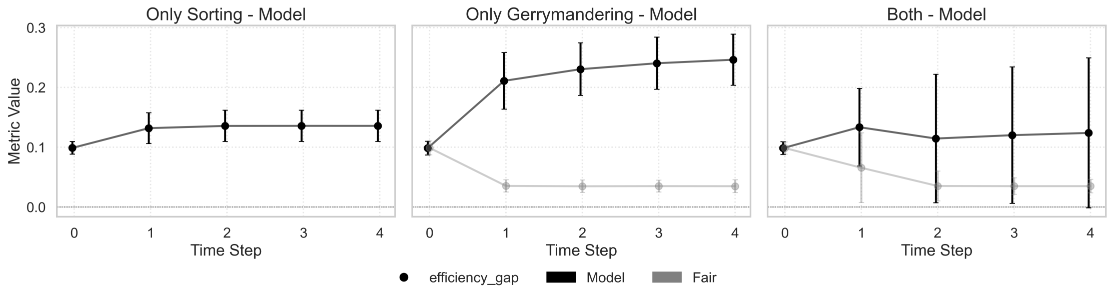

(B) Model-determined Control

FIGURE 5.2: Temporal evolution of the efficiency gap in the baseline experiments for ***GA*** under both fixed control and model-determined control scenarios.

In ***WI***, under fixed Democratic control, the gerrymandering-only scenario under fixed Democratic control demonstrates that Democrats can draw a map that clearly favors their party. However, this advantage is reduced when partisan sorting is introduced, likely due to the added unpredictability it brings (Fig. 5.3a). The Democrats' primary strategy involves cracking their voter base in the Milwaukee area and connecting it with the Democratic-leaning Madison region, while incorporating rural areas to dilute Republican strength (Fig. 5.1). Under fixed Republican control, the initial map produced in the gerrymandering-only scenario is already close to optimal for the party, leaving limited room for further advantage. The Republicans' main strategy centers on packing Democratic voters into a small number of districts concentrated around Milwaukee and Madison. As in the Democratic case, partisan sorting diminishes their advantage, softening the Republican edge (Fig. 5.3a). These dynamics mirror those observed in

GA: both parties are capable of leveraging gerrymandering to produce favorable outcomes, with Republicans typically gaining more from the underlying political geography. Additionally, the strategies employed by both parties show striking similarities across states.

In the model-determined control scenario with only partisan sorting, the efficiency gap decreases in favor of the Democratic Party (Fig. 5.3b), suggesting that WI's initial congressional map structurally favors Democrats when voters self-sort. In the gerrymandering-only condition, early Republican control tends to persist throughout the simulation, allowing them to continue optimizing maps in their favor. However, when both sorting and gerrymandering are active, this advantage is less reliably maintained due to the disruptive effects of sorting. In some cases, this unpredictability results in redistricting control eventually transferring to the Democratic Party (Fig. 5.6b). Across all scenarios, however, it remains possible to produce a relatively fair map, with an efficiency gap of $0 \leq 0.05$.

In the gerrymandering-only experiments under fixed Democratic and Republican control in ***MI***, both parties are able to draw advantageous maps (Fig. 5.4a). The Democrats primarily concentrate on constructing districts around urban centers with strong Democratic leanings—namely Detroit, Grand Rapids, Flint, Lansing, Kalamazoo, and Portage (Fig. 5.1). In contrast, the Republicans adopt a familiar strategy: packing Democratic voters into a few districts centered around Detroit, while cracking Democratic support in other metropolitan areas by extending districts into surrounding rural regions (Fig. 5.1). As in GA and WI, Republicans prove slightly more effective at exploiting the spatial distribution of voters for partisan gain. However, the introduction of partisan sorting reduces the effectiveness of gerrymandering for both parties (Fig. 5.4a).

In the model-determined control scenario with only partisan sorting, the efficiency gap increases in favor of the Republican Party (Fig. 5.4b), suggesting that MI's initial congressional map structurally benefits Republicans when voters self-sort. In the gerrymandering-only experiment, control is initially awarded to Democrats in about 60% of simulations and is typically retained, allowing them to continue optimizing maps (Fig. 5.4b and 5.6c). However, the resulting efficiency gaps are not as extreme as in the fixed Democratic control scenario, largely because control is more contested in MI than in GA or WI. (Fig. 5.6c). This variation in initial control introduces some Republican-favored runs, which in turn pull the average efficiency gap closer to zero. When both sorting and gerrymandering are active, Democrats still tend to secure favorable maps, but the unpredictability introduced by sorting—combined with the more competitive initial control landscape—reduces the magnitude of their advantage compared to the

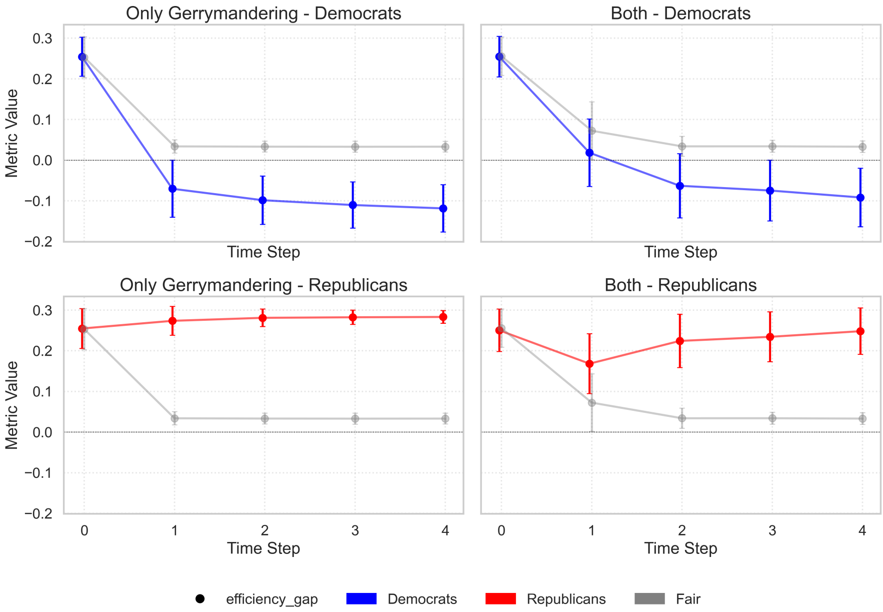

(A) Fixed Party Control

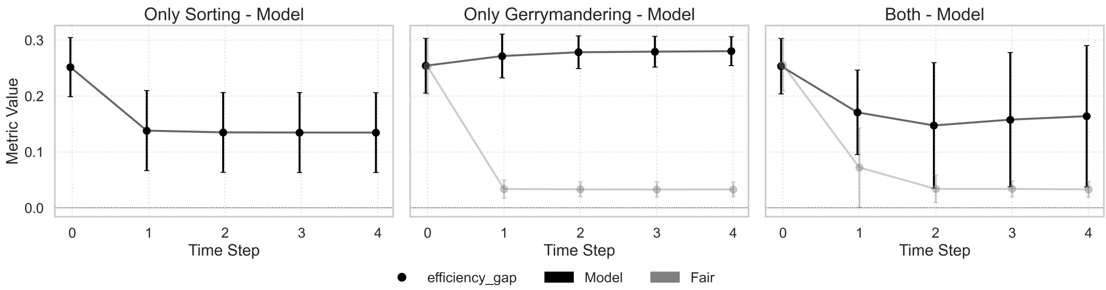

(B) Model-determined Control

FIGURE 5.3: Temporal evolution of the efficiency gap in the baseline experiments for ***WI*** under both fixed control and model-determined control scenarios.

gerrymandering-only scenario. Notably, the distribution of initial and final control remains relatively stable across all experimental conditions in MI (Fig. 5.6c). Nonetheless, in every scenario, it remains possible to generate a relatively fair map with an efficiency gap of $0 \leq 0.05$.

In the gerrymandering-only experiments under fixed Democratic and Republican control in ***PA***, both parties are able to produce advantageous maps. However, Republicans are significantly more effective at exploiting the initial spatial distribution of voters, indicating that PA's political geography is inherently more favorable to them (Fig. 5.5a). This pattern persists when both gerrymandering and partisan sorting are modeled: while sorting slightly reduces the Republican advantage, it substantially hampers the Democrats' ability to produce favorable outcomes. The Democrats' primary strategy involves cracking their voter base in strongholds like Philadelphia and Pittsburgh and combining

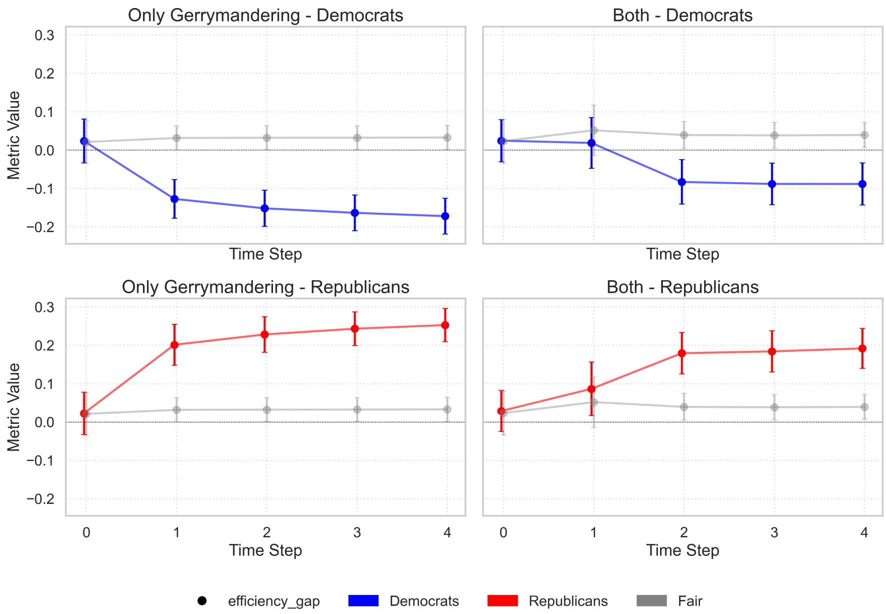

(A) Fixed Party Control

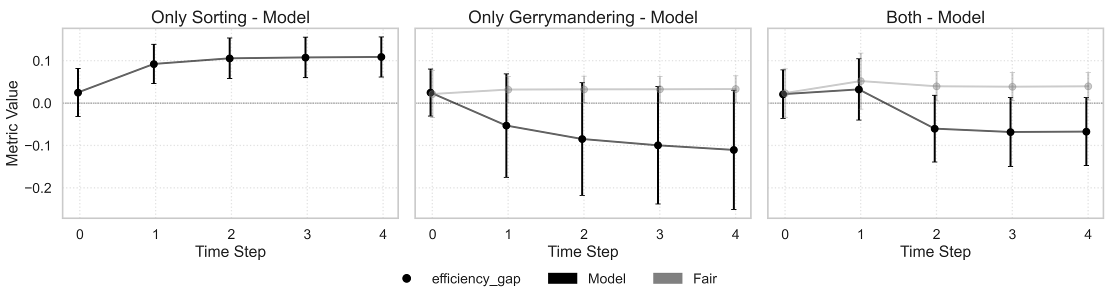

(B) Model-determined Control

FIGURE 5.4: Temporal evolution of the efficiency gap in the baseline experiments for ***MI*** under both fixed control and model-determined control scenarios.

them with rural areas to stretch their influence. Conversely, Republicans rely on packing Democratic voters into a small number of districts centered on those same urban areas. These results suggest that PA's underlying political geography severely limits Democratic gerrymandering potential, a disadvantage that is only amplified by the effects of partisan sorting. The reasons behind this asymmetry are explored further in Section 5.2.

In the model-determined control scenario simulating only partisan sorting, the efficiency gap increases in favor of the Republican Party (Fig. 5.5b), indicating that PA's initial congressional map structurally benefits Republicans as voters self-sort. This is further evidenced by shifts in control: although Democrats begin with initial control in roughly 50% of the simulations, the final control moves toward a tied outcome in approximately 80% of cases (Fig. 5.6d). In the gerrymandering-only scenario, the efficiency gap remains close to zero, likely because initial control is contested, and the party that starts with control generally retains it, limiting extreme partisan gains. When both sorting and gerrymandering are modeled together, a more notable shift occurs: although Democrats hold initial control in 50% of simulations, Republicans ultimately secure final control in 60% of runs (Fig. 5.6d). Correspondingly, the efficiency gap skews in favor of Republicans in the final maps (Fig. 5.5b). These results reinforce the idea that post-sorting voter distributions disproportionately benefit Republicans. While it remains possible to produce a relatively fair map in the gerrymandering-only scenario (efficiency gap $0 \leq 0.05$), achieving fairness becomes significantly more difficult when both dynamics are active (efficiency gap ≥ 0.05), highlighting the structural disadvantage Democrats face due to political geography in PA.

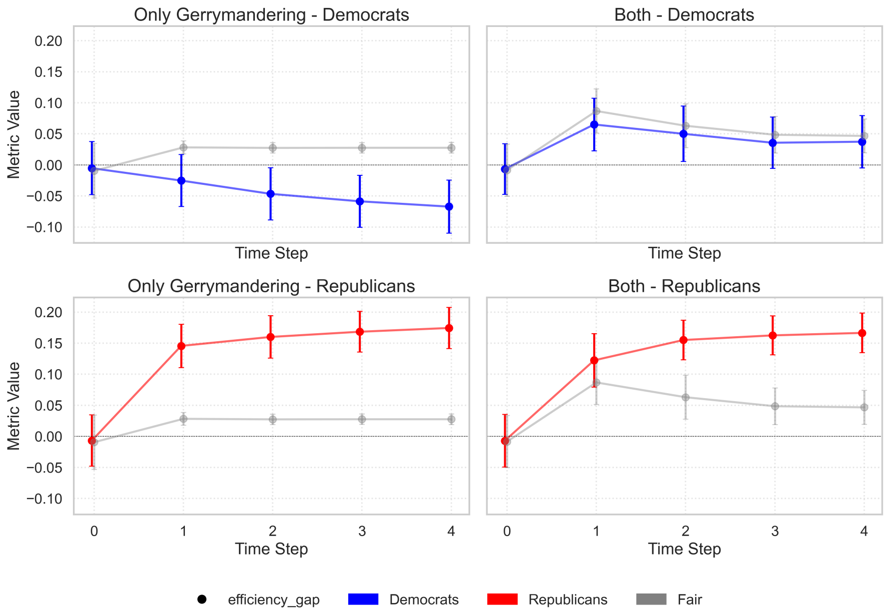

(A) Fixed Party Control

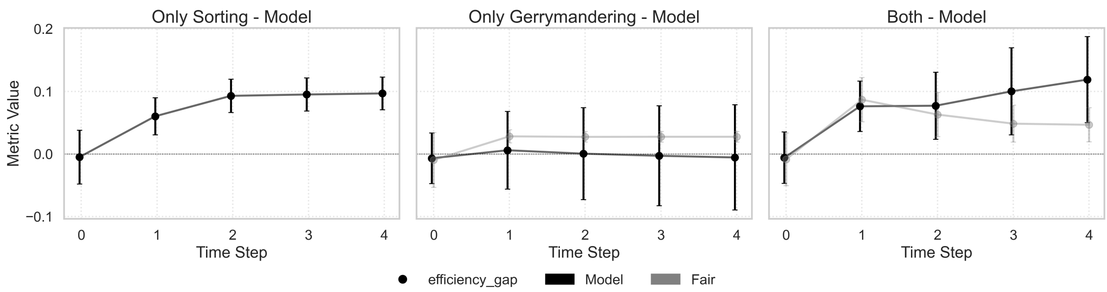

(B) Model-determined Control

FIGURE 5.5: Temporal evolution of the efficiency gap in the baseline experiments for ***PA*** under both fixed control and model-determined control scenarios.

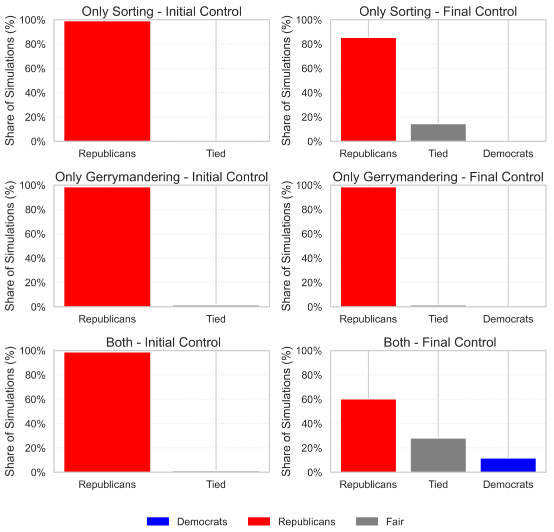

(A) GA

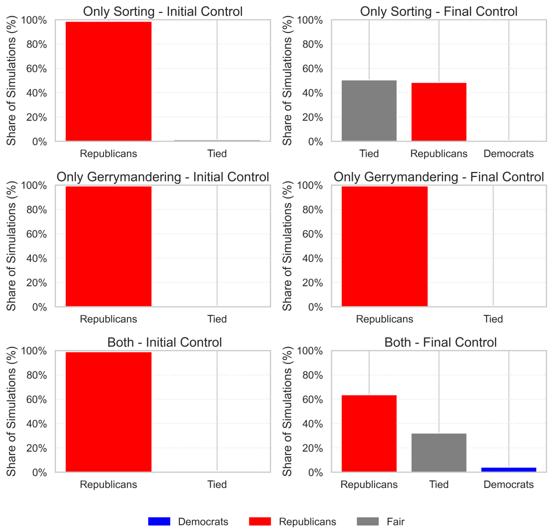

(B) WI

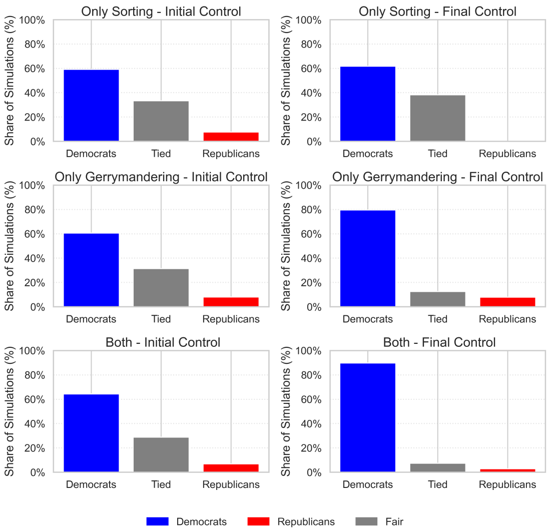

(C) MI

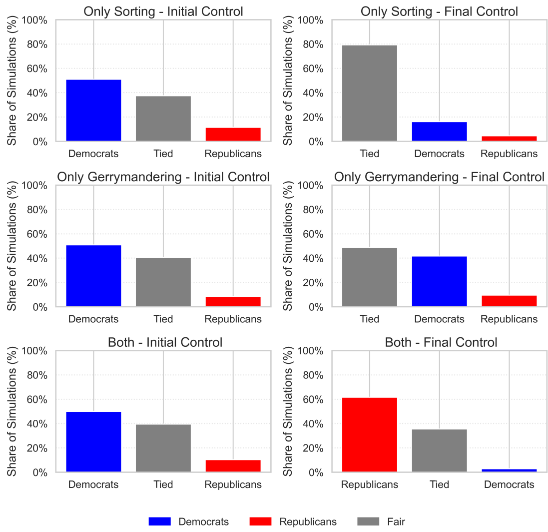

(D) PA

FIGURE 5.6: Comparison of party control from initial to final cycle in baseline experiments, where redistricting control is based on electoral outcomes.

General Observations Beyond the specific dynamics observed in each state, the baseline experiments reveal several consistent patterns that hold across all four cases:

- In gerrymandering-only scenarios under fixed party control, both parties can effectively exploit the initial spatial distribution of voters; however, Republicans consistently achieve higher efficiency gap scores. This pattern suggests that the political geography in these states structurally favors the Republican Party, potentially due to the underlying urban–rural divide, which provides them with greater leverage when drawing district boundaries. Similarly, in scenarios where both gerrymandering and partisan sorting are simulated, the Democratic Party is disproportionately negatively affected by the impact of sorting compared to the Republican Party.

- Partisan sorting increases the variability of partisan fairness metrics by introducing unpredictable population shifts. This unpredictability makes it more difficult for either party to maintain a consistent advantage through gerrymandering and increases the likelihood that redistricting control shifts between parties across cycles, leading to less stable electoral outcomes as mapmakers haven't accounted for partisan migration patterns.

- In gerrymandering-only scenarios under model-determined control, the party initially in control tends to retain control, demonstrating that, in the absence of sorting, it is easier to secure and sustain partisan advantage through redistricting.

- Across all states, Republicans predominantly employ a *packing* strategy, concentrating Democratic voters into a few heavily Democratic districts, while Democrats more often rely on a *cracking* strategy, attempting to split clusters of Democratic voters across multiple districts by merging urban centers with surrounding rural areas. This asymmetry reflects structural differences in each party's voter base: Democrats are heavily concentrated in urban areas, which makes them more susceptible to packing by Republicans, while also forcing Democrats to rely on cracking these dense urban centers as the only viable strategy to distribute their voters across multiple districts.

- Relatively fair maps, defined by efficiency gap values between $0 \leq 0.05$ and typically skewed slightly toward the Republican Party, are achievable across all states and simulation scenarios. An exception is PA under combined gerrymandering and sorting, where partisan sorting significantly diminished the Democrats' ability to gerrymander effectively and reduces the likelihood of producing fair maps.

- Due to the selected baseline parameter values, the majority of partisan sorting occurs within the first time step of the model (see Figs. C.3, C.6, C.9, C.12 in

Appendix C.1). This results in a rapid shift to a highly segregated state, after which only limited voter movement takes place. Agents who remain dissatisfied after this initial sorting phase typically continue to move between equally unsatisfying locations or choose to stay put. Importantly, since congressional district-level partisan alignment is not included in the agents' utility function, their satisfaction remains unchanged in the gerrymandering-only experiments. Moreover, in experiments where partisan sorting is modeled, the sorting dynamics unfold identically regardless of whether gerrymandering is also being simulated.

- Across all partisan sorting scenarios, sorting consistently reduces the average competitiveness of congressional maps, as it tends to create more politically homogeneous precincts, counties, and districts (See Figs. C.2, C.5, C.8, C.11 in Appendix C.1). This homogenization makes it more difficult to draw competitive electoral boundaries.
- Across all gerrymandering scenarios under fixed and model-determined control, gerrymandering consistently reduces the average compactness of congressional maps (See Figs. C.2, C.5, C.8, C.11 in Appendix C.1). This suggests that securing partisan advantage often depends on drawing irregularly shaped districts.
- In gerrymandering-only scenarios under fixed and model-determined control, gerrymandering can increase the average competitiveness of the congressional map, suggesting that, counterintuitively, gerrymandering can enhance electoral competition (See Figs. C.2, C.5, C.8, C.11 in Appendix C.1).

5.2 Testing the Role of Democratic Strongholds

The baseline results for PA revealed that Democrats were unable to produce a favorable map when both gerrymandering and partisan sorting were simulated (Fig. 5.5a), making it notably different from the results observed in GA, WI, MI (Figs. 5.2a, 5.3a, 5.4a). The fact that PA displayed these irregular dynamics indicates that state-specific factors—such as political geography—may substantially influence the effectiveness of gerrymandering.

A closer look at the initial and final spatial distribution of voters could potentially explain this discrepancy. In PA, after four rounds of sorting, roughly 60% of the Democratic voter base is concentrated in a single major urban cluster centered around Philadelphia[1], with an additional 13% located in the Pittsburgh area[2]. In contrast, the other three

[1] This includes the counties of Philadelphia, Delaware, Chester, Montgomery, Bucks, Berks, Lehigh, and Northampton.

[2] Including Allegheny and Westmoreland counties.

states (GA, WI, and MI) have multiple Democratic-leaning urban centers that are more geographically dispersed (Fig. C.13a, C.13b, and 5.7a). For instance, in MI, around 50% of Democratic voters are concentrated in the Detroit metropolitan area,[3] but the remainder are spread across additional urban hubs throughout the state. This contrast suggests that both the number and geographic dispersion of Democratic strongholds play a critical role in shaping the degree of structural partisan bias exacerbated by sorting. When Democratic voters are highly concentrated in one or two locations, the effects of unintentional gerrymandering appear to be magnified. Conversely, when Democratic voters are more spatially distributed, the impact of sorting on gerrymandering is less severe.

To examine this further, we conducted an additional experiment in which the initial spatial distribution of voters was systematically altered. This experiment investigates whether the number and dispersion of Democratic strongholds affect each party's ability to gerrymander effectively and directly addresses S-RQ4. The experimental design and results are presented below.

State	**Before Sorting**	**After Sorting**
GA	0.3582	0.4079
WI	0.3170	0.4123
MI	0.1644	0.1815
MI (Fabricated)	0.2392	0.3532
PA	0.1004	0.1077
PA (Fabricated)	0.0283	0.0481

Table 5.1: Global Moran's I measurements before and after partisan sorting averaged over 25 simulations.

5.2.1 Experimental Set-Up

This experiment focuses on two test cases: MI and PA. In PA, under fixed Democratic control with sorting enabled, Democrats are unable to create favorable maps. We hypothesize that this outcome is influenced by the number and spatial dispersion of Democratic urban centers. Specifically, when Democratic voters are concentrated in one or two large urban hubs—as in PA—it becomes more difficult for Democrats to draw favorable districts beyond those areas. In contrast, when Democratic voters are spread across multiple urban centers—as seen in MI—it becomes possible for the Democratic Party obtain a favorable map.

To test this hypothesis, new baseline experiments were conducted with fabricated initial voter distributions designed to produce different spatial outcomes after sorting. In the

[3] Including Wayne, Macomb, Oakland, and Washtenaw counties.

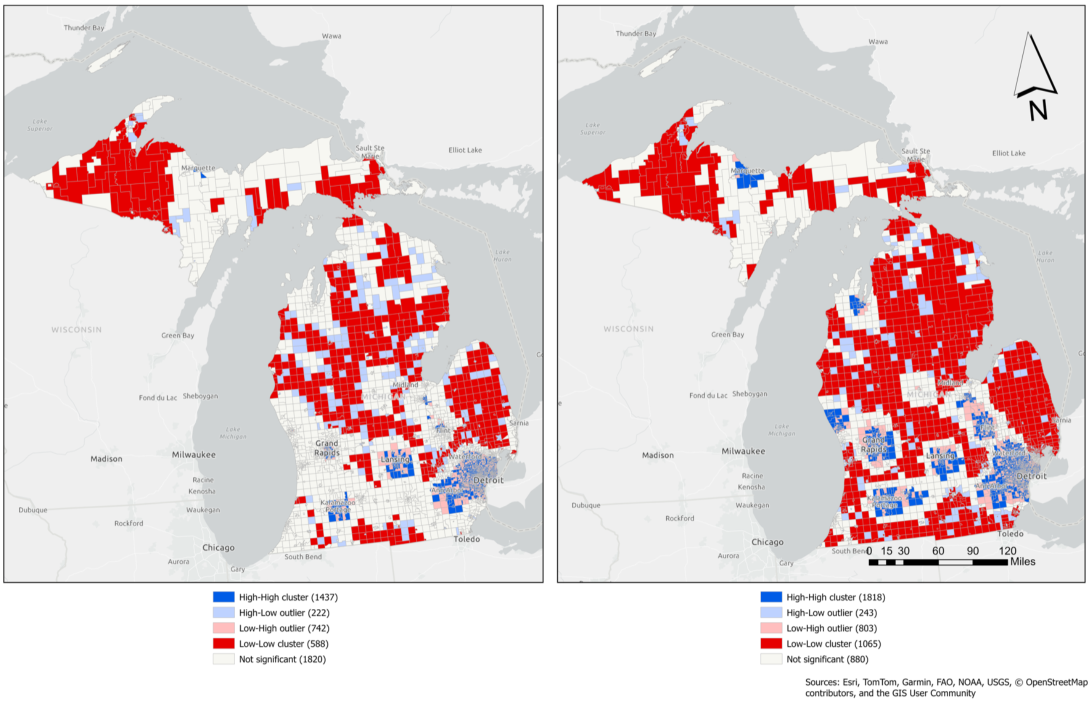

(A) MI

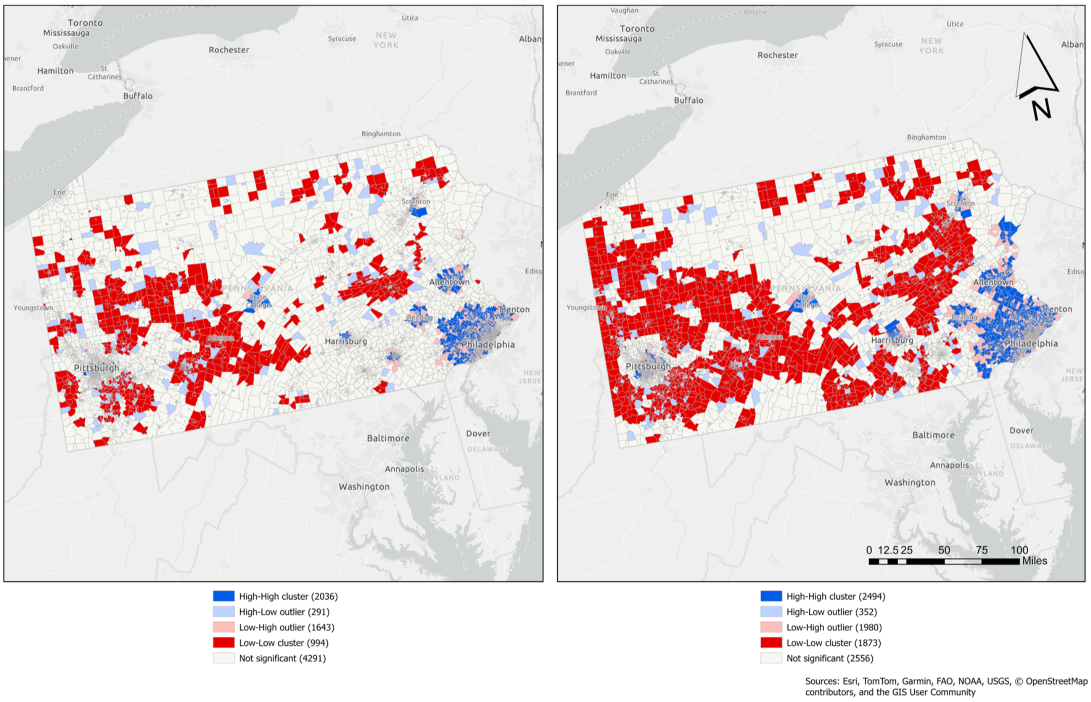

(B) PA

FIGURE 5.7: Local Moran's I classification for MI and PA precincts before (left) and after (right) partisan sorting using default model parameters. The classification distinguishes four cluster types: **high-high** clusters represent Democratic enclaves, where precincts with high Democratic vote shares are surrounded by similar precincts; **low-low** clusters represent Republican enclaves, where precincts with low Democratic vote shares (i.e., high Republican support) are adjacent to similarly Republican-leaning areas; **low-high** outliers are Republican precincts surrounded by Democratic precincts; and **high-low** outliers are Democratic precincts surrounded by Republican ones.

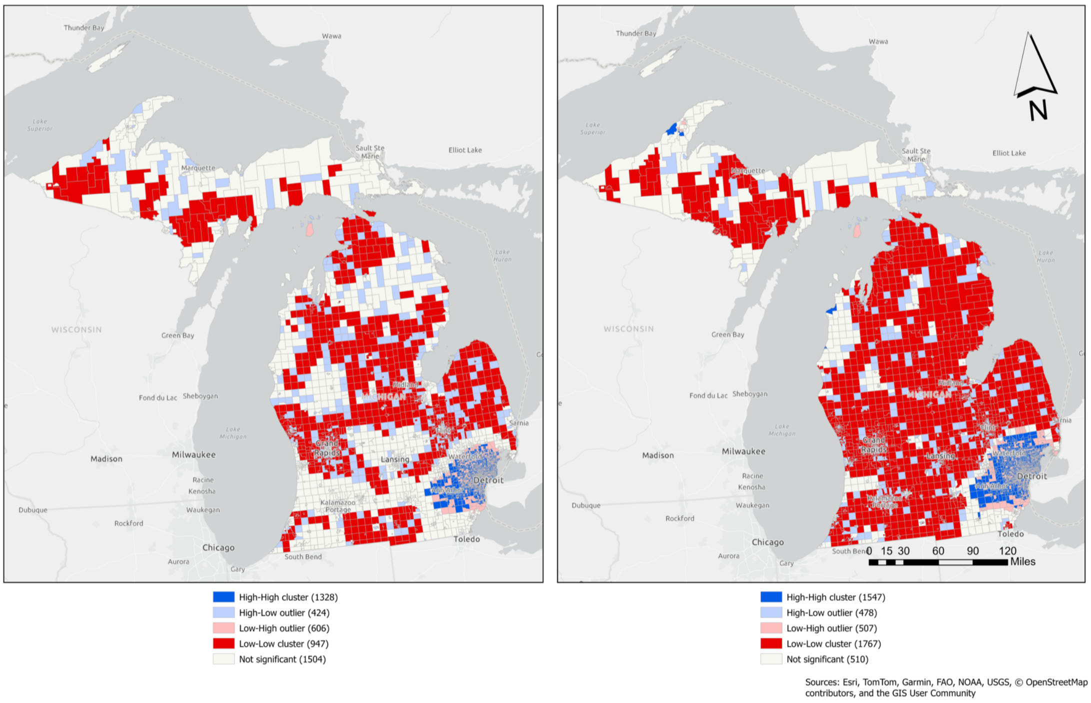

(A) MI (Fabricated)

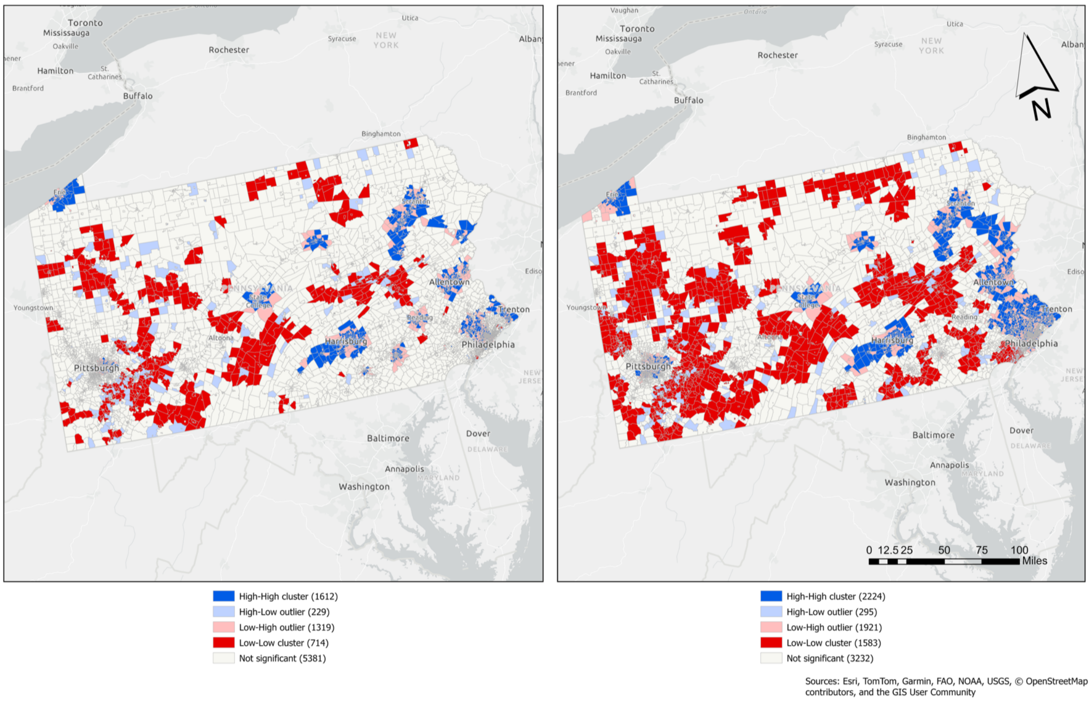

(B) PA (Fabricated)

FIGURE 5.8: Local Moran's I classification for MI and PA precincts using fabricated initial voter distributions before (left) and after (right) partisan sorting using default model parameters. The classification distinguishes four cluster types: **high-high** clusters represent Democratic enclaves, where precincts with high Democratic vote shares are surrounded by similar precincts; **low-low** clusters represent Republican enclaves, where precincts with low Democratic vote shares (i.e., high Republican support) are adjacent to similarly Republican-leaning areas; **low-high** outliers are Republican precincts surrounded by Democratic precincts; and **high-low** outliers are Democratic precincts surrounded by Republican ones.

fabricated PA scenario, a 300,000 Democratic voters from Philadelphia were relocated to slightly Democratic-leaning counties, while an equal number of Republican voters were moved in the opposite direction (Fig. 5.7b, 5.8b). This redistribution reduced Philadelphia's dominance as PA's sole Democratic hub and instead produced a pattern of several smaller Democratic strongholds across the state (Fig. 5.8b), with only about 44% of Democratic voters now residing in the Philadelphia area after sorting. In contrast, the modified MI scenario concentrated 250,000 Democratic voters in the Detroit region while redistributing an equal number of Republican voters elsewhere (Fig. 5.7a, 5.8a), effectively establishing Detroit as the state's dominant Democratic stronghold, home to approximately 67% of Democratic voters after sorting (Fig. 5.8a). The correct redistribution of voters is confirmed by the Global Moran's I values for both states (Table 5.1). The results show that MI becomes more spatially segregated under the fabricated initial voter distribution, while PA becomes less segregated—both before and after sorting.

These new baseline experiments followed the exact same structure and process as the original baseline simulations, with the only difference being the change in initial voter distribution. The results are compared to the original experiments to assess whether Democrats in PA can now create more favorable maps, and whether Democrats in MI are hindered by their concentrated support in Detroit. If the outcomes shift accordingly, it would offer further substantiation for the hypothesis that the number and spatial arrangement of urban Democratic strongholds can influence the fairness and manipulability of redistricting outcomes.

5.2.2 Results

This section presents the results of the additional baseline experiments using fabricated initial voter distributions for MI and PA, and compares them to the original baseline results based on empirical voter distributions (Section 5.1.2). Results are discussed separately for each state.

MI In the baseline experiments using empirical data for MI, Democrats were able to generate a favorable map under fixed control whether partisan sorting was modeled or not (Fig. 5.4a). However, with the fabricated voter distribution—where Democratic voters were concentrated in Detroit—Democrats lost their ability to draw favorable maps under both sorting and non-sorting scenarios (Fig. 5.9a). This marks a complete reversal of the original baseline results and underscores how the spatial concentration of Democratic voters can severely undermine their gerrymandering potential while enhancing Republican advantage.

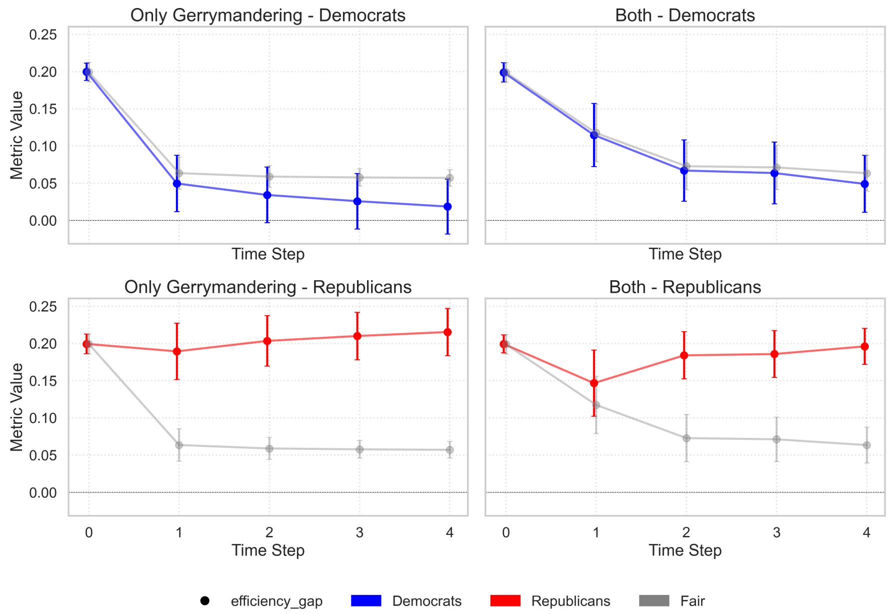

(A) Fixed Party Control

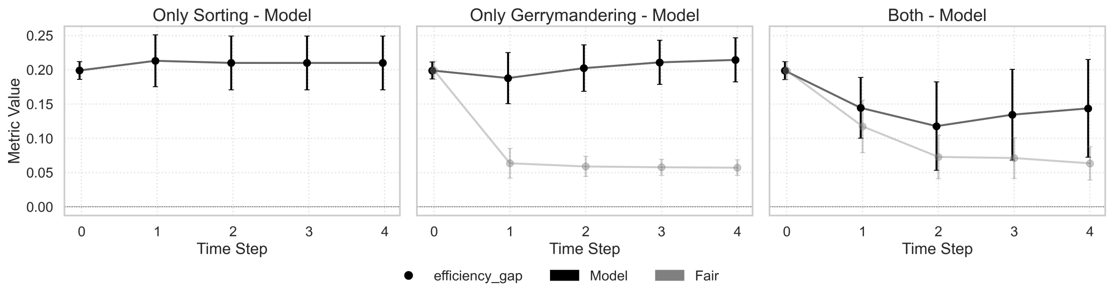

(B) Model-determined Control

FIGURE 5.9: Temporal evolution of the efficiency gap in the baseline experiments for ***MI***, using ***fabricated*** initial voter distribution, under both fixed control and model-determined control scenarios.

In the model-determined control scenarios, the fabricated distribution led to Republicans gaining initial control in 100% of simulations (Fig. 5.11a). This generally allowed them to retain control throughout. However, the randomness introduced by sorting occasionally resulted in transitions to fair control, which in turn lowered the average efficiency gap toward zero (Fig. 5.9b).

PA In the original baseline results for PA, Democrats struggled to generate favorable maps under fixed control when sorting was present and achieved only marginal advantage in the gerrymandering-only scenario (Fig. 5.5a). After redistributing Democratic voters away from Philadelphia, Democrats were able to produce significantly more favorable maps in the gerrymandering-only condition and achieved somewhat advantageous outcomes even when sorting was included (Fig. 5.10a). This indicates that a more spatially

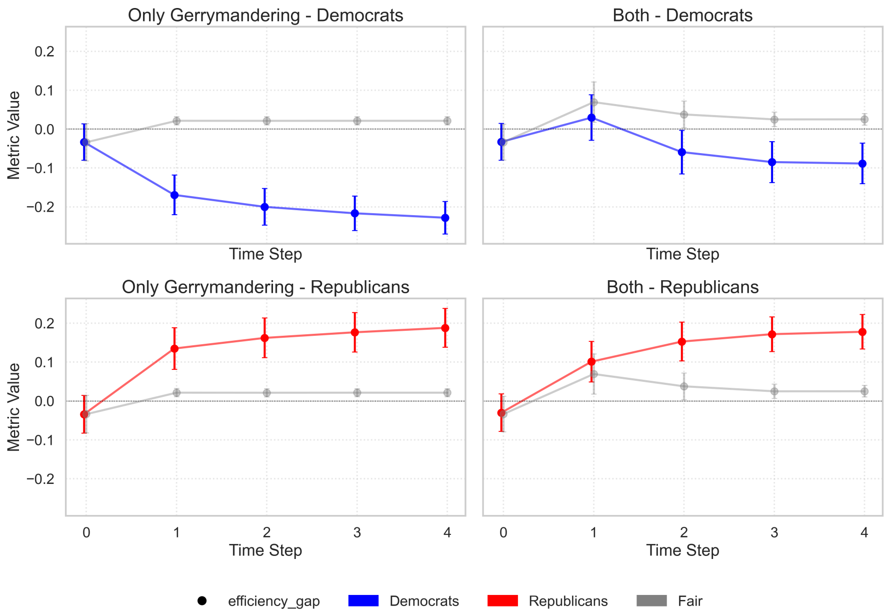

(A) Fixed Party Control

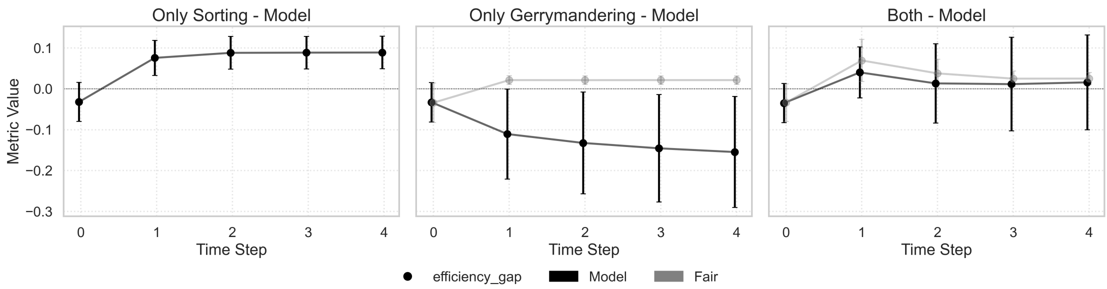

(B) Model-determined Control

FIGURE 5.10: Temporal evolution of the efficiency gap in the baseline experiments for ***PA***, using ***fabricated*** initial voter distribution, under both fixed control and model-determined control scenarios.

dispersed Democratic voter base substantially improves their ability to gerrymander and counteract sorting effects. Meanwhile, the Republican Party's ability to gerrymander remained largely unchanged.

In model-determined scenarios, Democrats were granted initial control in just over 75% of simulations (Fig. 5.11b). This typically enabled them to maintain control throughout. However, as in MI, sorting occasionally shifted control to a fair process, reducing the average efficiency gap (Fig. 5.10b). Importantly, under sorting-only conditions, the results reaffirm that the initial congressional map heavily favors Republicans, despite the fabricated initial voter distribution.

In conclusion, these experiments provide a preliminary exploration of how the spatial distribution of Democratic voters influences redistricting outcomes. Concentrating Democratic voters into a single urban hub, as in the modified MI scenario, significantly

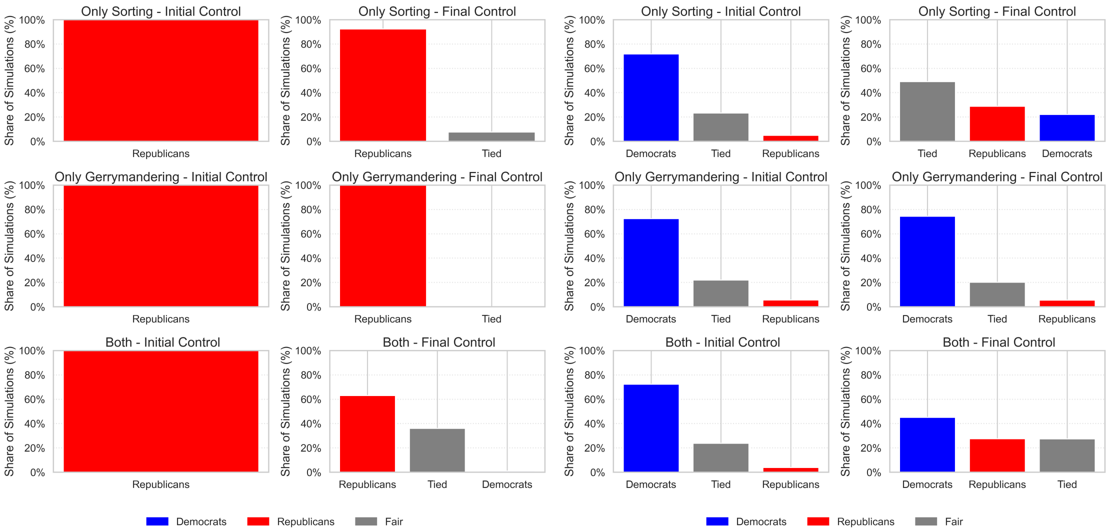

(A) MI (B) PA

FIGURE 5.11: Comparison of party control from initial to final cycle in baseline experiments for PA and MI, based on fabricated initial voter distributions, where redistricting control is based on electoral outcomes.

undermines their ability to gerrymander effectively and amplifies Republican advantage, particularly under sorting. Conversely, redistributing Democratic voters into multiple smaller strongholds, as done in PA, enhances their ability to generate fairer and more competitive maps. These findings highlight that not only the partisan makeup, but also the geographic configuration of voter populations, fundamentally shapes the fairness and effectiveness of redistricting under both gerrymandering and sorting dynamics. However, it is important to note that these results are not conclusive evidence but rather serve as an illustrative demonstration of possible mechanisms at play. The simplified nature of the model and its assumptions mean that the findings should be interpreted as exploratory insights rather than definitive conclusions.

5.3 Redistricting Reform Experiments

To address sub-research questions S-RQ5 and S-RQ6, concerning the efficacy of redistricting reforms in mitigating the adverse effects of gerrymandering and partisan sorting, this experiment incorporates three redistricting reforms: (1) a requirement for electoral *competitiveness*; (2) a requirement for district *compactness*; and (3) a requirement for *both* district competitiveness and compactness criteria.

5.3.1 Experimental Set-Up

To evaluate the effectiveness of redistricting reforms, three sets of redistricting reform experiments are conducted. Each experiment introduces a constraint into the redistricting optimization function: one promoting district compactness, one promoting competitiveness, and one promoting both. The reforms are integrated into a modified optimization function that represents the trade-off between partisan objectives and the chosen reform criteria. The optimization function used for redistricting is redefined as follows:

$$\mathcal{O}(x) = \begin{cases} w_1 \cdot \text{Reform}(x) + w_2 \cdot \text{Gerrymandering}_P(x) + \varepsilon, & \text{if } P = R \vee D \\ \text{Reform}(x) + \varepsilon, & \text{if } P = T \end{cases} \tag{5.1}$$

where:

- **Gerrymandering Term ($P = R$)**: $\text{Gerrymandering}_R(x)$ represents the proportion of districts won by Republicans, defined as:

$$\text{Gerrymandering}_R(x) = \frac{1}{|\mathcal{D}(x)|} \sum_{i \in \mathcal{D}(x)} 1\left(N_R(i) > N_D(i)\right)$$

  where:

  - $\mathcal{D}(x)$ = represents the set of all districts in the proposed redistricting plan x,
  - $N_R(i)$ and $N_D(i)$ = denote the number of Republican and Democratic agents in district i.

- **Gerrymandering Term ($P = D$)**: $\text{Gerrymandering}_D(x)$ represents the proportion of districts won by Democrats, defined as:

$$\text{Gerrymandering}_D(x) = \frac{1}{|\mathcal{D}(x)|} \sum_{i \in \mathcal{D}(x)} 1\left(N_D(i) > N_R(i)\right)$$

- **Redistricting Reform Term**: $\text{Reform}(x)$ reflects the degree to which a given redistricting plan satisfies the redistricting criterion, either competitiveness or compactness:

$$\text{Reform}(x) = \begin{cases} 1 - \frac{1}{|\mathcal{D}(x)|} \sum_{i \in \mathcal{D}(x)} \frac{|N_D(i) - N_R(i)|}{N_D(i) + N_R(i)}, & \text{if Competitiveness} \\ \frac{1}{|\mathcal{D}(x)|} \sum_{i \in \mathcal{D}(x)} \frac{4\pi \cdot \text{Area}(i)}{\text{Perimeter}(i)^2}, & \text{if Compactness} \\ (1 - \frac{1}{|\mathcal{D}(x)|} \sum_{i \in \mathcal{D}(x)} \frac{|N_D(i) - N_R(i)|}{N_D(i) + N_R(i)}) + (\frac{1}{|\mathcal{D}(x)|} \sum_{i \in \mathcal{D}(x)}), & \text{if Both} \end{cases}$$

- **Stochastic Term**: ε is a random noise component drawn from a normal distribution, representing unpredictability in the redistricting process:

$$\varepsilon \sim \mathcal{N}(0, \sigma)$$

- **Weights**: w_1 and w_2 determine the trade-off between adhering to redistricting criteria and pursuing partisan advantage. w_1 ranges from 0 to 1 and reflects the importance given to the reform term, while $w_2 = 1 - w_1$ reflects the weight of maximizing partisan advantage.

The redistricting reform experiments are designed to evaluate the effectiveness of competitiveness and compactness criteria in mitigating partisan bias under varying simulation scenarios. Each reform is tested under two experimental setups: (1) with only gerrymandering enabled, and (2) with both gerrymandering and geographical partisan sorting enabled. This dual setup allows for assessing whether the reforms can still promote fairer outcomes even when sorting dynamics are at play. To simulate the trade-off between partisan advantage and reform goals, each reform is governed by a weight parameter (w_1) that balances the objective of the reform (competitiveness, compactness, or both) against partisan interest. This weight is systematically varied from 0 to 1 in increments of 0.1, with each value simulated for 250 independent iterations per state and condition. The complementary weight ($w_2 = 1 - w_1$) is applied to the partisan gerrymandering objective, ensuring a consistent total influence across objectives. Redistricting control is determined by the model's default mechanism, which assigns control based on electoral outcomes after each cycle, reflecting how political power would realistically shift over time. All simulations use the model's default parameter settings (Table 3.1) and are applied to four swing states—GA, WI, MI, and PA—to ensure comparability and generalizability of results. Each simulation tracks five outputs: three partisan fairness metrics (efficiency gap, mean-median difference, and declination), average district competitiveness, and average district compactness. These indicators provide an overview of how each redistricting reform shapes the quality and fairness of the resulting congressional maps.

5.3.2 Results

This section presents the results from experiments that apply redistricting reforms, specifically competitiveness and compactness criteria, under varying levels of enforcement by adjusting w_1. These experiments aim to evaluate whether such criteria can effectively counteract the influence of gerrymandering and partisan sorting to promote partisan fairness. Results are discussed in terms of their impact on partisan fairness metrics, average competitiveness, and average compactness across all four states. Partisan fairness will once again be evaluated using the efficiency gap, while results for the declination and mean-median difference are included in Appendix C.2.

Measuring the Effectiveness of Redistricting Reforms The impact of redistricting reforms is evaluated using three output metrics: partisan fairness, average district competitiveness, and average district compactness across all four states. For each state, we compare gerrymandering scenarios with and without partisan sorting to assess how sorting influences these metrics. Notably, the reforms perform as intended: increasing the reform weight for a given criterion consistently leads to improvements in its corresponding metric across all states both in the presence and absence of partisan sorting (Fig. 5.12a, 5.12b, 5.13a, 5.13b, 5.14a, 5.14b, 5.15a, and C.16b). Examples of maps generated under each reform with a weight of 1 after partisan sorting are shown in Figure C.17 in Appendix C.2.

In the absence of partisan sorting, increasing the reform weight for competitiveness leads to only modest improvements in average congressional map competitiveness (Fig. 5.12a, 5.13a, 5.14a, and 5.15a). This limited effect is largely due to already high baseline competitiveness—typically above 75%—which leaves little room for further gains. However, when partisan sorting is introduced, districts become more politically homogeneous, and average competitiveness drops sharply, often falling below 40%. In such cases, the competitiveness criterion has greater potential to make a difference, and its positive effect becomes more pronounced with higher reform weights. When both competitiveness and compactness criteria are applied simultaneously, a similar pattern emerges, although competitiveness tends to be slightly lower than in the scenario where competitiveness alone is prioritized. Importantly, the competitiveness reform alone does not contribute to improving compactness.

Raising the weight of the compactness criterion consistently increases average district compactness across all states. Unlike competitiveness, compactness is less affected by partisan sorting because it is structurally independent of voter distribution dynamics (Fig. 5.12b, 5.13b, and 5.14b). PA is the one exception, where the introduction of partisan sorting significantly weakens the effectiveness of the compactness reform (Fig. C.16b). A similar trend is seen when both criteria are optimized together, though the resulting compactness scores are slightly lower than when compactness alone is prioritized. Notably, when both criteria are applied, both metrics improve with increasing reform weight. However, as with competitiveness, the compactness reform alone does not lead to greater electoral competition.

Figures 5.12c, 5.13c, 5.14c, and 5.15c present efficiency gap outcomes across all four states under each of the three reform strategies, both with and without partisan sorting. In scenarios that include sorting, the variance in the efficiency gap is generally higher, reflecting the unpredictability introduced by shifting voter distributions. Despite this, a clear threshold effect emerges: across all states and reforms, meaningful improvements in partisan fairness—indicated by efficiency gaps near zero—only occur when reform weights are relatively high, typically in the 0.7 to 0.9 range. Although state-specific complexities in PA and WI slightly blur this pattern (explained further below), the overall results indicate that strong reform efforts are effective at reducing partisan bias. In contrast, weakly applied reforms have minimal impact, underscoring the importance of robust and sustained reform enforcement.

State-Specific Patterns In both ***GA*** and ***MI***, the competitiveness and compactness criteria, as well as their combination, are effective at producing fairer congressional maps, regardless of whether partisan sorting is present (Fig. 5.12c and 5.14c). However, these reforms only yield substantial improvements when their implementation is strong, typically at reform weights of 0.7 or higher. This indicates that while either criterion can act as a meaningful safeguard against gerrymandering and partisan sorting in these states, their effectiveness depends on a high level of enforcement and commitment.

In ***WI***, the competitiveness criterion is more effective than compactness in reducing partisan bias, a pattern that also holds when both criteria are combined. This trend remains consistent across scenarios with and without partisan sorting, suggesting that competitiveness is the more influential lever for reform in this context. As with other states, these improvements only emerge when the reform weight is high—generally 0.8 or above—reinforcing the need for strong policy enforcement.

PA continues to stand out as an exception in several ways:

- The variance in the efficiency gap outcomes is higher without partisan sorting (Fig. 5.15). This stems from the roughly balanced or tied initial control of redistricting between Democrats and Republicans (Fig. 5.6d), which introduces greater randomness in redistricting results. In contrast, when sorting is introduced, which consistently benefits Republicans, the efficiency gap becomes more stable, though biased in their favor.

- Even at high reform weights (≥ 0.9), improvements in the efficiency gap are less substantial compared to other states (Fig 5.15c). This suggests that the reforms are less effective at offsetting the effects of sorting. The reason is likely structural: sorting disproportionately disadvantages Democrats in PA, making it extremely

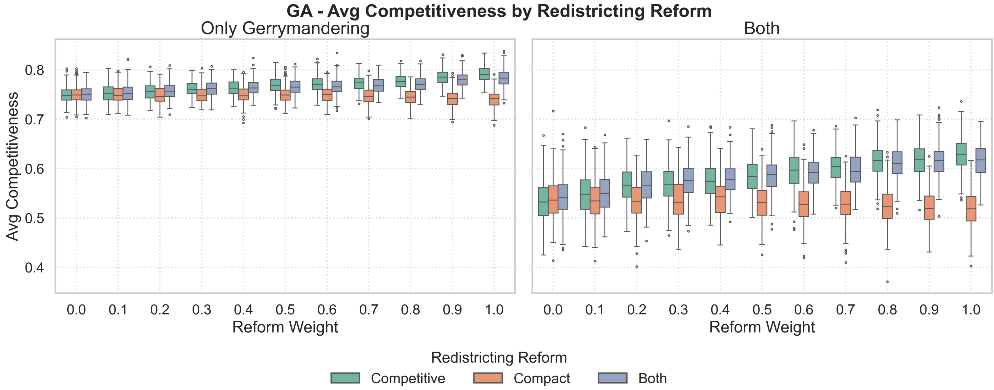

(A) Avg. Competitiveness

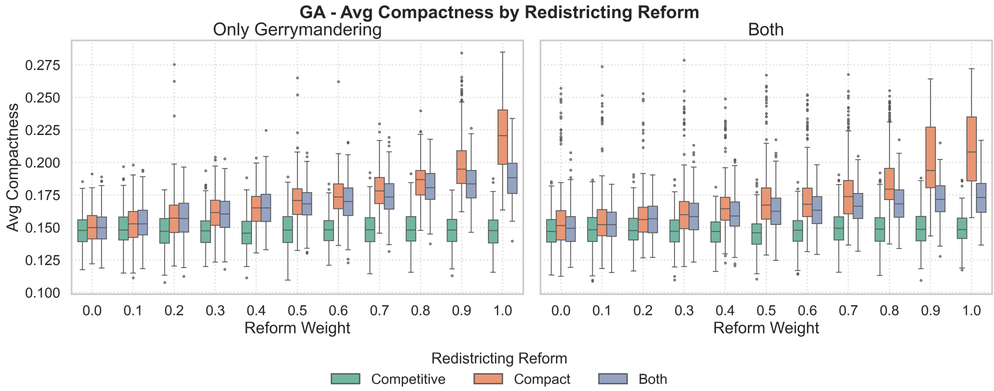

(B) Avg. Compactness

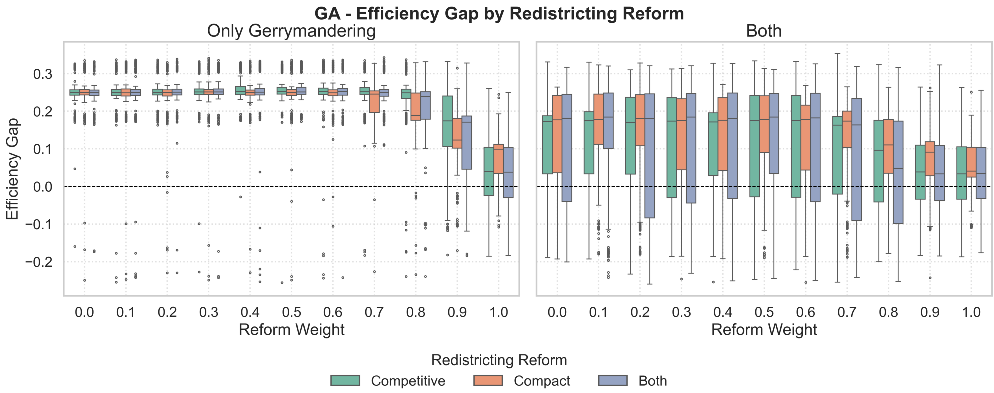

(C) Efficiency Gap

FIGURE 5.12: Effect of compactness and competitiveness reforms on redistricting outcomes in GA, under scenarios with and without partisan sorting.

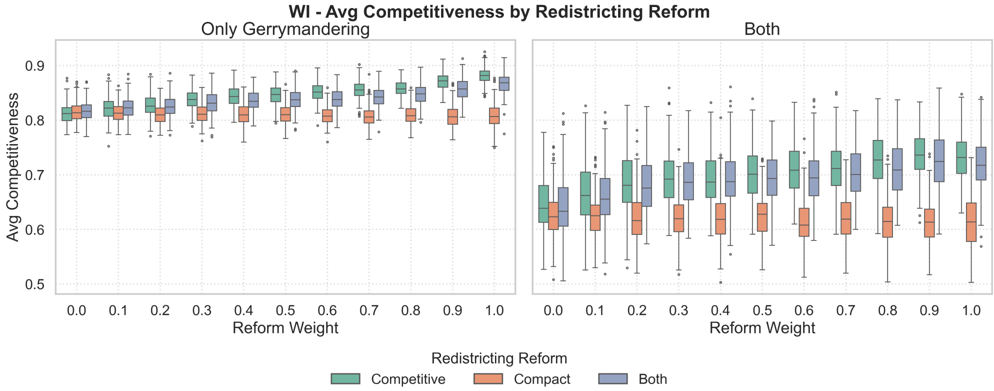

(A) Avg. Competitiveness

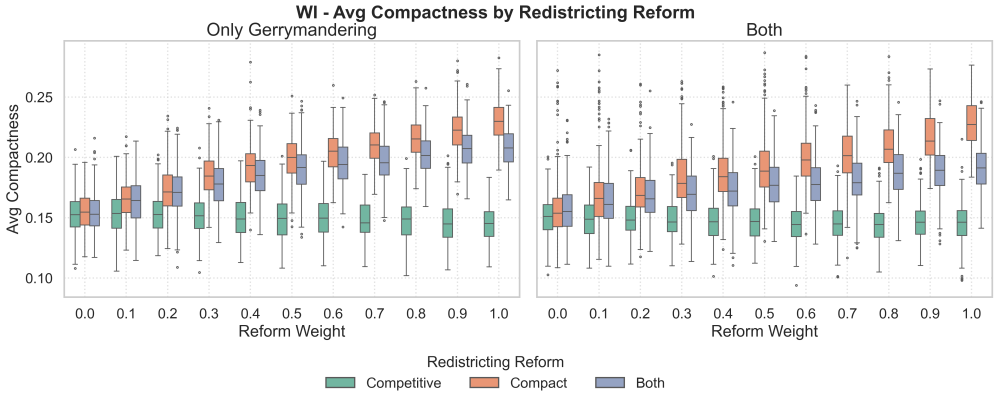

(B) Avg. Compactness

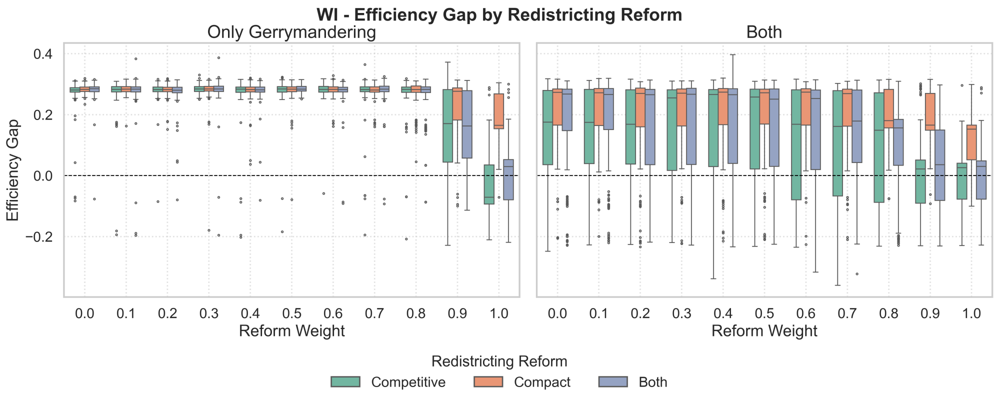

(C) Efficiency Gap

FIGURE 5.13: Effect of compactness and competitiveness reforms on redistricting outcomes in WI, under scenarios with and without partisan sorting.

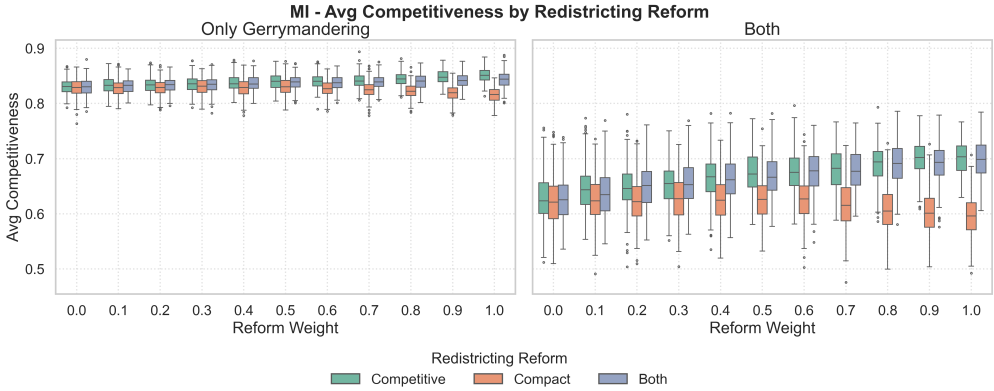

(A) Avg. Competitiveness

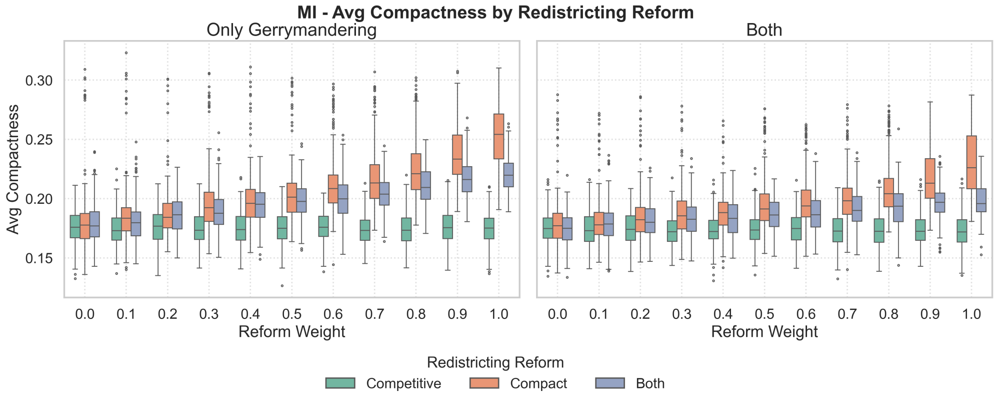

(B) Avg. Compactness

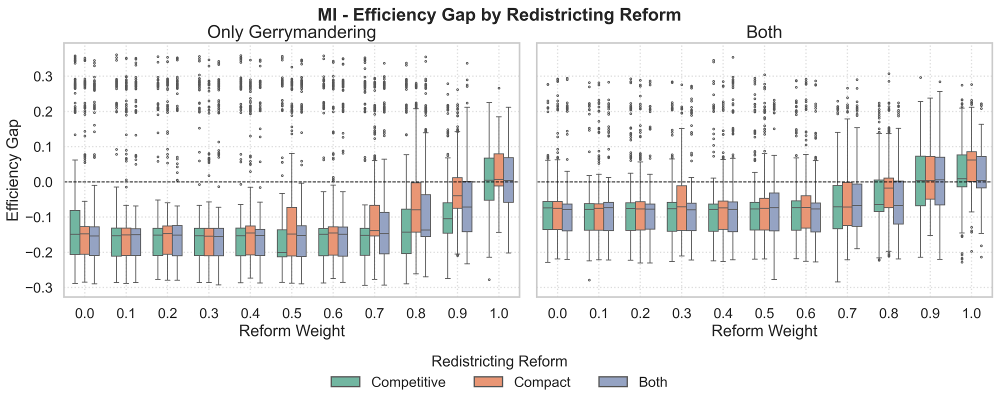

(C) Efficiency Gap

Figure 5.14: Effect of compactness and competitiveness reforms on redistricting outcomes in MI, under scenarios with and without partisan sorting.

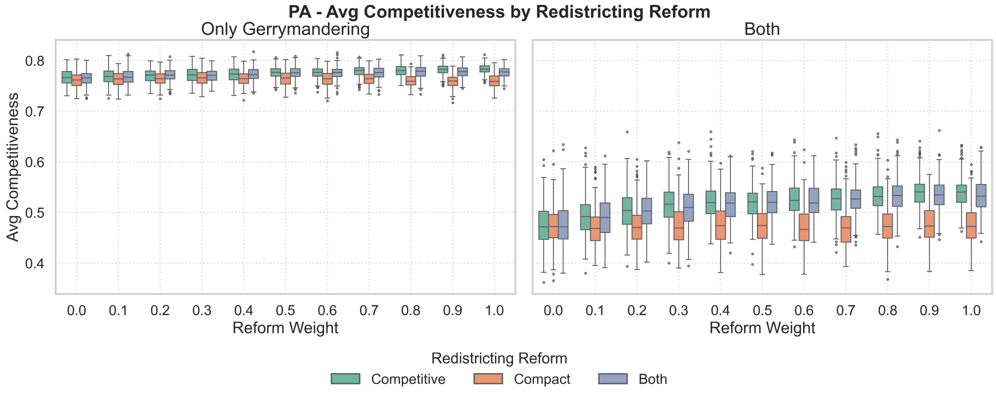

(A) Avg. Competitiveness

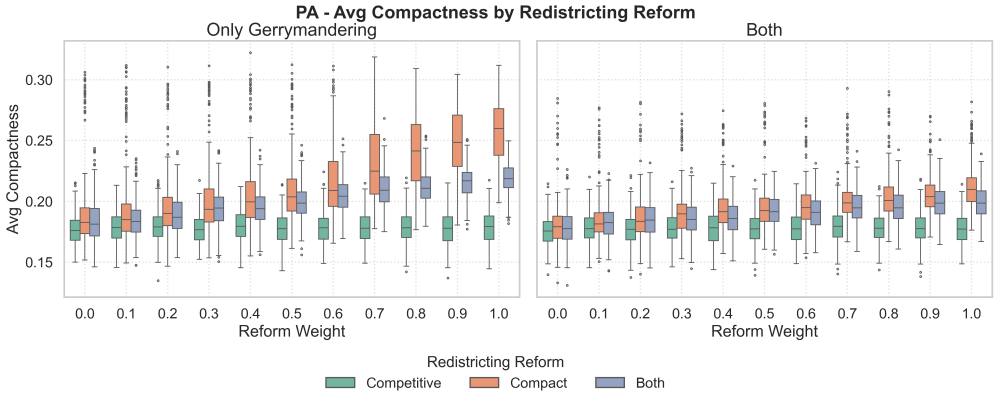

(B) Avg. Compactness

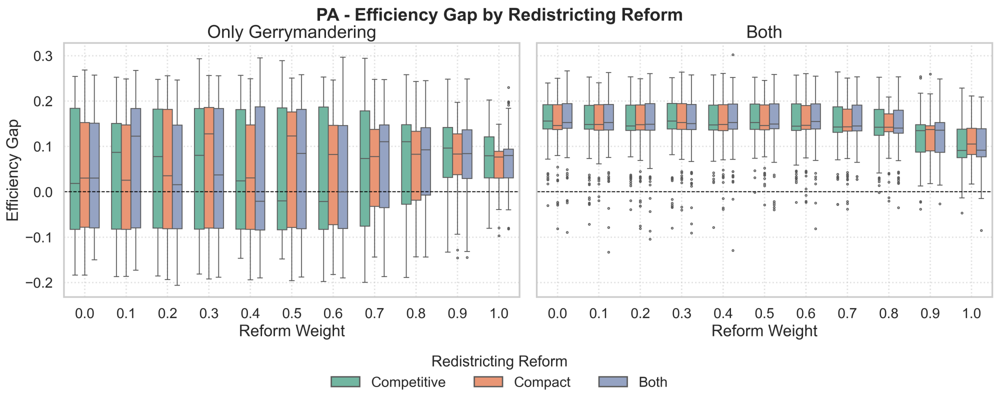

(C) Efficiency Gap

FIGURE 5.15: Effect of compactness and competitiveness reforms on redistricting outcomes in PA, under scenarios with and without partisan sorting.

difficult—if not impossible—to draw maps favoring them. As a result, the underlying political geography severely limits the reforms' potential impact.

- The compactness reform becomes notably less effective under sorting (Fig. C.16b). While it achieves an average compactness score of ≈ 0.26 without sorting, this drops significantly to around ≈ 0.21 when sorting is modeled.

- Similarly, the competitiveness criterion loses effectiveness under sorting (Fig. 5.15a). The resulting average competitiveness score hovers around 0.55, which is considerably lower than in other states, where scores typically exceed 0.65.

PA's continued outlier status may again be attributed to its unique political geography. To test this hypothesis, the reform experiments were rerun using the fabricated voter distribution (as described in Section 5.2). Under these conditions, the previously observed anomalies disappear (Fig. C.16 in Appendix C.2). The efficiency gap improves more consistently with higher reform weights, and the competitiveness and compactness reforms remain effective even when partisan sorting is simulated. This preliminary result suggests that PA's underlying voter distribution, particularly the spatial concentration of Democratic voters, plays a critical role in limiting the impact of redistricting reforms in the state.

General Observations In addition to the state-specific dynamics, the reform experiments reveal several consistent trends that emerge across all four states:

- Redistricting reforms only begin to meaningfully counteract gerrymandering and the effects of partisan sorting when implemented with high reform weights. Minimal or moderate enforcement yields little impact against partisan interference. Nonetheless, in both sorting and non-sorting scenarios, the reforms contribute to fairer electoral maps. An exception is PA, where the underlying political geography structurally benefits Republicans, limiting the reforms' effectiveness.

- The competitiveness and compactness criteria function as independent reform objectives; improving one does not inherently improve the other. This underscores the need to treat them as separate, complementary tools in redistricting reform design.

- Partisan sorting amplifies electoral volatility by introducing unpredictable population shifts, which increase the variance in partisan fairness metrics and reduce average competitiveness through the formation of more politically homogeneous districts.

Chapter 6

Discussion

This section reflects on the main findings of the thesis, placing them in the context of broader redistricting and political geography literature. It discusses the implications of the results for understanding the dynamic relationship between gerrymandering, partisan sorting, and redistricting reforms. Additionally, it identifies the limitations of the modeling approach and provides directions for future research to improve and extend the current work.

6.1 Main Contributions

The most interesting contribution of this thesis, that the spatial concentration and dispersion of Democratic strongholds critically shape redistricting outcomes, closely aligns with the theory of unintentional gerrymandering put forward by Chen and Rodden [65]. Their study demonstrated that Democrats tend to be highly clustered in dense urban areas, which systematically disadvantages them under single-member district systems due to the inefficiency of vote distribution. Even in the absence of intentional partisan manipulation, these geographic patterns result in a consistent electoral bias favoring Republicans. This structural bias arises because Democratic votes are "wasted" in overwhelmingly blue districts, while Republican voters are more evenly distributed and thus more electorally efficient.

The experiments in this thesis provide support for this theory by simulating how varying the number and spatial arrangement of Democratic strongholds influences partisan advantage. The PA baseline results, where Democrats were unable to gerrymander effectively due to their high concentration in the Philadelphia region, align with Chen and Rodden's broader findings [65], as well as with a study showing that PA's political geography makes it virtually impossible for Democrats to draw a favorable map [168]. When

Democratic voters were redistributed into smaller, more geographically dispersed urban clusters, the party was able to produce significantly more favorable and competitive maps. Conversely, in MI, concentrating Democratic voters in the Detroit area reversed the original pattern, making it easier for Republicans to generate favorable outcomes under both gerrymandering and sorting conditions. These results highlight that not only the partisan composition of a state, but also the geographic configuration of its voters, plays a decisive role in determining the fairness and manipulability of redistricting. By integrating agent-based modeling with redistricting simulation, this thesis extends the literature by operationalizing and testing the mechanisms behind unintentional gerrymandering in a dynamic setting. It shows that political geography is not only a passive backdrop to redistricting but an active factor that affects it and shapes partisan fairness of electoral maps. These findings reaffirm the structural nature of electoral bias and demonstrate the importance of considering geographic voter patterns to design fairer redistricting systems.

The secondary contribution is that redistricting reforms, specifically those enforcing district competitiveness and compactness, can improve the fairness of congressional maps, but only when implemented with high rigor and minimal partisan interference. Prior research has shown that redistricting reforms incorporating compactness criteria can restrict partisan gerrymandering by limiting the geometric manipulation available to mapmakers [26, 27, 65]. Likewise, promoting competitive districts has been found to enhance electoral responsiveness while reducing the prevalence of safe seats and mitigating political polarization [19, 26–28, 169]. However, these safeguards are not foolproof and rely heavily on strict enforcement. They should be removed from the control of partisan actors, as even with such measures in place, those actors can still exploit loopholes—technically complying with the reforms while securing a partisan advantage.

The experiments in this thesis reinforce this skepticism: unless reforms are implemented with a high weight—effectively sidelining partisan goals—their influence on partisan fairness metrics remains marginal. This suggests that merely including competitiveness or compactness criteria in redistricting frameworks is insufficient if these constraints can be easily overridden or diluted by partisan actors. Furthermore, the findings contribute a valuable perspective to the literature by showing that the effectiveness of redistricting criteria is strongly influenced by a state's political geography. Specifically, these criteria tend to lose impact when one party's electorate is heavily concentrated in one or two densely populated urban centers, as observed in PA. This highlights the importance of accounting for state-specific geographic patterns when designing redistricting reforms, as such patterns can significantly limit the reforms' ability to mitigate partisan gerrymandering.

6.2 Limitations

While this thesis provides valuable insights into the relationship between geographical partisan sorting and partisan gerrymandering, several limitations should be acknowledged.

First, political control within the simulation is determined by which party wins the most congressional districts, a simplification made for computational feasibility purposes. In reality, redistricting decisions are often controlled by the party holding both chambers of a state legislature, and gerrymandering also takes place at the state legislative level. This simplification may limit the realism of modeled redistricting dynamics, particularly in states with split control.

Second, the mechanisms used to simulate mapmaker behavior, whether optimizing for partisan advantage or adherence to reform principles, do not fully capture the complexity of real-world redistricting processes. Important considerations such as preserving communities of interest, respecting natural geographic features, and ensuring minority representation through majority-minority districts are not explicitly modeled. As a result, the realism and applicability of the simulated maps are necessarily constrained.

Furthermore, the utility function guiding agents' residential sorting behavior includes weights that are somewhat arbitrary; while informed by plausible assumptions, they may not capture the full heterogeneity of individual preferences. The model also assumes a fixed proportion and initial spatial distribution of Republican and Democratic voters in each state, based on the 2020 presidential election results. This static setup neglects potential political shifts over time, thereby limiting the model's dynamic realism. Moreover, the model does not allow for cross-state migration, agents can only relocate within the state in which they reside. As a result, the model cannot capture interstate mobility trends that may significantly influence local partisan composition and district outcomes in the real world.

Finally, the experiments are conducted on only four U.S. swing states, selected for their competitive political environments. While this allows for focused analysis, it restricts the generalizability of the findings to other states with different political geographies or partisan balances.

6.3 Future Work

Several promising directions for future research could deepen our understanding of the relationship between political geography and gerrymandering and how they affect redistricting outcomes. One such avenue involves modeling different forms of segregation. While this thesis centers on partisan sorting, future work could examine how racial or income-based segregation patterns affect redistricting outcomes.

Another opportunity lies in testing alternative redistricting reforms. The current model evaluates compactness and competitiveness criteria as reform mechanisms, but future experiments could include additional criteria such as community preservation or majority-minority district protections. Examining these reforms both individually and in combination can help identify which criteria—or mix of criteria—most effectively counteract partisan gerrymandering, while accounting for a state's unique political geography.

Expanding the model to include a broader range of states would also enhance the robustness of the findings. While this thesis focuses on four swing states, applying the framework to more geographically and politically diverse states could uncover state-specific dynamics and improve the generalizability of results. Additionally, experimenting with different initial voter distributions—such as fabricated or counterfactual spatial arrangements—could help clarify which aspects of political geography most strongly influence partisan bias.

Finally, future work could enhance realism by simulating gerrymandering across all levels it pertains to, and determining redistricting control based on state legislative election outcomes. Currently, redistricting and elections are only modeled at the congressional level, whereas in practice, partisan control is often preserved through coordinated gerrymandering at the state house, state senate, and congressional levels. Incorporating these different layers of government—though computationally intensive—could substantially enhance the model's accuracy and its reflection of the real-world redistricting procedure.

Chapter 7

Conclusion

This thesis set out to investigate how partisan gerrymandering and geographical partisan sorting influence the fairness of congressional redistricting in the U.S. Using a novel agent-based model, the study examined the two phenomena in isolation and in combination across four swing states. It also evaluated the effectiveness of redistricting reforms focused on promoting compactness and competitiveness. The overarching goal—framed in the main research question (M-RQ)—was to understand the relationship between gerrymandering and partisan sorting and how it shapes the fairness, competitiveness, and compactness of electoral maps. In the remainder of this chapter, the main research question (M-RQ) and the sub-research questions (S-RQs) are addressed based on the results of the study.

Effects of Gerrymandering and Partisan Sorting (S-RQ1–S-RQ3):
The first part of the thesis explored the effects of geographical partisan sorting and gerrymandering independently. When only partisan sorting was simulated (S-RQ1), partisan biases emerged even in the absence of intentional manipulation. Democratic voters, often concentrated in urban areas, "wasted" more votes, while Republicans, being more evenly spread across rural and suburban regions, gained an electoral advantage. In three of the four modeled states (PA, MI, GA), this spatial imbalance increased partisan bias in favor of Republicans, only in WI did fairness decline in favor of Democrats. These findings replicate and extend previous research on unintentional gerrymandering, demonstrating that partisan bias can emerge naturally from the spatial distribution of voters—particularly disadvantaging electorates that are highly concentrated in dense urban areas, as is often the case for the Democratic Party.

When only gerrymandering was simulated (S-RQ2), both parties were able to manipulate district boundaries to their advantage when given control. However, the extent of this advantage varied depending on the spatial distribution of voters. In PA, where

Democratic voters were highly clustered, the Democratic Party was significantly disadvantaged by the spatial distribution of voters. Conversely, in states with multiple Democratic strongholds that were more evenly dispersed—like MI, GA, and WI—Democrats found it easier to draw favorable maps. However, overall, the initial spatial configuration of voters tended to favor Republicans, who benefited more consistently across states. These findings further emphasize the critical role of political geography in shaping the partisan fairness of redistricting outcomes.

When gerrymandering and partisan sorting were combined (S-RQ3), the combined effects introduced unpredictability into redistricting outcomes. Partisan migration patterns disrupted partisan control, making it harder for either party to consistently gerrymander successfully. In all states, these effects disproportionately harmed Democrats, as their urban clustering became more pronounced over time. Only in PA did the introduction of partisan sorting make it virtually impossible for Democrats to draw favorable maps. This outcome raised the question of how sensitive partisan bias is to underlying spatial voter distribution, motivating S-RQ4.

Sensitivity to Political Geography (S-RQ4):
To test this sensitivity, additional experiments were conducted using fabricated initial voter distributions (S-RQ4). The results confirmed that even modest changes in how voters are spatially arranged can flip redistricting outcomes. This finding reinforces the idea that political geography, how concentrated or dispersed each party's supporters are, is a key determinant of how gerrymandered a map can be. Importantly, the combined effects of gerrymandering and sorting are not uniform across states; it is highly contingent on the political landscape and the spatial distribution of partisan voters. Thus, evaluating redistricting fairness requires attention not only to overall partisan balance but also to the geographic configuration of voters.

Evaluating Redistricting Reforms (S-RQ5–S-RQ6):
The final set of sub-questions (S-RQ5 and S-RQ6) examined whether redistricting reforms, namely promoting competitiveness and compactness, could mitigate the distortions caused by gerrymandering and partisan sorting. Enforcing competitive districts (S-RQ5) generally improved the fairness and competitiveness of congressional maps. Likewise, promoting compactness (S-RQ6) constrained the geometric manipulation options available to partisan mapmakers, thereby limiting opportunities for extreme gerrymandering. However, these reforms only proved effective when strongly enforced. When compactness or competitiveness criteria were given low priority or allowed to be overridden by partisan interests during map optimization, their influence on partisan fairness was negligible. In contrast, high-weight enforcement produced meaningful improvements in fairness and reduced partisan asymmetries. Still, the effectiveness of

these reforms varied across states. In PA, for instance, the political landscape and the spatial advantage of Republicans limited the impact of reform. These results suggest that while reform can help, its success is conditional, it depends not only on rigorous implementation but also on a state's underlying political geography.

Summary (M-RQ):
In summary, this thesis demonstrates that the fairness of congressional redistricting is shaped by a dynamic relationship between partisan gerrymandering and geographical partisan sorting. While each mechanism alone can tilt the bias of congressional electoral maps, their combination produces more unpredictable and state-specific effects. Critically, the political geography of a state, including how clustered or dispersed electorates are, plays a pivotal role in determining who benefits and to what extent.

Redistricting reforms that prioritize competitiveness and compactness can counteract these biases and produce fairer electoral maps. However, they are not a universal solution. Their effectiveness hinges on strong enforcement mechanisms and an awareness of a state's political geography. Reforms must be binding, insulated from partisan influence, and account for structural biases introduced by political geography; otherwise, their impact will be inherently limited.

Chapter 8

Ethics and Data Management

This thesis adheres to the ethical code of the Informatics Institute of the University of Amsterdam[1] and complies complies with the university's research data management policies[2]. All research was conducted in accordance with the principles of academic integrity, including transparency, reproducibility, and appropriate acknowledgment of sources.

The research presented in this thesis involves computational modeling and simulation of politically driven residential segregation and political redistricting processes in the United States. No personal or sensitive data from individuals was used at any stage of the research. All input data is derived from publicly available shapefiles, election results, and demographic statistics at the precinct and county level. These data sources were aggregated, processed and stored in accordance with the university's data management policies, ensuring that all steps are well-documented and reproducible.

Ethically, this thesis engages with politically sensitive topics such as electoral fairness, gerrymandering, and political polarization. While the model is a simplification of real-world processes, it aims to provide insight into the complex dynamics that emerge from partisan sorting and redistricting. The goal of the research is not to support or criticize any political party, but to increase understanding of the systemic mechanisms that can affect fair representation. By doing so, the work contributes to informed public discourse and reflects the broader societal responsibility of computational scientists to use modeling tools in ways that support fairness, transparency, and accountability.

[1] https://ivi.uva.nl/research/ethical-code/ethical-code.html
[2] https://rdm.uva.nl/en

Appendix A

Additional Model Description

A.1 Entity Attributes

A.1.1 Individual Agents

Attribute	**Description**
`unique_id`	A unique identifier assigned to each agent.
`model`	The instance of the model the agent is part of.
`geometry`	The *(x, y)* coordinates of the agent on the map, used for visualization.
`crs`	The coordinate reference system used for mapping and display.
`utility`	A value between **0 and 1** indicating the agent's happiness, calculated using local precinct and county-level data.
`is_unhappy`	A Boolean indicating if the agent is dissatisfied (`True`) and likely to move. An agent is unhappy when their utility drops below a model-defined `tolerance` threshold.
`precinct_id`, `county_id`, `congdist_id`	The unique identifiers of the precinct, county, and congressional district where the agent resides.
`last_moved`	The number of time steps since the agent last changed residence.
`color`	The agent's political affiliation: `Red` for Republican or `Blue` for Democrat.

Table A.1: Overview of attributes for each individual agent.

A.1.2 Congressional Districts

Attribute	**Description**
`unique_id`	Unique identifier for the district.
`model`	Reference to the model instance the district belongs to.
`geometry`	Geometric boundaries of the district, used for visualization.
`crs`	Coordinate Reference System used for spatial rendering.
`type`	Specifies the kind of geographic unit: `congdist`, `county`, or `precinct`.
`rep_cnt`, `dem_cnt`	Counters that track the number of Republican and Democratic voters in the district.
`color`	Indicates majority party: `Red` for Republican or `Blue` for Democrat, or `Grey` in case of a tie.
`competitive`	Boolean indicating whether the district is electorally competitive. This is `True` if the vote margin between parties is below the user-defined `competitive_threshold`.
`precincts`	List of precinct IDs currently assigned to the district, which is updated during redistricting.

Table A.2: Overview of attributes for each congressional district.

A.1.3 Precincts

Similarly to congressional districts the precincts also possess the `unique_id`, `model`, `geometry`, `crs`, `type`, `rep_cnt`, `dem_cnt`, and `color` attributes. Table A.3 lists the attributes unique to precincts.

Attribute	**Description**
`reps`, `dems`	Lists of agent IDs representing Republican and Democratic voters residing in the precinct.
`PRES20R`, `PRES20D`, `PRES20TOT`	Republican, Democratic, and total vote counts from the 2020 U.S. presidential election. This data is used to estimate partisan composition and initialize agent placement.
`CONGDIST`	The unique ID of the congressional district that the precinct currently belongs to. This value may change during redistricting.
`COUNTY_NAME`	Identifier for the county the precinct is part of. This is fixed throughout the simulation.
`TOTPOP`	The real-world total population of the precinct. Used to determine the initial spatial allocation of agents across precincts.

Table A.3: Overview of attributes for each precinct.

A.1.4 Counties

Similarly to the congressional districts the counties also have a `unique_id`, `model`, `geometry`, `crs`, `type`, `rep_cnt`, `dem_cnt`, `color`, and `precincts`. Table A.4 lists the attributes that are unique to counties.

Attribute	**Description**
`CAPACITY`	Maximum number of agents that can live in the county, estimated from real-world data (see Section 3.1.3.1). Once full, no additional agents can relocate to this county.
`RUCACAT`	RUCA classification of the county: `rural`, `small_town`, `large_town`, or `urban`. Used in individual agents' utility calculations.
`HOUSEHOLDS`, `HOUSING_UNITS`	Real-world counts of households and housing units in the county, used to estimate the county's residential capacity.
`TOTPOP`	Total population of the county, used to determine the initial number of agents placed in the county.

Table A.4: Overview of attributes for each county.

A.2 Other Model Parameters

Parameter	**Type**	**Range**	**Description**
`state`	Str	`GA, WI, MI, PA, MN, TX`	U.S. state to simulate.
`print`	Bool	`True/False`	Whether to print intermediate results.
`vis_level`	Str	`CONGDIST, COUNTY, PRECINCT`	Level of visualization detail.
`data`	Str	Path or None	Path to input data.
`election`	Str	`PRES12, PRES16, PRES20`	Election dataset to use.
`sorting`	Bool	`True/False`	Whether to enable partisan sorting.
`gerrymandering`	Bool	`True/False`	Whether to enable redistricting.
`control_rule`	Str	`CONGDIST, FIXED`	Rule for assigning control during redistricting.
`initial_control`	Str	`Model, Democrats, Republicans`	Who initially controls redistricting. When `initial_control` is set to `FIXED`, the party that is given initial control retains control throughout the entire simulation run.

Table A.5: Overview of other model parameters.

A.3 Process Overview and Scheduling

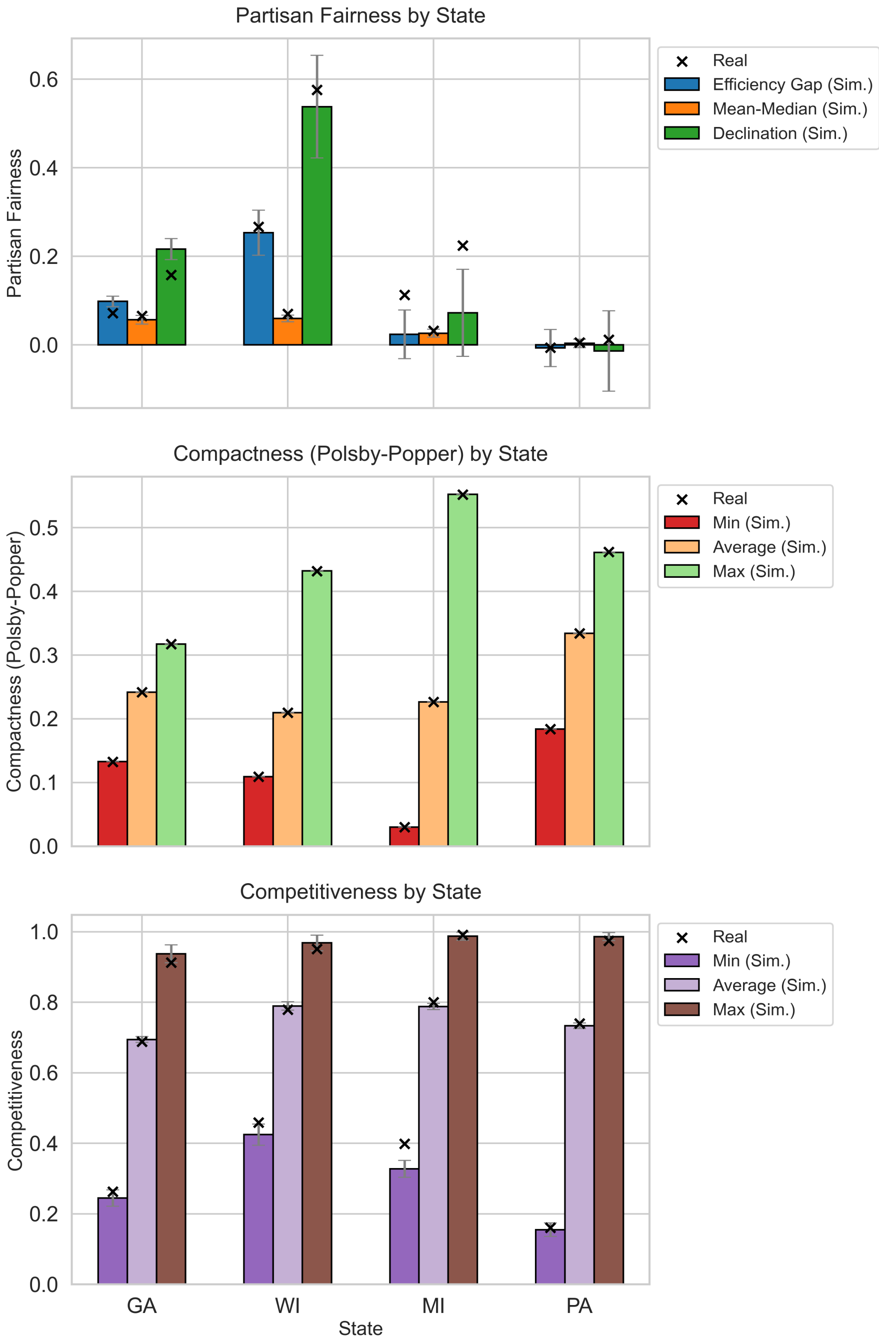

FIGURE A.1: Mean and standard deviation of initial redistricting metrics across 10,500 simulation runs per state.

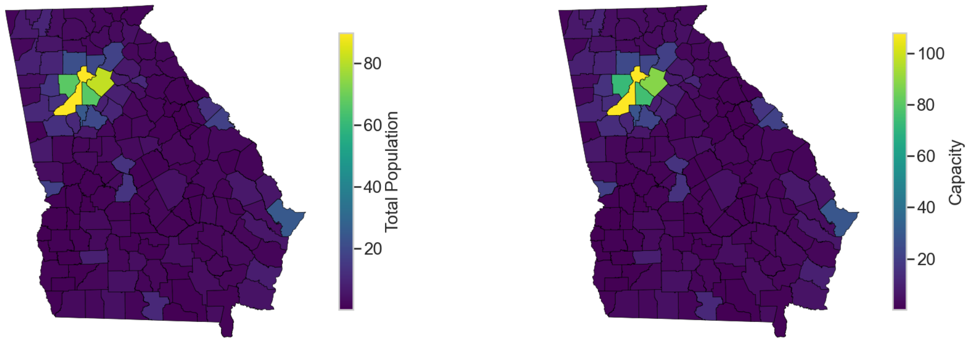

(A) GA

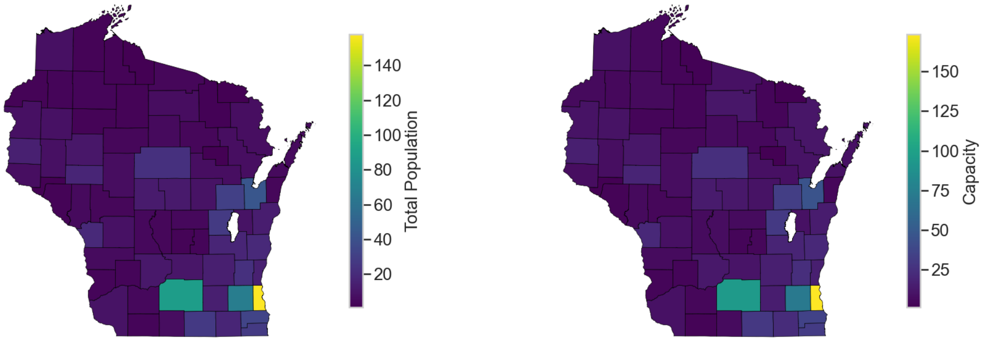

(B) WI

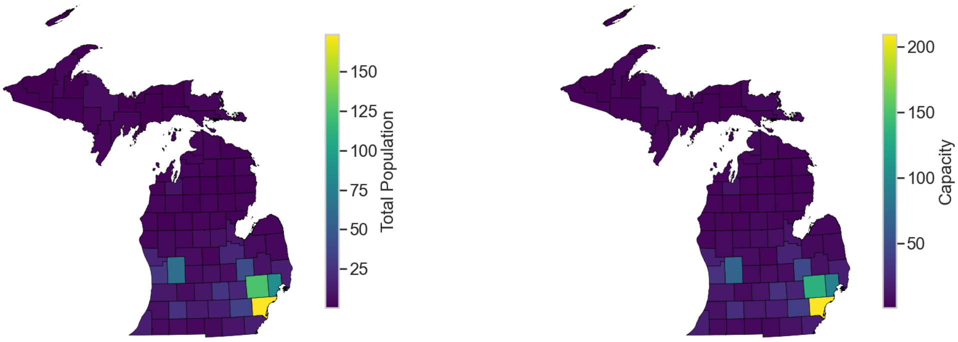

(C) MI

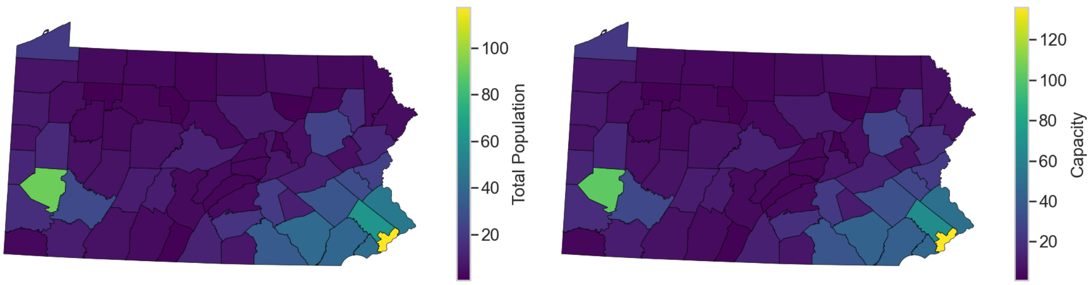

(D) PA

FIGURE A.2: Total number of agents and capacity per county across each state.

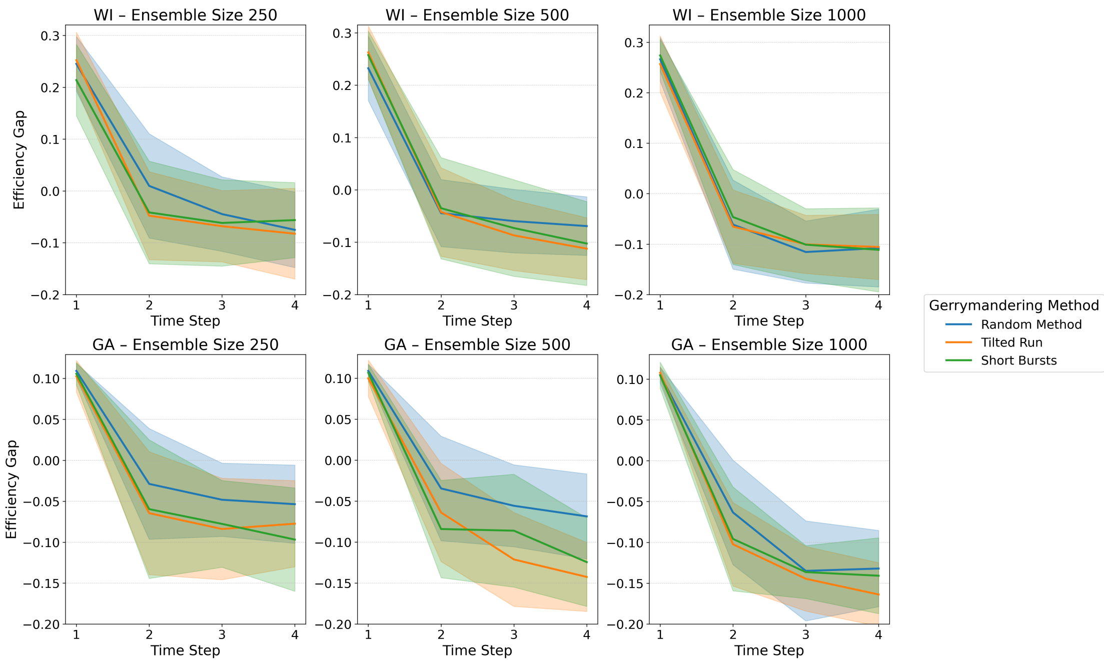

FIGURE A.3: Comparison of efficiency gaps for three algorithms that generated gerrymandered maps favoring the Democratic Party across three ensemble sizes in two states.

Algorithm 1 Redistricting via GerryChain Optimization

procedure REDISTRICT(`model`)
    Extract current demographic data from precincts as a `GeoDataFrame`
    Create graph from `GeoDataFrame` with relevant updaters (e.g., `TOTPOP`, `NREPS`, `NDEMS`)
    if `pop_dev` $> \epsilon$ **then**
        Start from a randomly generated assignment using population balance constraint
    else
        Start from current congressional district assignment
    end if
    Define proposal function as `ReCom` with bipartition tree
    Apply constraints (e.g., contiguity), depending on the state
    if `control` = Republicans **then**
        $\mathcal{O}(x) \leftarrow \frac{1}{|\mathcal{D}(x)|}\sum_i 1(N_R(i) > N_D(i)) + \varepsilon$
    else if `control` = Democrats **then**
        $\mathcal{O}(x) \leftarrow \frac{1}{|\mathcal{D}(x)|}\sum_i 1(N_D(i) > N_R(i)) + \varepsilon$
    else if `control` = Fair **then**
        $\mathcal{O}(x) \leftarrow \left|\frac{1}{|\mathcal{D}(x)|}\sum_i 1(N_D(i) > N_R(i)) - \frac{N_D}{N_D+N_R}\right|$
        $\triangleright$ Use fairness metric to minimize seat deviation from statewide vote share
    end if
    Initialize optimizer (`SingleMetricOptimizer`) with:
        initial partition, proposal, constraints, and objective
    $best\_score \leftarrow -\infty$
    for $i \leftarrow 1$ to E_S **do**
        Generate new plan via `tilted_run`
        Evaluate objective function on new plan
        if score $> best\_score$ **then**
            $best\_score \leftarrow$ new score
            Save current plan as best plan
        end if
    end for
    Update congressional district boundaries in `model` with best plan
    Update precinct-to-district assignments for vote counting
end procedure

A.4 Individual Decision-Making

State	Max Distance (miles)
Georgia (GA)	385
Wisconsin (WI)	360
Michigan (MI)	500
Pennsylvania (PA)	330

TABLE A.6: Maximum relocation distances by state (in miles).

A.5 Other Observations

- `unhappy` and `happy`: The total number of unhappy and happy agents, respectively.
- `unhappyreps`, `unhappydems`, `happyreps`, and `happydems`: The total counts of unhappy and happy agents categorized by party affiliation (Republican or Democrat).
- `avg_utility`: The average utility score across all agents.
- `total_moves`: The total number of agents that relocated during the simulation step.
- `rep_congdist_seats`, `dem_congdist_seats`, and `tied_congdist_seats`: The total number of Congressional districts in which Republicans, Democrats, or neither party (tied) hold a majority.
- `avg_county_segregation` and `avg_congdist_segregation`: Average segregation scores computed at the county and Congressional district levels, respectively. These are calculated by averaging the majority vote share across all geographic units. Formally, the majority vote percentage for a geographic unit g is defined as:

$$\text{majority\_pct}(g) = \begin{cases} \frac{N_R}{N}, & \text{if } g.\text{color} = \text{'Red'} \\ \frac{N_D}{N}, & \text{if } g.\text{color} = \text{'Blue'} \\ 0.5, & \text{otherwise} \end{cases} \tag{A.1}$$

  where N, N_D, and N_R are the total, Democrat, and Republican agent counts in geographical unit g, respectively. Then, the average segregation scores are:

$$\texttt{avg\_congdist\_segregation} = \frac{1}{N_{congdist}} \sum_{i=1}^{N_{congdist}} \text{majority\_pct}(congdist_i) \tag{A.2}$$

$$\texttt{avg\_county\_segregation} = \frac{1}{N_{county}} \sum_{i=1}^{N_{county}} \text{majority\_pct}(county_i) \tag{A.3}$$

where $N_{congdist}, N_{county}$ are the total number of Congressional districts and counties in the state, and $congdist_i, county_i$ are the specific Congressional district or county.

- `competitive_seats`: Total number of districts considered competitive according to a user-defined parameter `competitive_threshold`. A district i is defined as competitive if the difference between Democrat and Republican vote shares is less than the threshold:

$$dist_i.\text{competitive} = \begin{cases} 1, & \text{if } \left| \frac{N_{D,i}}{N_i} - \frac{N_{R,i}}{N_i} \right| < \texttt{competitive\_threshold} \\ 0, & \text{otherwise} \end{cases} \tag{A.4}$$

where N_i, $N_{D,i}$, and $N_{R,i}$ are the total, Democrat, and Republican agent counts in district i, respectively. The total number of competitive seats is:

$$\texttt{competitive\_seats} = \sum_{i=1}^{N_{congdist}} dist_i.\text{competitive} \tag{A.5}$$

- `max_popdev`: The maximum population deviation across districts, measuring how far each district's population deviates from the ideal equal population. The ideal population is:

$$N_{ideal} = \frac{N_{total}}{N_{congdist}} \tag{A.6}$$

where N_{total} is the total agent count and $N_{congdist}$ is the total number of Congressional districts in the state. For each district i, the population deviation is:

$$pop\_dev_i = \frac{|N_i - N_{ideal}|}{N_{ideal}} \tag{A.7}$$

and the maximum population deviation is:

$$\texttt{max\_popdev} = \max_{i=1,\ldots,N_{congdist}} pop\_dev_i \tag{A.8}$$

- `predicted_seats`: The number of seats predicted to be won by the party in control after redistricting and before partisan sorting. If the state legislature is split, this value is zero. This metric highlights whether partisan self-sorting can offset predicted seat gains.

- `change_map`: The percentage of precincts reassigned to a different Congressional district after redistricting. Calculated as:

$$\texttt{change\_map} = \frac{\text{number of reassigned precincts}}{\text{total number of precincts}} \tag{A.9}$$

This indicates the extent to which the map has changed due to redistricting.

- `projected_winner`: A ternary indicator of the party controlling the redistricting process in the next time step (`Republican`, `Democratic`, or `Tied`). It is updated after redistricting, sorting, and elections, and is set only if a party holds a majority in both state legislatures.

- `projected_margin`: The seat margin held by the projected winner over the opposing party.

- `control`: A ternary indicator of the party currently controlling the redistricting process (`Republican`, `Democratic`, or `Tied`). This is updated at the end of the previous time step when the projected winner assumes control for the next.

A.6 Input Data

Property Name	Type	Description
VTDID	Str	Unique precinct identifier.
VTD_NAME	Str	Name of the voting precinct.
VTDST	Str	State abbreviation.
COUNTY_NAME	Str	Name of the county.
COUNTYFP	Str	FIPS code for the county.
CONGDIST	Str	Congressional district code.
SENDIST	Str	State Senate district code.
LEGDIST	Str	State legislative district code.
PRES20R	Int	2020 Republican presidential votes.
PRES20D	Int	2020 Democratic presidential votes.
PRES20O	Int	2020 votes for other candidates.
PRES20TOT	Int	Total 2020 presidential votes.
PRES16R	Int	2016 Republican presidential votes.
PRES16D	Int	2016 Democratic presidential votes.
PRES16O	Int	2016 votes for other candidates.
PRES16TOT	Int	Total 2016 presidential votes.
PRES12R	Int	2012 Republican presidential votes.
PRES12D	Int	2012 Democratic presidential votes.
PRES12O	Int	2012 votes for other candidates.
PRES12TOT	Int	Total 2012 presidential votes.
TOTPOP	Int	Total precinct population.
COUNTY_TOTPOP	Int	Total county population.
COUNTY_TOTPOP_SHARE	Float	County's share of total population.
COUNTY_HOUSEHOLDS	Int	Number of households in the county.
COUNTY_HOUSING_UNITS	Int	Number of housing units in the county.
COUNTY_PERSONS_PER_HOUSEHOLD	Float	Average household size in the county.
COUNTY_CAPACITY	Float	Maximum relocation capacity for the county.
COUNTY_CAPACITY_SHARE	Float	County's share of total capacity.
COUNTY_RUCA	Int	Rural-Urban Commuting Area (RUCA) code.
COUNTY_RUCA2	Int	Alternate RUCA code.
COUNTY_RUCACAT	Str	RUCA classification category.
geometry	Object	Polygon geometry for spatial representation.

Table A.7: Overview of properties in the GeoJSON file.

Appendix B

Supplementary SA

B.1 GSA

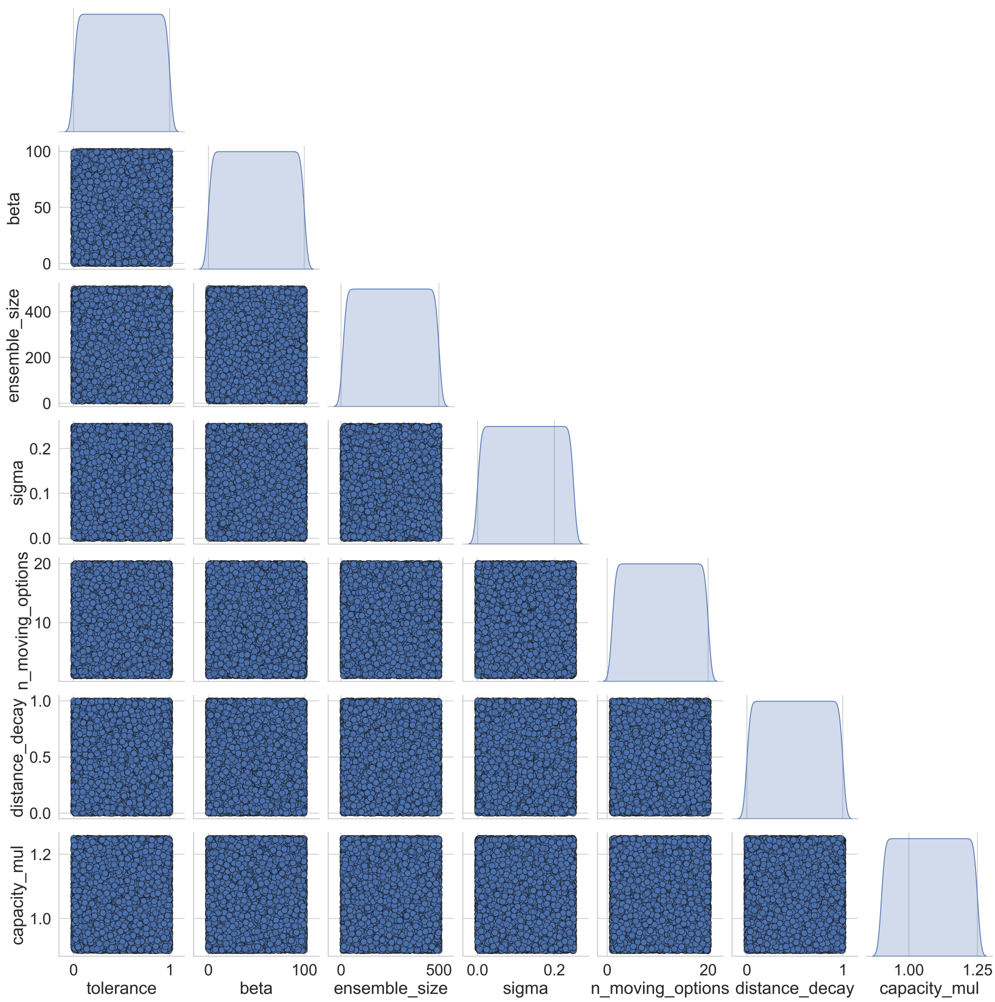

FIGURE B.1: Visualization of the full parameter space covered using Saltelli's sampling method. With a base sample size of $N = 4096$ and $k = 7$ input parameters, a total of $N(2k + 2) = 65{,}536$ simulations were generated to support the Sobol' sensitivity analysis.

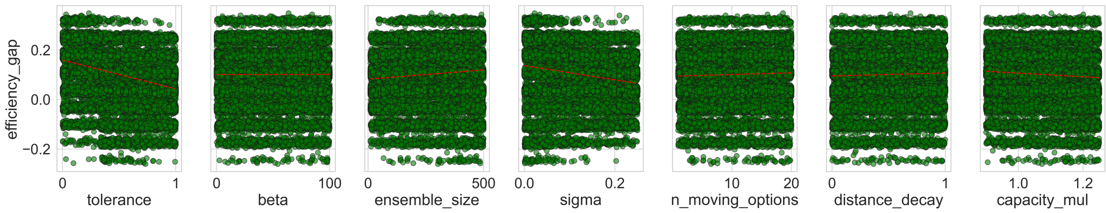

(A) GA

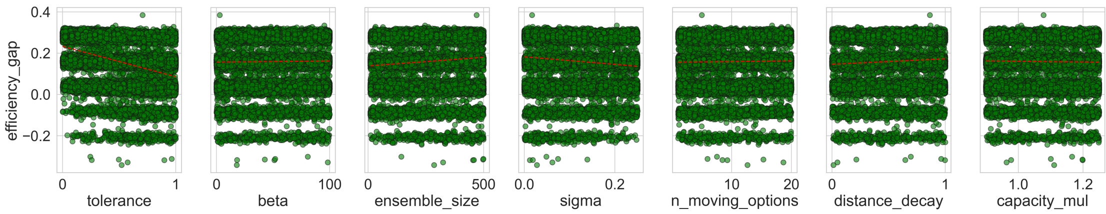

(B) WI

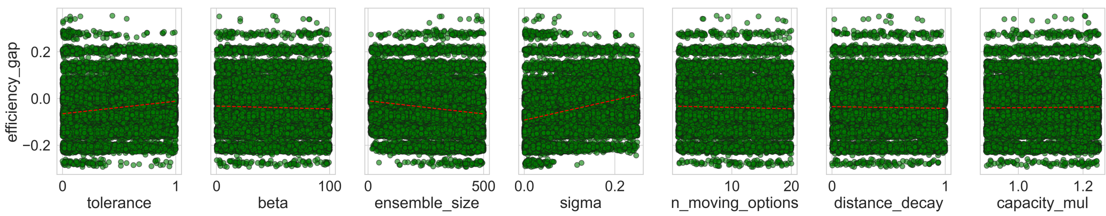

(C) MI

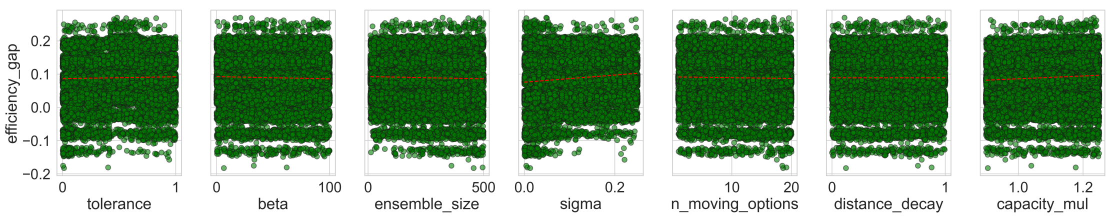

(D) PA

Figure B.2: Scatter plots showing the relationship between each input parameter and the efficiency gap output for four states. Each subplot displays output data points from the Sobol' sample ($N = 4096$) alongside a linear regression line (in red) to illustrate the direction and strength of each parameter's influence.

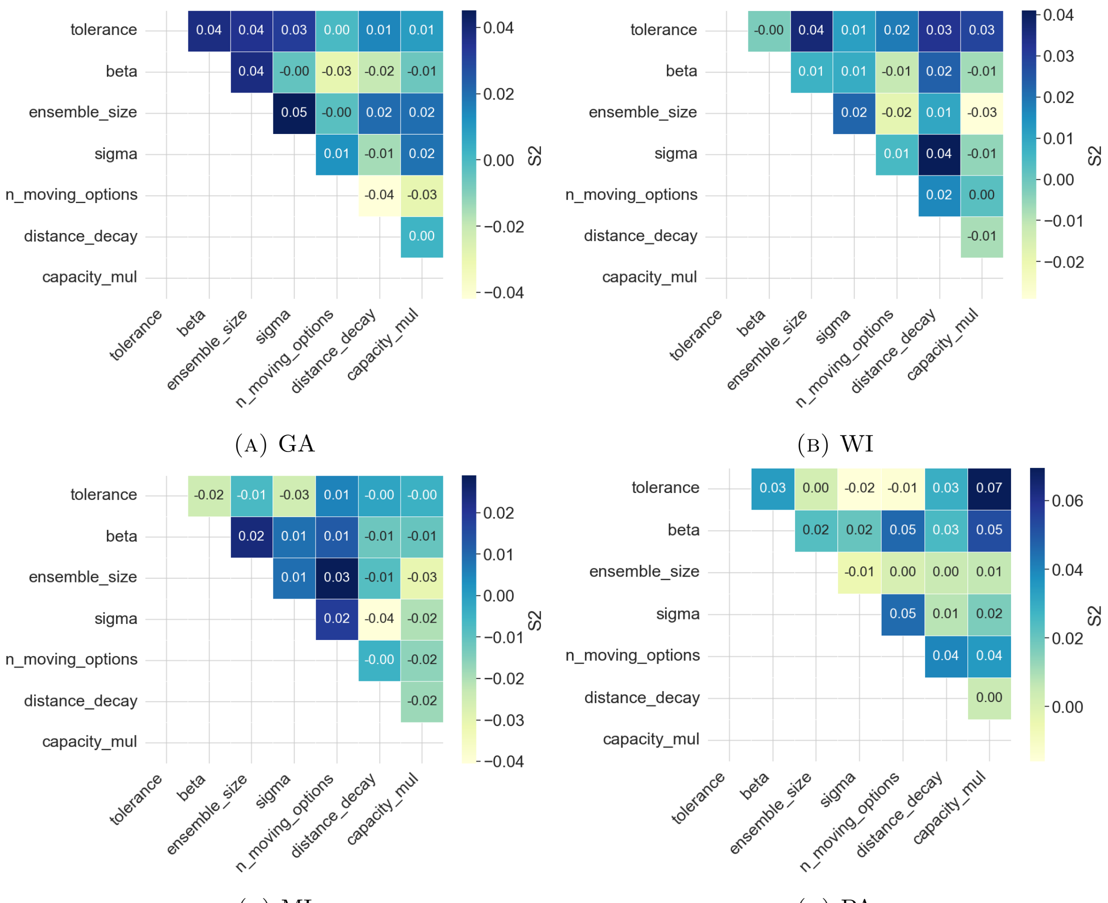

(A) GA

(B) WI

(C) MI

(D) PA

FIGURE B.3: Second-order Sobol' sensitivity indices (S_2) for the efficiency gap output across four states. Each heatmap visualizes pairwise interaction effects between model input parameters, where higher values indicate stronger interaction influence on model variance.

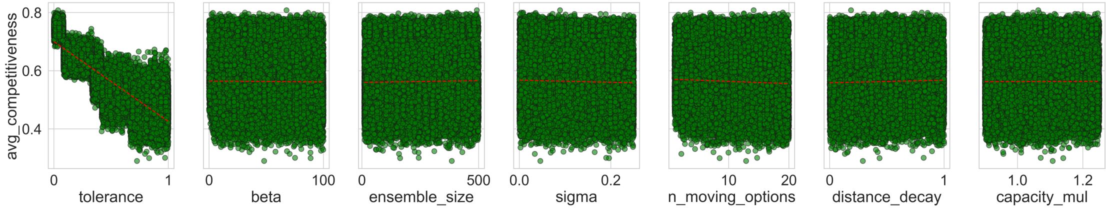

(A) Scatter plots for the average competitiveness output.

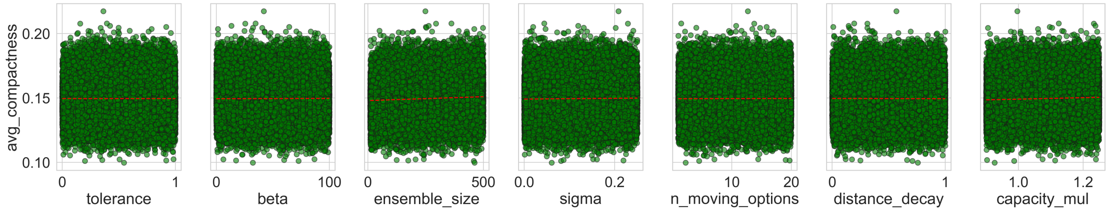

(B) Scatter plots for the average compactness output.

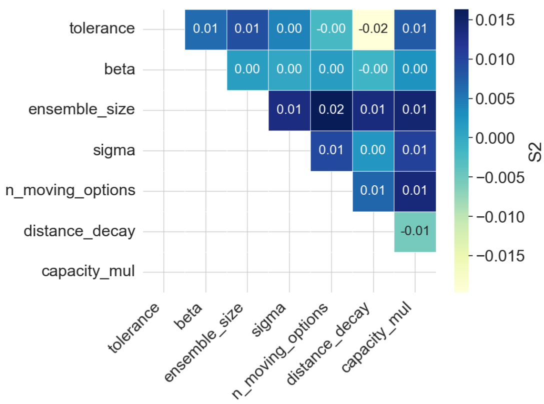

(C) S_2 for the average competitiveness output.

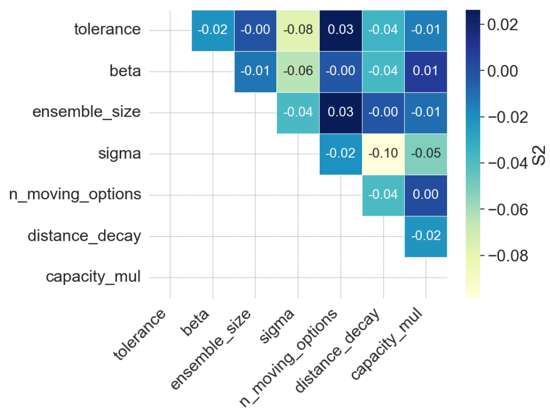

(D) S_2 for the average compactness output.

FIGURE B.4: GSA results for average competitiveness and average compactness outputs in GA, combining scatter plots with regression lines and second-order Sobol' interaction indices (S_2).

B.2 LSA

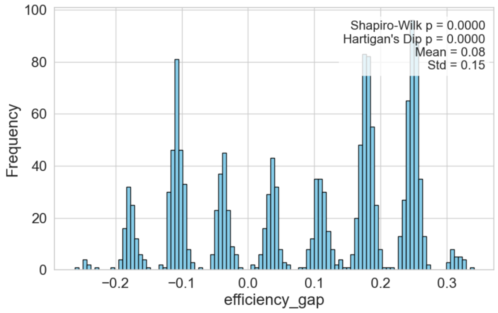

(A) Output distribution of efficiency gap for tolerance parameter (T) in GA.

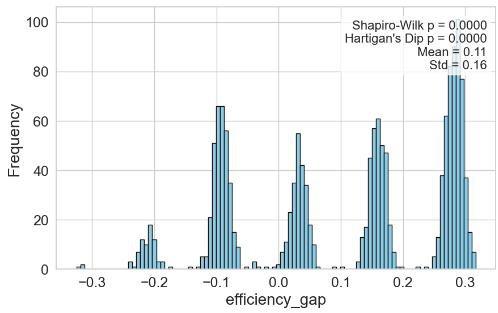

(B) Output distribution of efficiency gap for tolerance parameter (T) in WI.

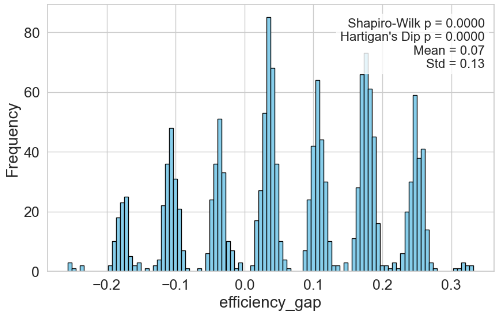

(C) Output distribution of efficiency gap for ensemble size parameter (E_S) in GA.

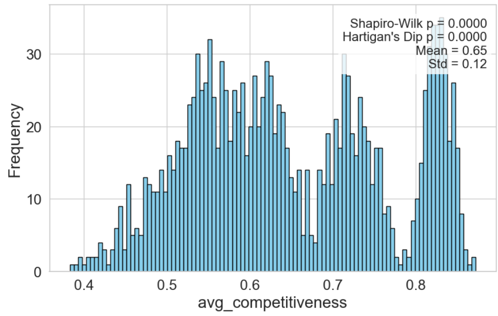

(D) Output distribution of average competitiveness for tolerance parameter (T) in MI.

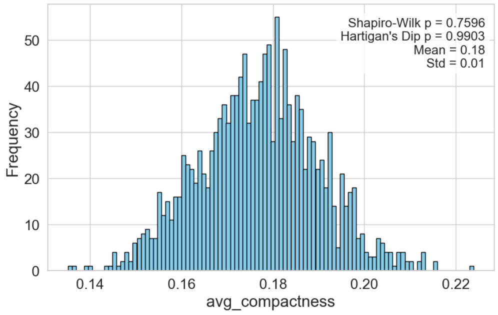

(E) Output distribution of average compactness for tolerance parameter (T) in PA.

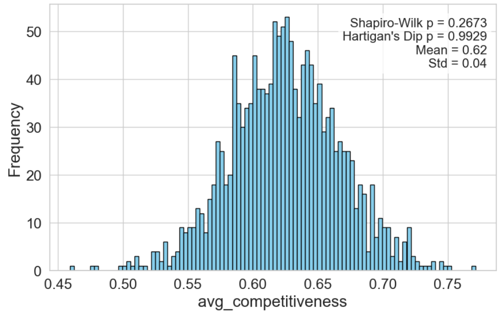

(F) Output distribution of average competitiveness for beta parameter (β) in MI.

FIGURE B.5: Examples of output distributions for output metrics (efficiency gap, average competitiveness, average compactness) obtained through OFAT sensitivity analysis.

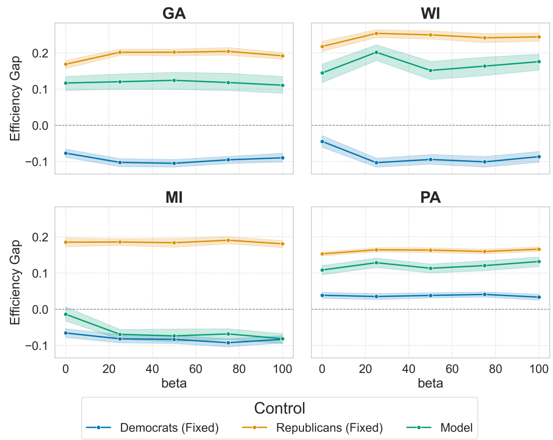

(A) Sensitivity of the efficiency gap to the relocation randomness parameter (β).

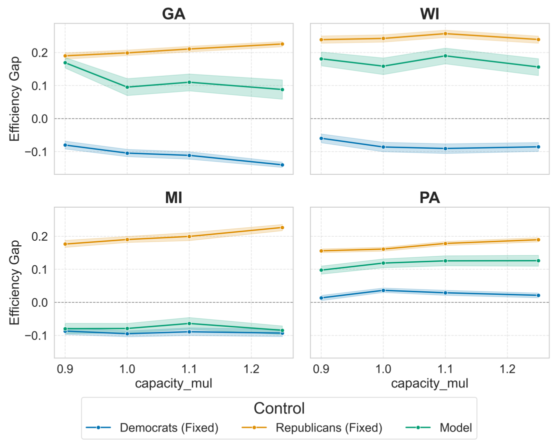

(B) Sensitivity of the efficiency gap to the county capacity multiplier (C_M).

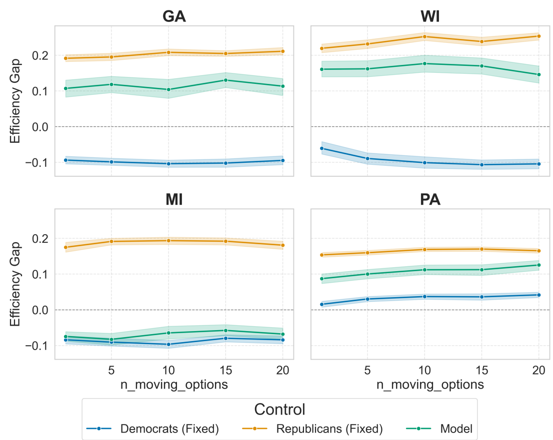

(C) Sensitivity of the efficiency gap to the number of moving options (M_O).

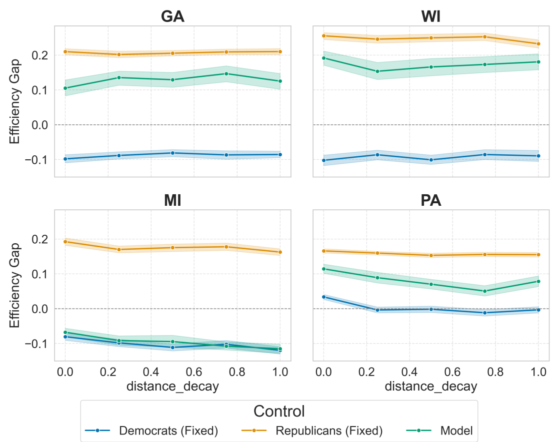

(D) Sensitivity of the efficiency gap to the distance decay factor (D_D).

FIGURE B.6: OFAT sensitivity analysis results for selected model parameters (randomness in relocation decision-making (β), county capacity multiplier (C_M), number of moving options (M_O), and distance decay factor (D_D)). The plots show the effect of varying each parameter on the efficiency gap across four states and under different redistricting control regimes: fixed Democratic, fixed Republican, and model-determined control.

Appendix C

Supplementary Results

C.1 Baseline Experiments

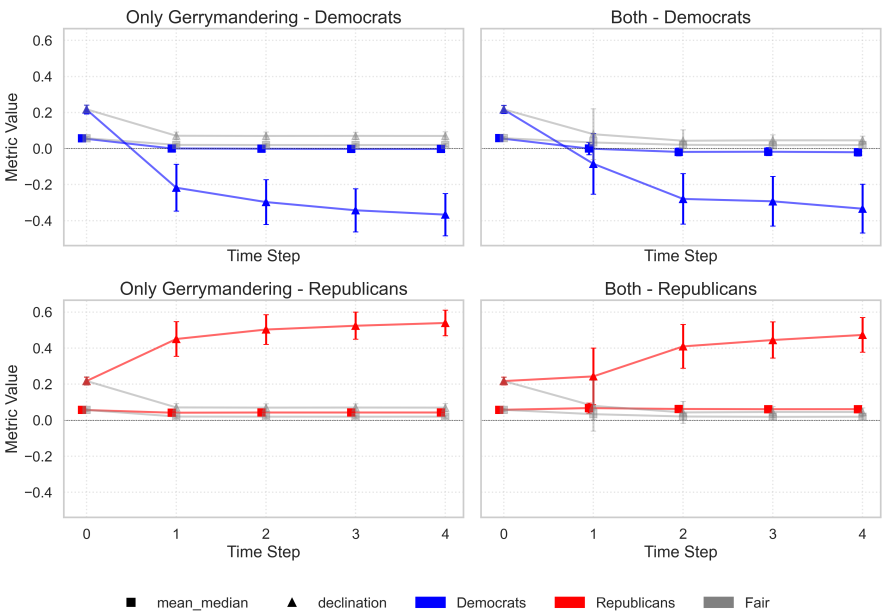

(A) Fixed Party Control

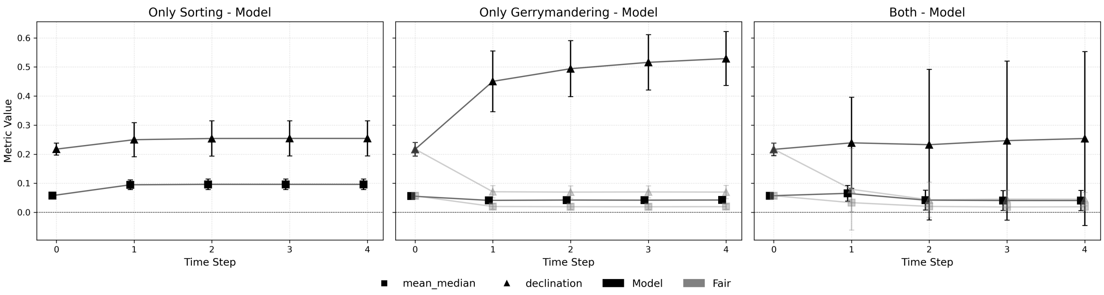

(B) Model-determined Control

Figure C.1: Temporal evolution of the declination and mean-median difference in the baseline experiments for GA under both fixed control and model-determined control scenarios.

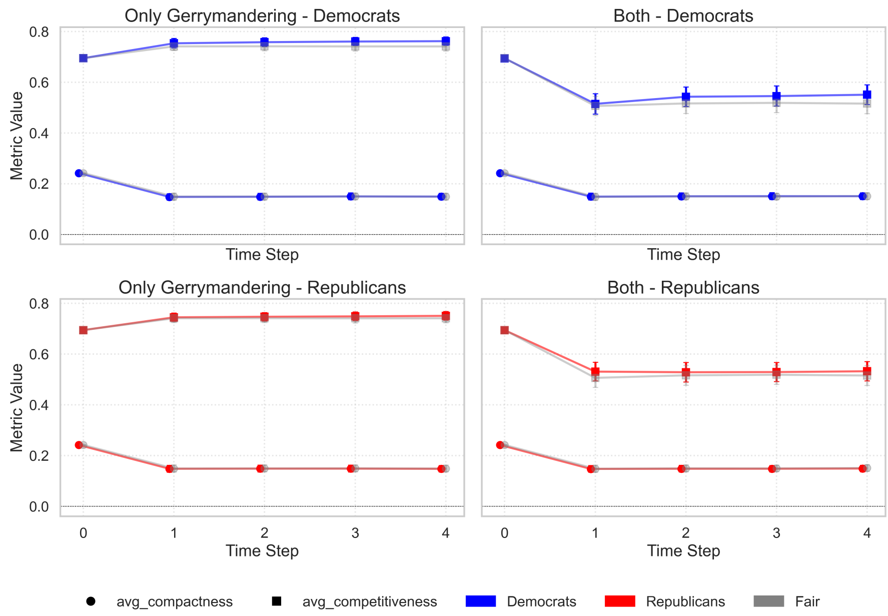

(A) Fixed Control

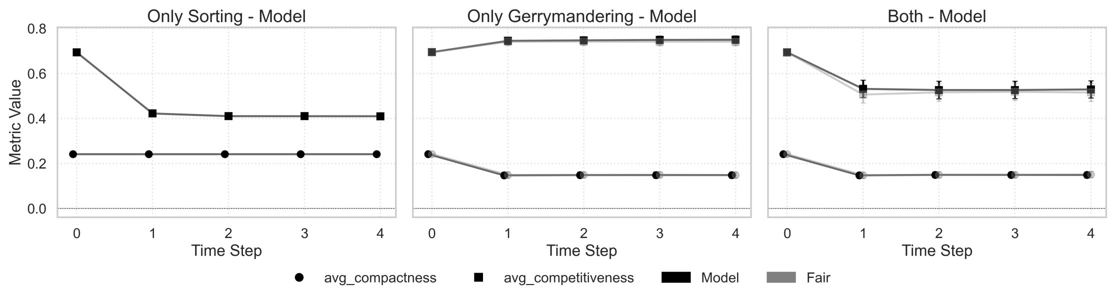

(B) Model Control

FIGURE C.2: Temporal evolution of the average district competitiveness and compactness in the baseline experiments for GA under both fixed control and model-determined control scenarios.

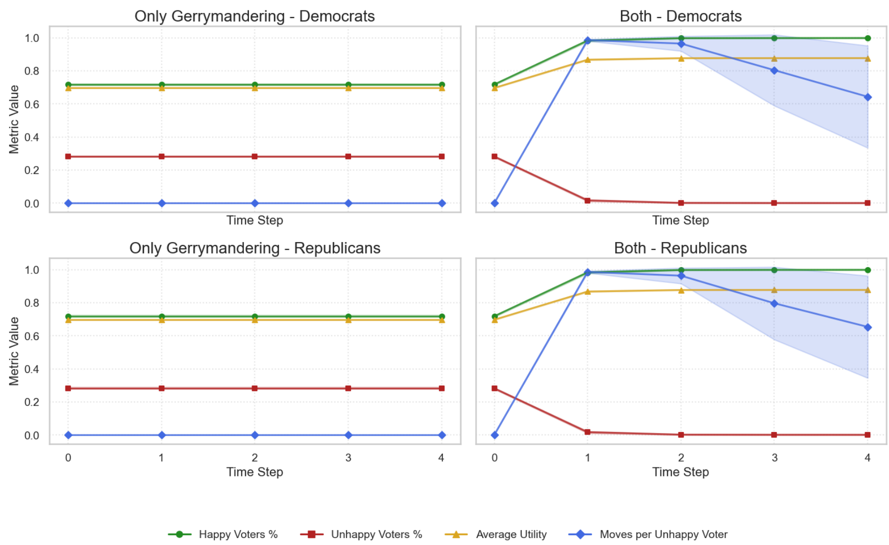

(A) Fixed Control

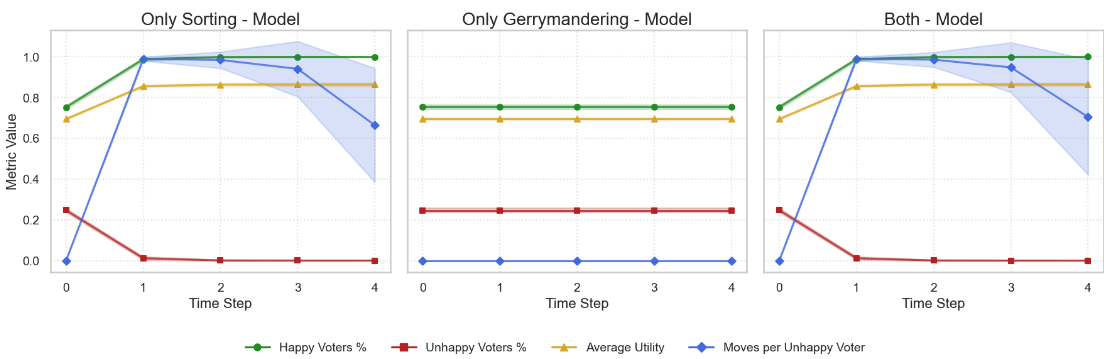

(B) Model Control

FIGURE C.3: Temporal evolution of agent-based dynamics in the baseline experiments for GA, under both fixed and model-determined control scenarios. The plots show the percentage of happy and unhappy agents, the average utility score, and the share of unhappy agents who decide to move at each time step.

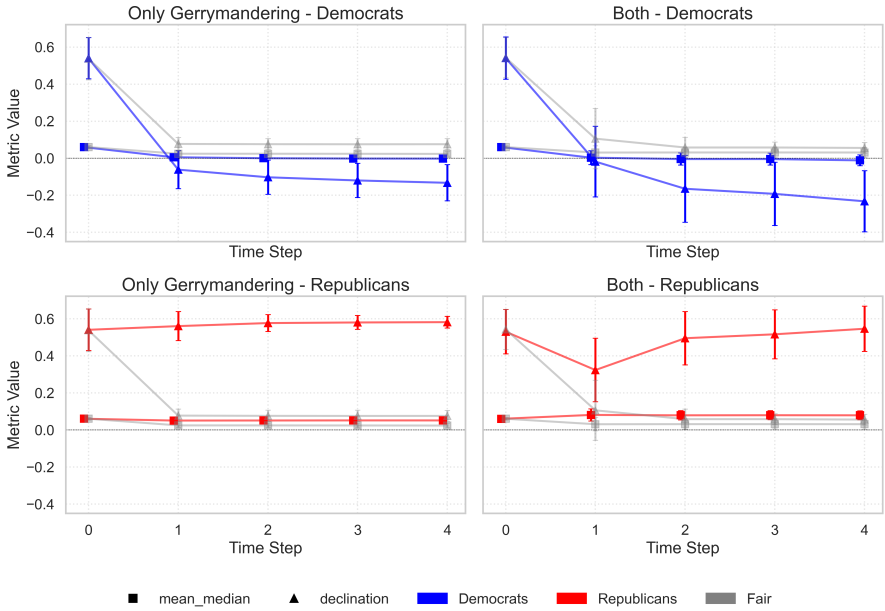

(A) Fixed Party Control

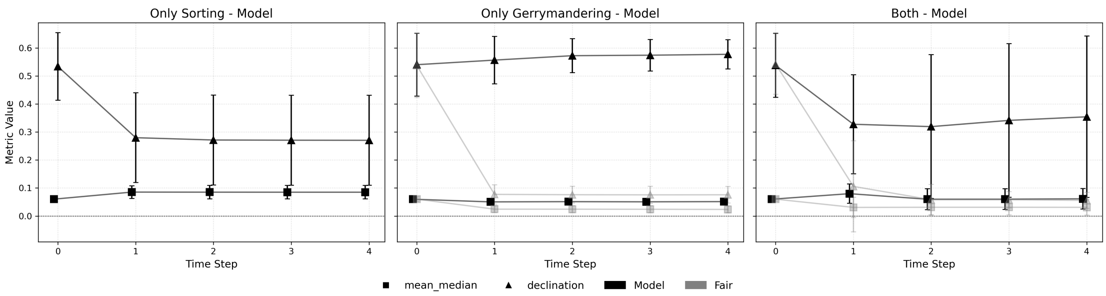

(B) Model-determined Control

FIGURE C.4: Temporal evolution of the declination and mean-median difference in the baseline experiments for WI under both fixed control and model-determined control scenarios.

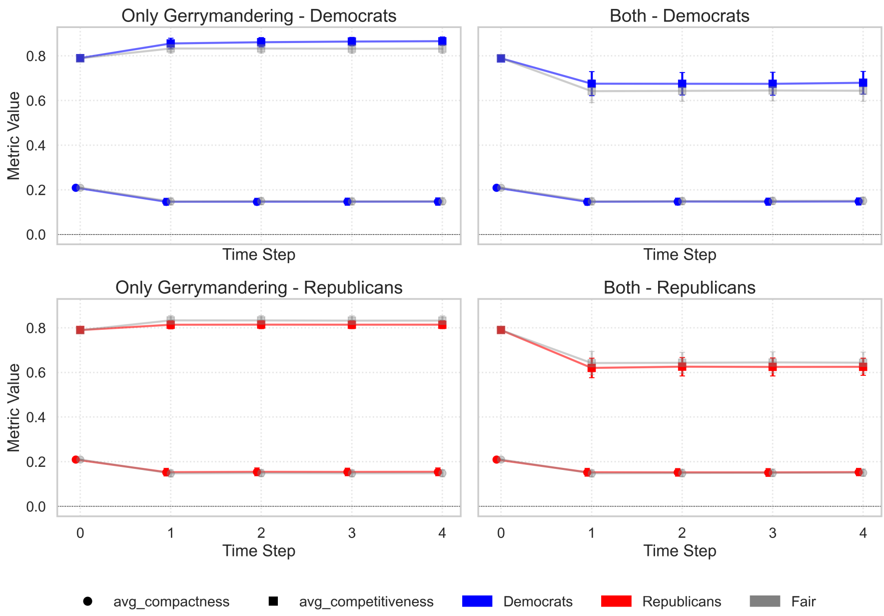

(A) Fixed Control

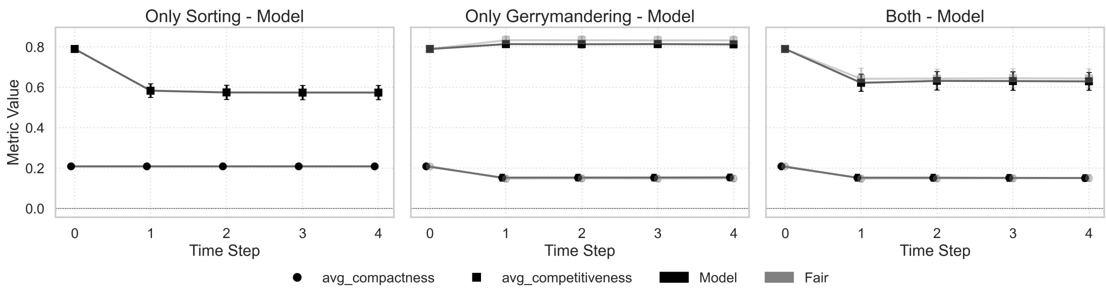

(B) Model Control

FIGURE C.5: Temporal evolution of the average district competitiveness and compactness in the baseline experiments for WI under both fixed control and model-determined control scenarios.

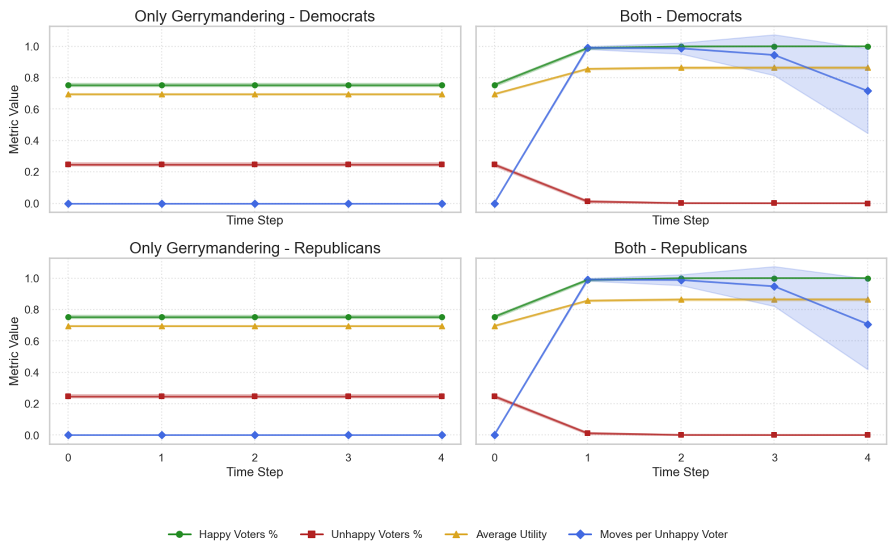

(A) Fixed Control

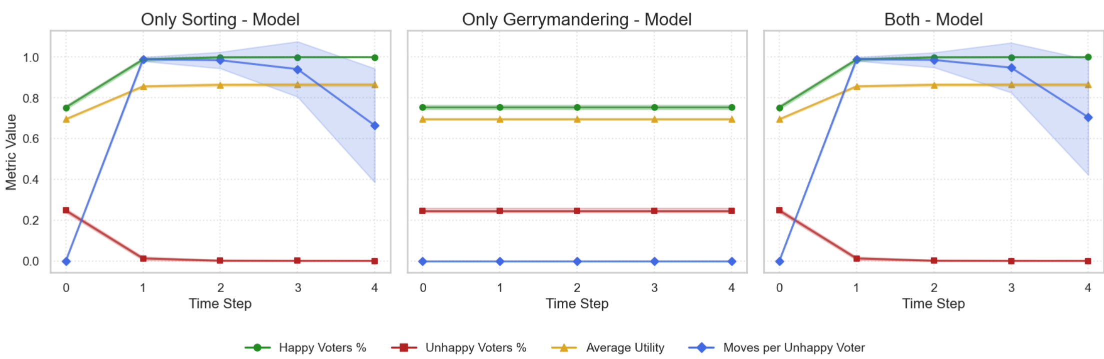

(B) Model Control

FIGURE C.6: Temporal evolution of agent-based dynamics in the baseline experiments for WI, under both fixed and model-determined control scenarios. The plots show the percentage of happy and unhappy agents, the average utility score, and the share of unhappy agents who decide to move at each time step.

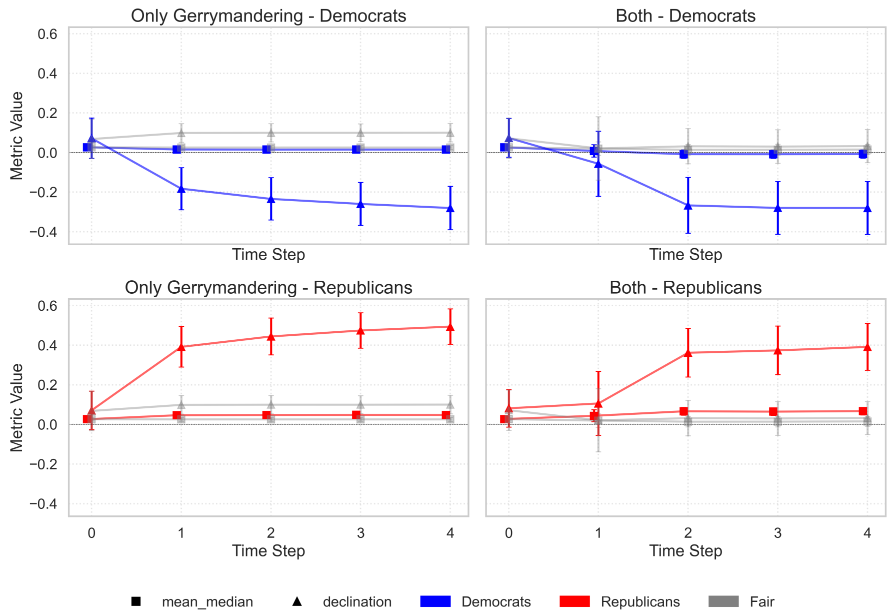

(A) Fixed Party Control

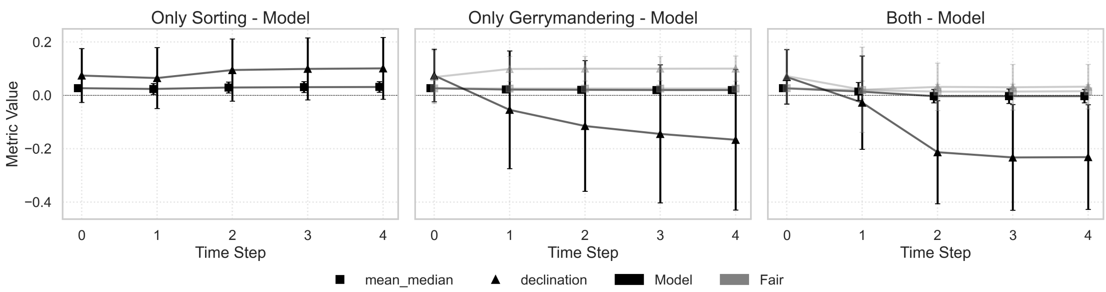

(B) Model-determined Control

FIGURE C.7: Temporal evolution of the declination and mean-median difference in the baseline experiments for MI under both fixed control and model-determined control scenarios.

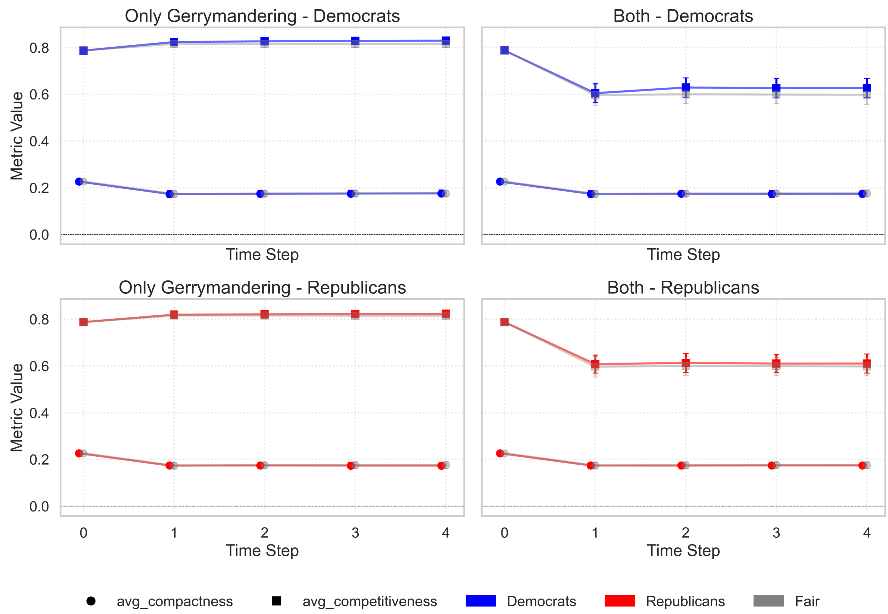

(A) Fixed Control

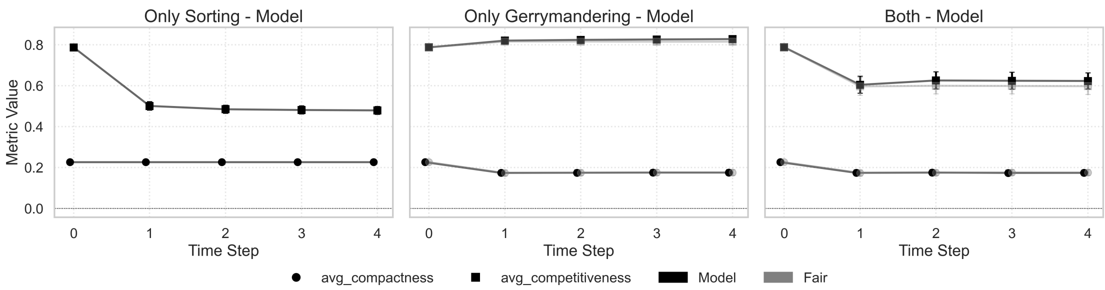

(B) Model Control

FIGURE C.8: Temporal evolution of the average district competitiveness and compactness in the baseline experiments for MI under both fixed control and model-determined control scenarios.

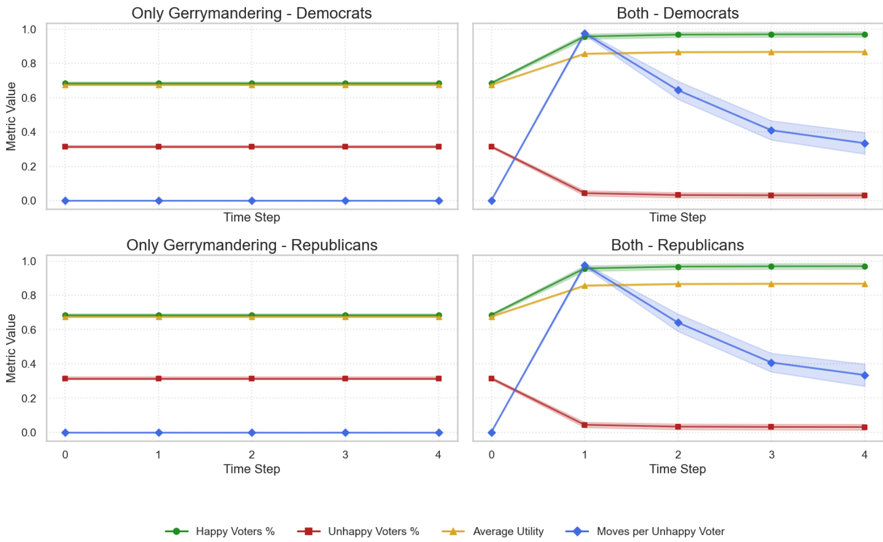

(A) Fixed Control

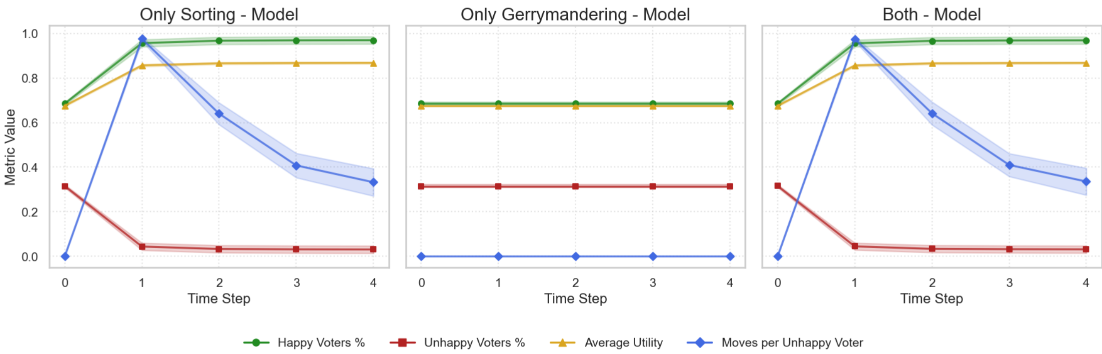

(B) Model Control

FIGURE C.9: Temporal evolution of agent-based dynamics in the baseline experiments for MI, under both fixed and model-determined control scenarios. The plots show the percentage of happy and unhappy agents, the average utility score, and the share of unhappy agents who decide to move at each time step.

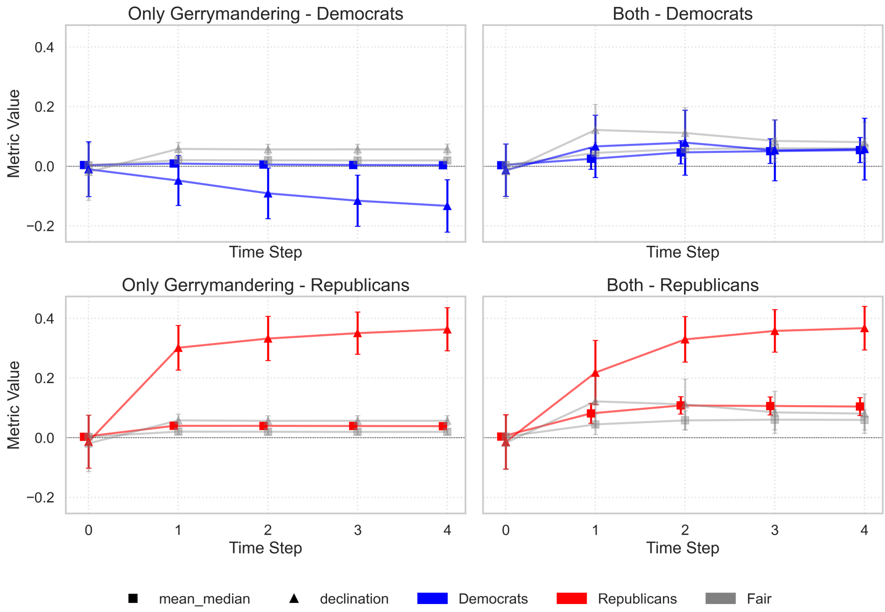

(A) Fixed Party Control

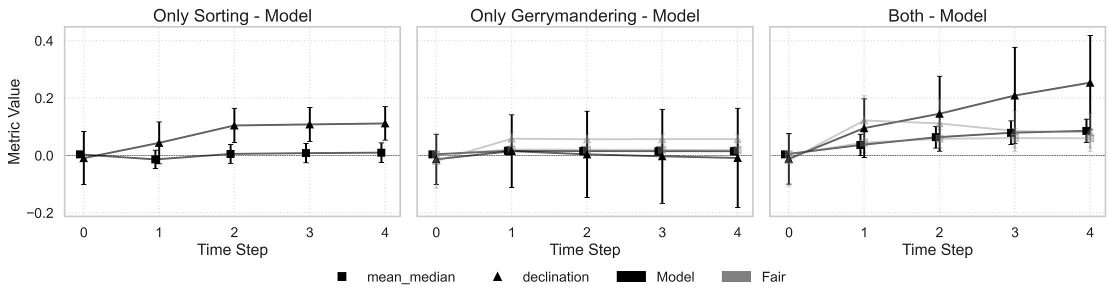

(B) Model-determined Control

[Baseline results for declination and mean-median difference outputs in PA.]

FIGURE C.10: Temporal evolution of the declination and mean-median difference in the baseline experiments for PA under both fixed control and model-determined control scenarios.

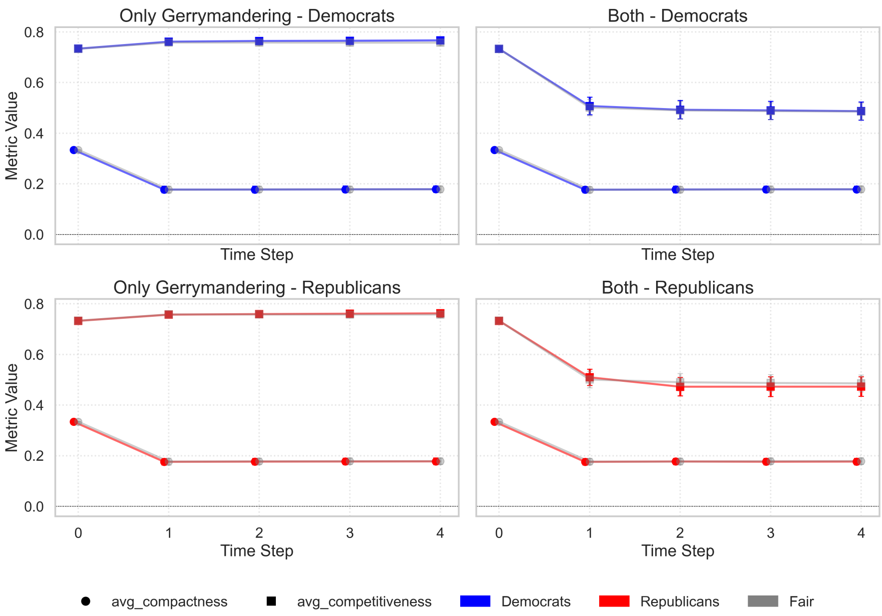

(A) Fixed Control

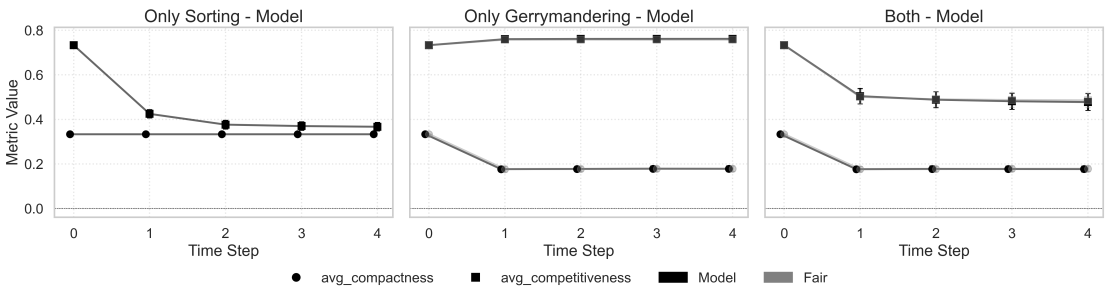

(B) Model Control

FIGURE C.11: Temporal evolution of the average district competitiveness and compactness in the baseline experiments for PA under both fixed control and model-determined control scenarios.

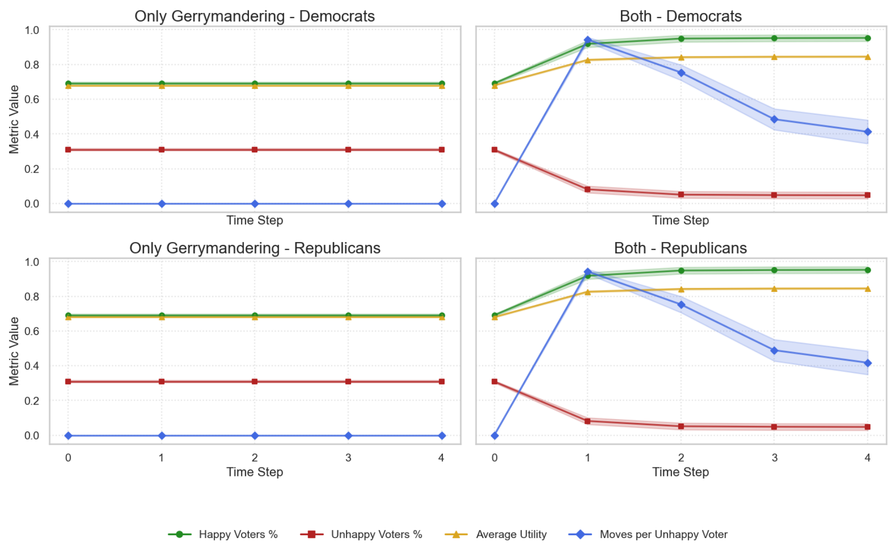

(A) Fixed Control

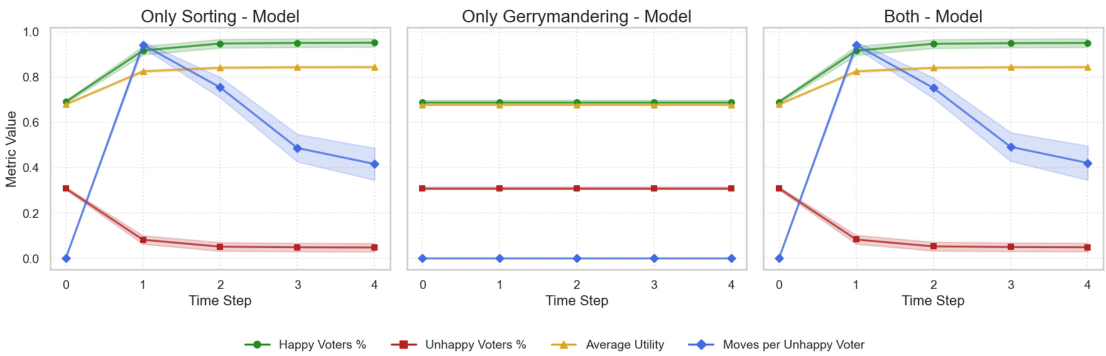

(B) Model Control

FIGURE C.12: Temporal evolution of agent-based dynamics in the baseline experiments for PA, under both fixed and model-determined control scenarios. The plots show the percentage of happy and unhappy agents, the average utility score, and the share of unhappy agents who decide to move at each time step.

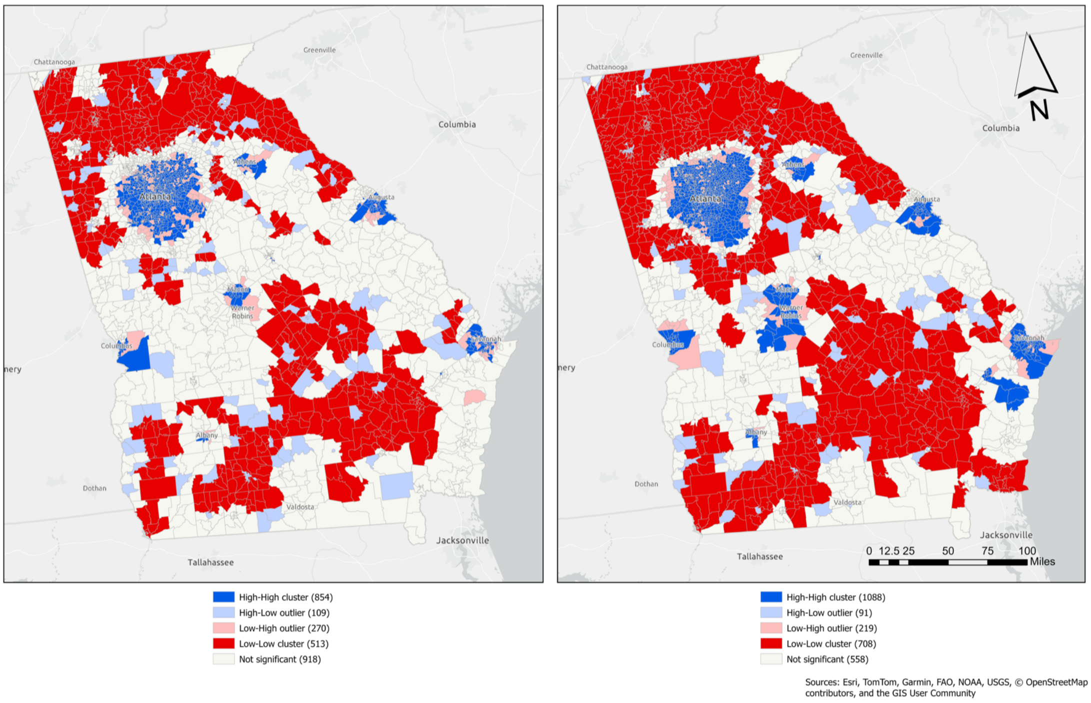

(A) GA

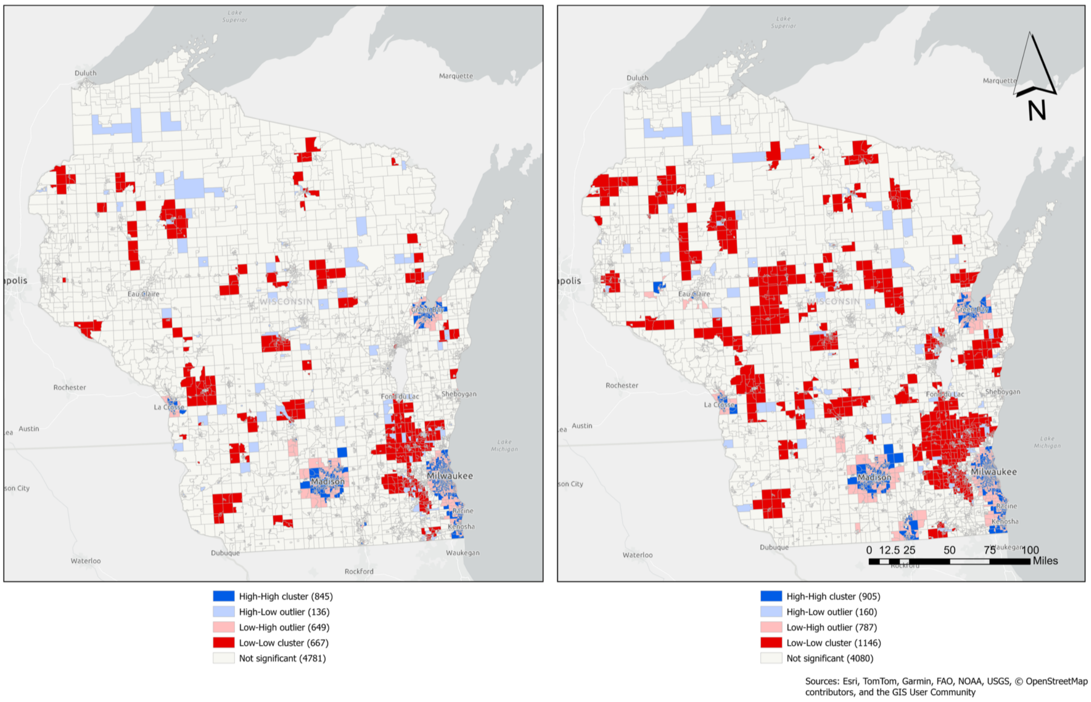

(B) WI

FIGURE C.13: Local Moran's I classification for GA and WI precincts before (left) and after (right) partisan sorting using default model parameters. The classification distinguishes four cluster types: **high-high** clusters represent Democratic enclaves, where precincts with high Democratic vote shares are surrounded by similar precincts; **low-low** clusters represent Republican enclaves, where precincts with low Democratic vote shares (i.e., high Republican support) are adjacent to similarly Republican-leaning areas; **low-high** outliers are Republican precincts surrounded by Democratic precincts; and **high-low** outliers are Democratic precincts surrounded by Republican ones.

C.2 Redistricting Reform Experiments

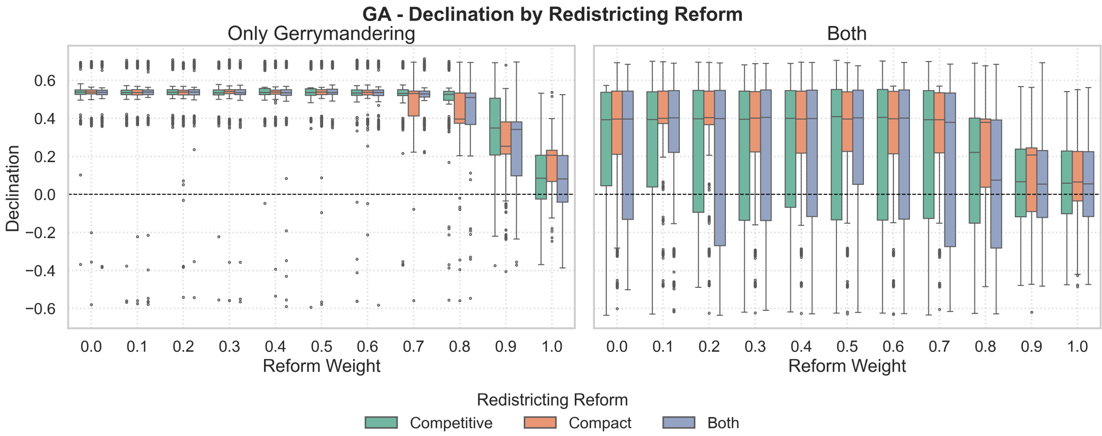

(A) GA

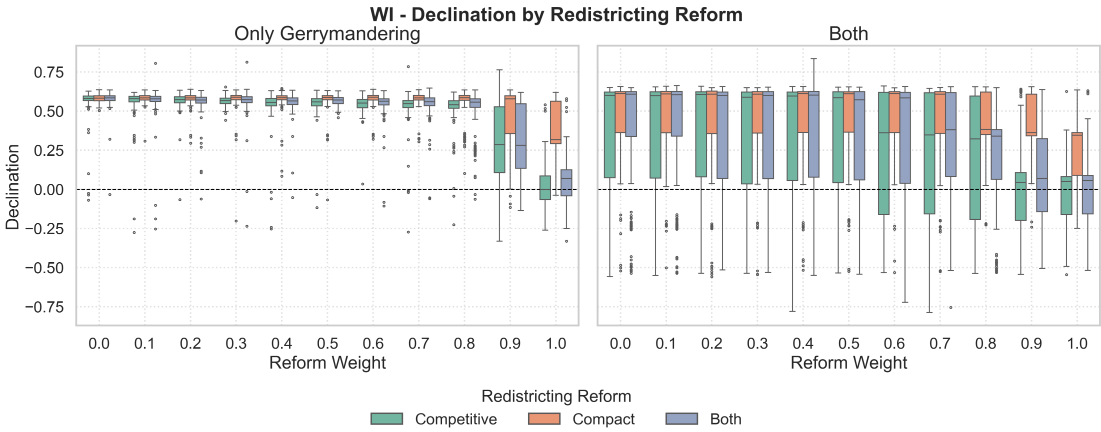

(B) WI

FIGURE C.14: Effect of compactness and competitiveness reforms on the declination in GA and WI.

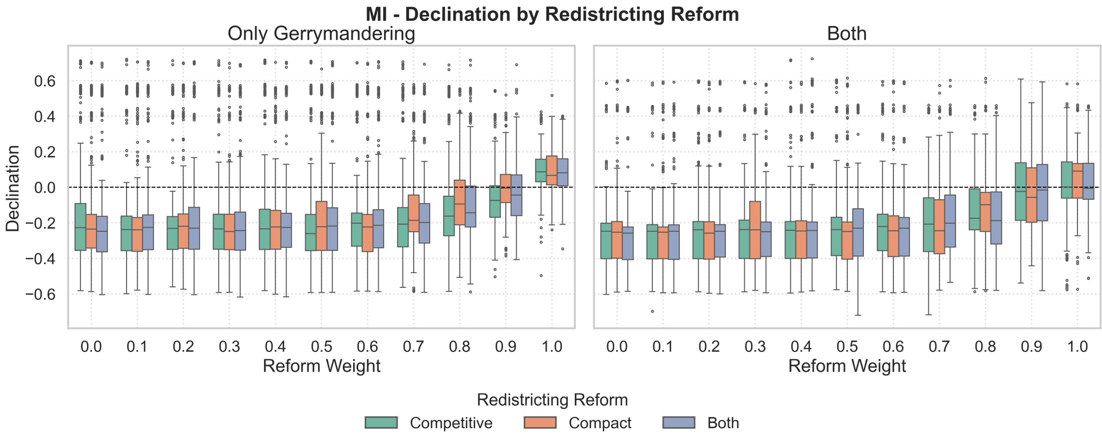

(c) MI

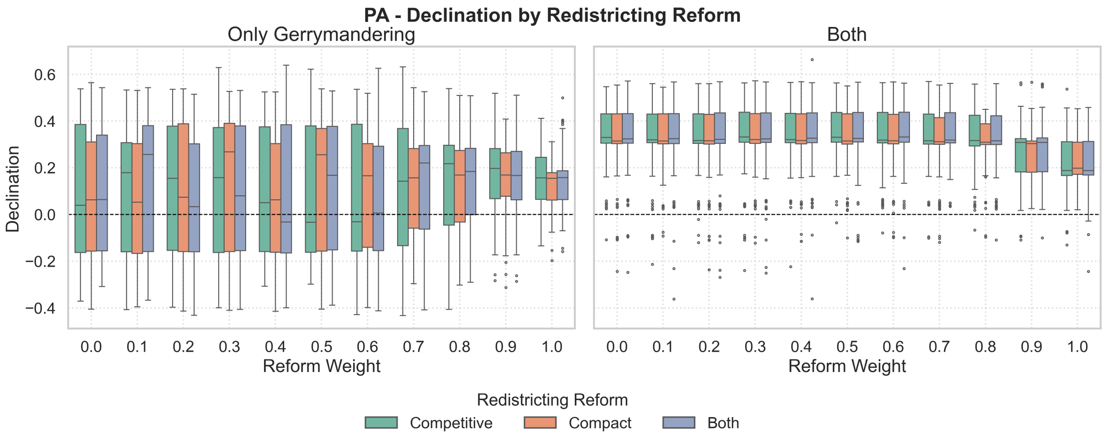

(d) PA

Figure C.14: Effect of compactness and competitiveness reforms on the declination in MI and PA.

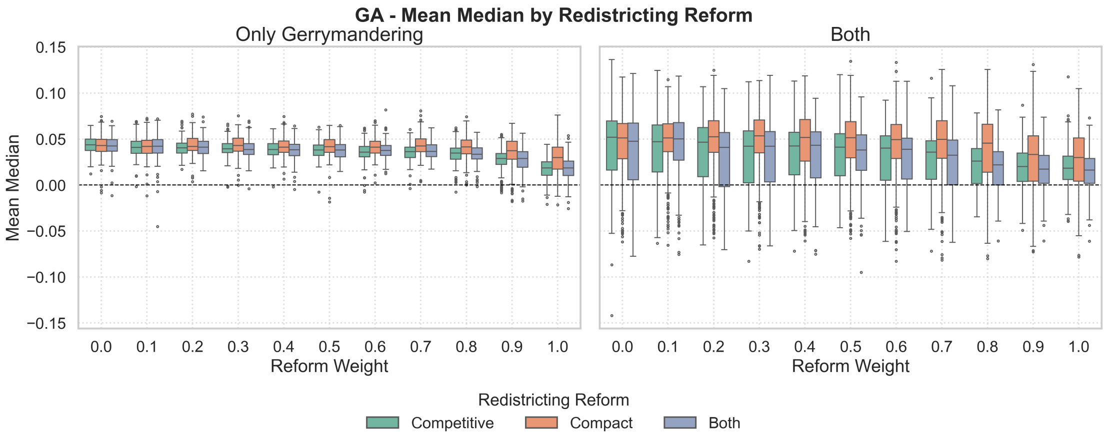

(A) GA

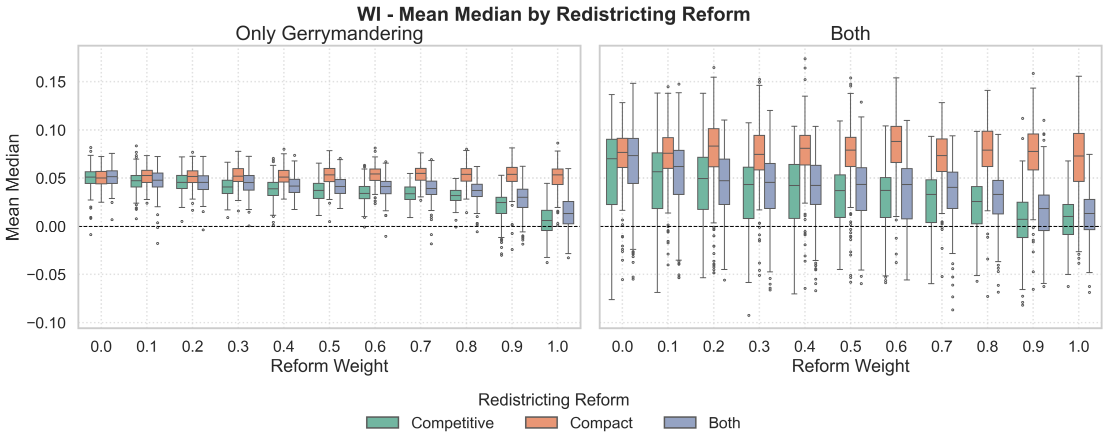

(B) WI

FIGURE C.15: Effect of compactness and competitiveness reforms on the mean-median difference in GA and WI.

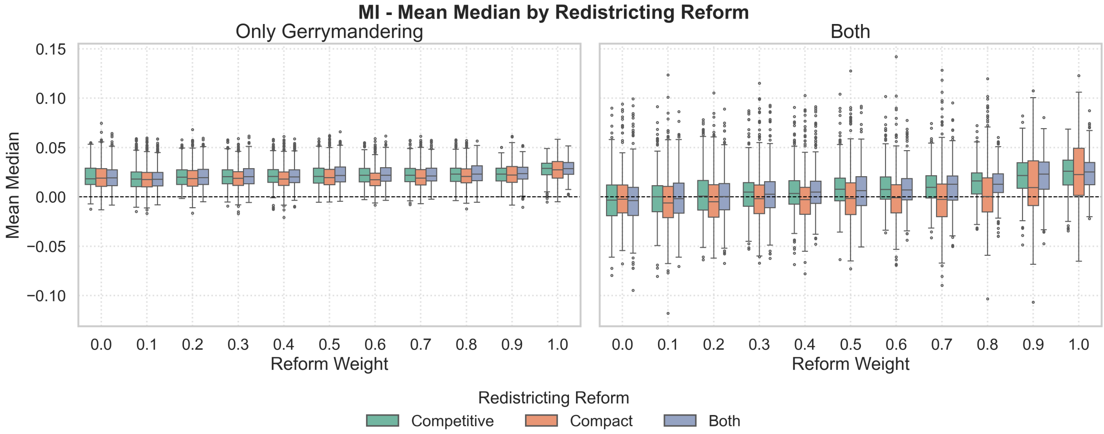

(c) MI

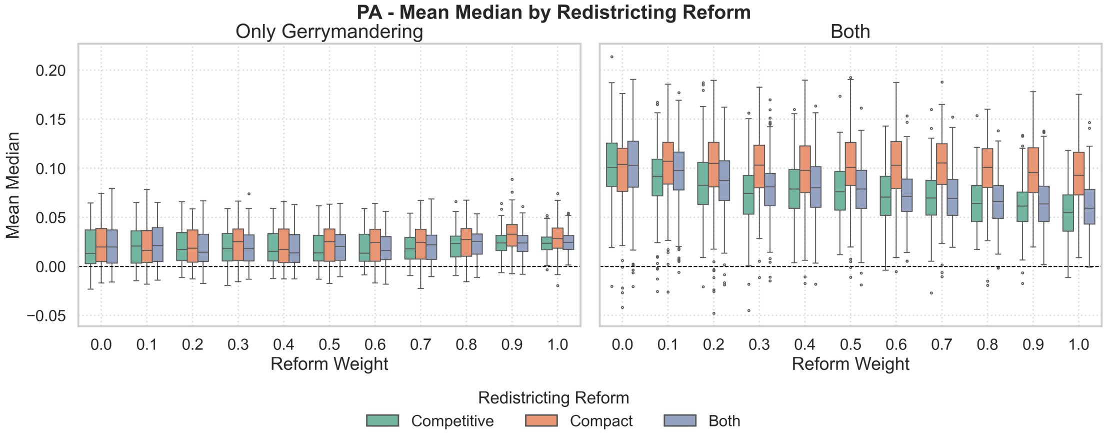

(d) PA

Figure C.15: Effect of compactness and competitiveness reforms on the mean-median difference in MI and PA.

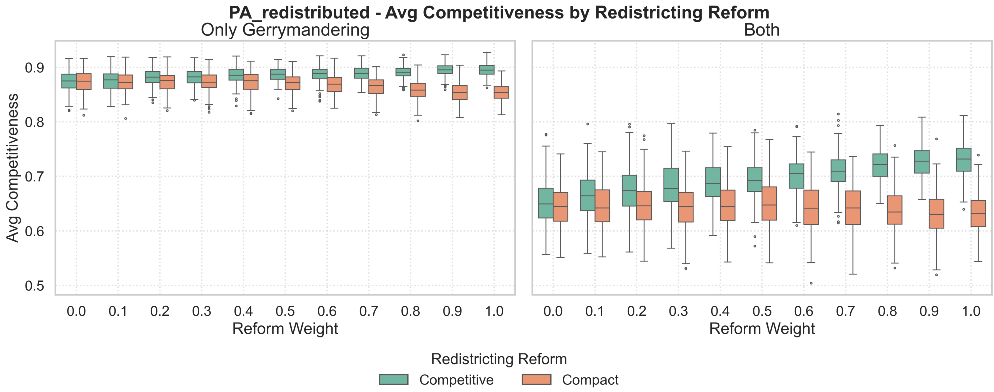

(A) Avg. Competitiveness

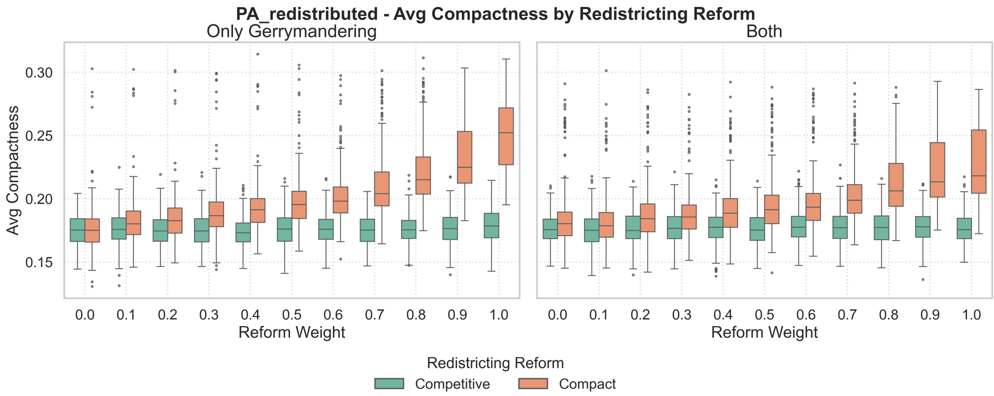

(B) Avg. Compactness

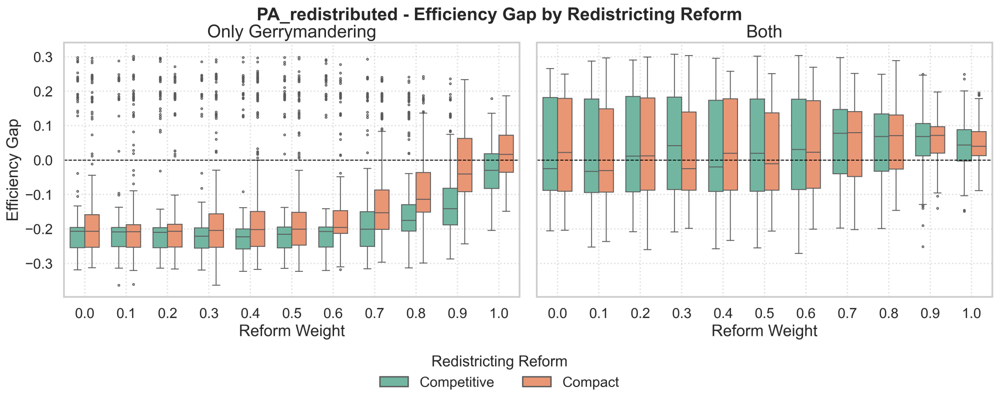

(C) Efficiency Gap

FIGURE C.16: Effect of compactness and competitiveness reforms on gerrymandering outcomes in PA using fabricated voter distribution (as described in Section 5.2), under scenarios with and without partisan sorting.

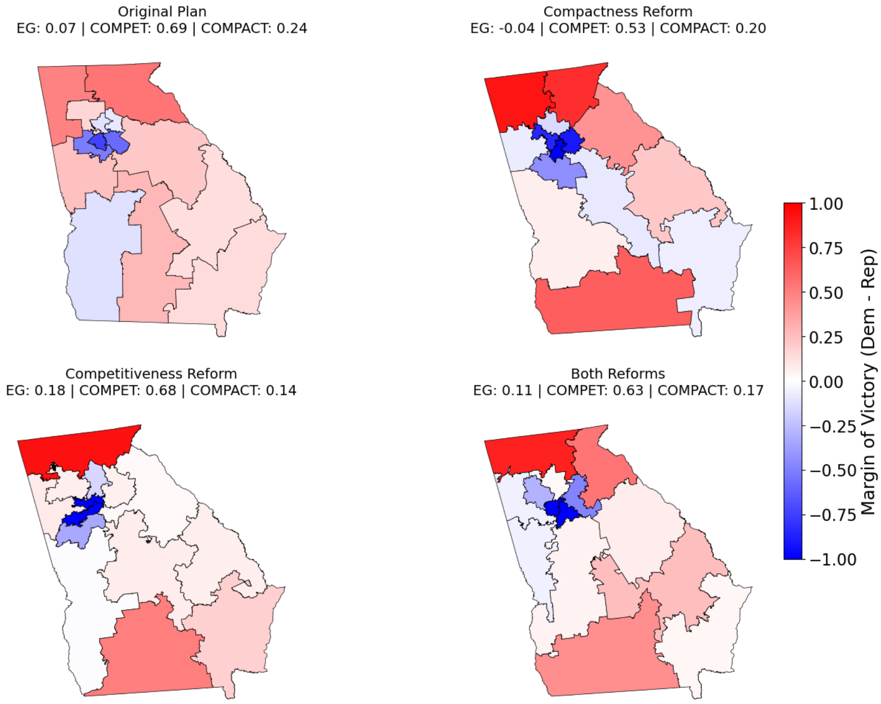

(A) GA

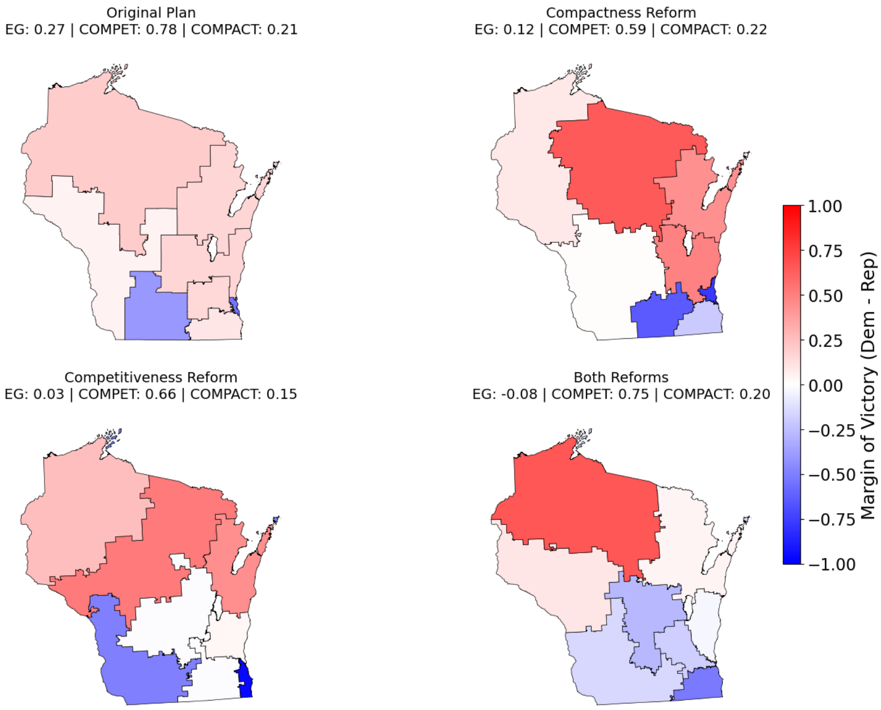

(B) WI

FIGURE C.17: Examples of generated congressional maps after partisan sorting for each redistricting reform in GA and WI. District color and intensity reflect the winning party's margin of victory. Each map also displays its efficiency gap (EG), average competitiveness (COMPET), and average compactness (COMPACT). Note that the "original plan" refers to the actual 2020 congressional map, with margins based on the initial placement of individual agents.

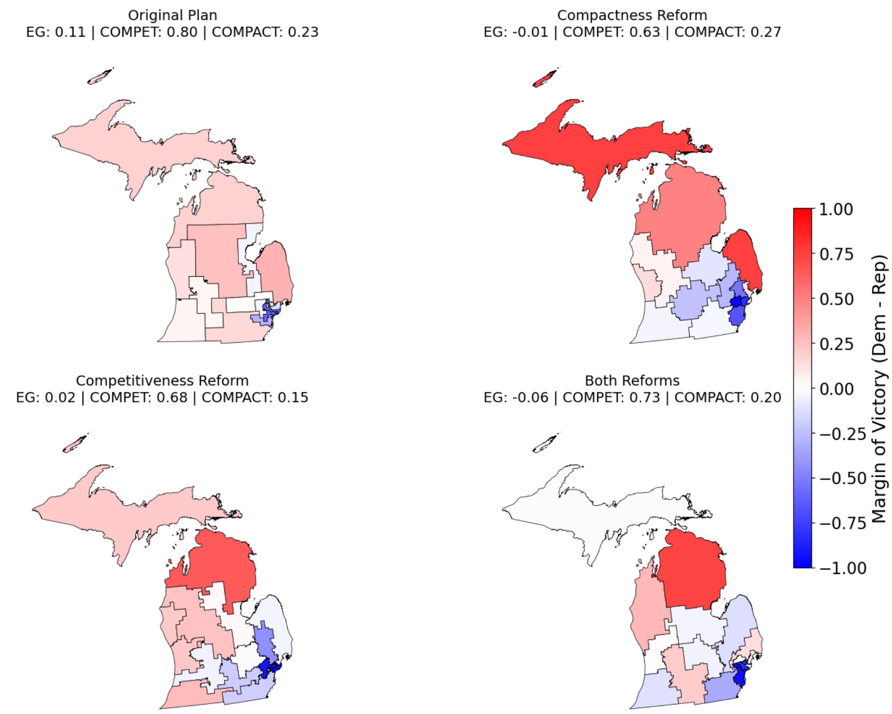

(c) MI

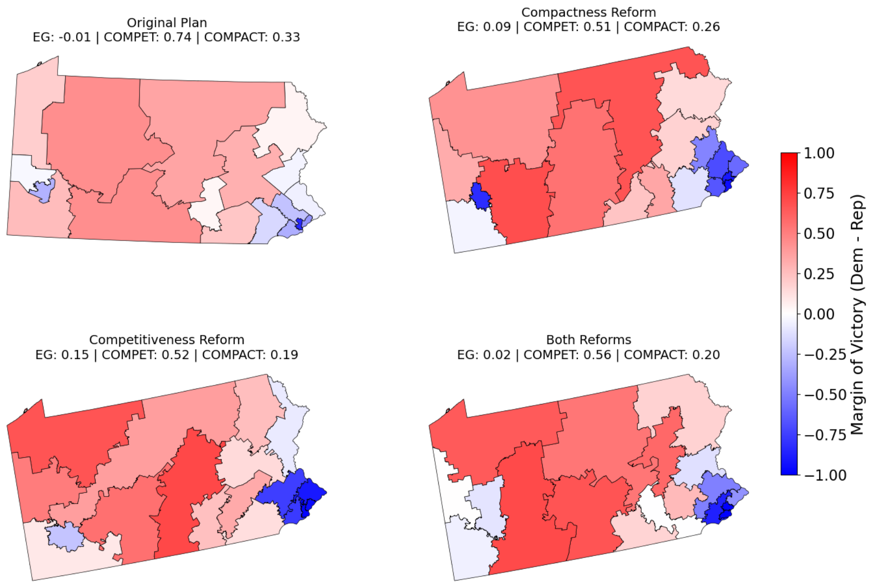

(d) PA

Figure C.17: Examples of generated congressional maps after partisan sorting for each redistricting reform in WI and PA. District color and intensity reflect the winning party's margin of victory. Each map also displays its efficiency gap (EG), average competitiveness (COMPET), and average compactness (COMPACT). Note that the "original plan" refers to the actual 2020 congressional map, with margins based on the initial placement of individual agents.

Bibliography

[1] C. O. Sauer. Geography and the Gerrymander. *American Political Science Review*, 12(3):403–426, 1918. URL https://doi.org/10.2307/1946093.

[2] Anthony J. McGann, Charles Anthony Smith, Michael Latner, and Alex Keena. *Gerrymandering in America: The House of Representatives, the Supreme Court, and the Future of Popular Sovereignty*. Cambridge University Press, 2016. URL https://doi.org/10.1017/CBO9781316534342.

[3] Nicholas O. Stephanopoulos and Eric M. McGhee. Partisan Gerrymandering and the Efficiency Gap. *The University of Chicago Law Review*, 82(2):831–900, 2015. URL https://chicagounbound.uchicago.edu/uclrev/vol82/iss2/4.

[4] Brennan Center for Justice. 50 State Guide to Redistricting, 2019. URL https://www.brennancenter.org/our-work/research-reports/50-state-guide-redistricting.

[5] Ballotpedia. State-by-State Redistricting Procedures, 2024. URL https://ballotpedia.org/State-by-state_redistricting_procedures.

[6] Leroy Clyde Hardy. *The Gerrymander: Origin, Conception and Re-emergence*. Rose Institute of State and Local Government, 1990. URL https://roseinstitute.org/wp-content/uploads/2014/02/The-Gerrymander-Origin-Conception-and-Re-emergence.pdf.

[7] Erik J. Engstrom. *Partisan Gerrymandering and the Construction of American Democracy*. Legislative Politics and Policy Making. University of Michigan Press, 2013. URL https://doi.org/10.2307/j.ctt1gk086k.

[8] James E. Pate. Redistricting for the Purpose of Representation. *Kentucky Law Journal*, 23(3), 1935. URL https://uknowledge.uky.edu/cgi/viewcontent.cgi?article=4617&context=klj.

[9] Richard L. Morrill. Redistricting, Region and Representation. *Political Geography Quarterly*, 6(3):241–260, 1987. URL https://doi.org/10.1016/S0260-9827(87)80003-4.

[10] Gary King. Representation Through Legislative Redistricting: A Stochastic Model. *American Journal of Political Science*, 33(4):787–824, 1989. URL https://doi.org/10.2307/2111110.

[11] Nicholas O. Stephanopoulos. The Causes and Consequences of Gerrymandering. *William and Mary Law Review*, 59(5):2115, 2018. URL https://chicagounbound.uchicago.edu/journal_articles/9803/.

[12] David Lublin and Michael P. McDonald. Is It Time to Draw the Line?: The Impact of Redistricting on Competition in State House Elections. *Election Law Journal*, 5(2):144–157, 2006. URL https://doi.org/10.1089/elj.2006.5.144.

[13] Alan I. Abramowitz, Brad Alexander, and Matthew Gunning. Incumbency, Redistricting, and the Decline of Competition in U.S. House Elections. *The Journal of Politics*, 68(1):75–88, 2006. URL https://www.journals.uchicago.edu/doi/10.1111/j.1468-2508.2006.00371.x.

[14] David Cottrell. Using Computer Simulations to Measure the Effect of Gerrymandering on Electoral Competition in the U.S. Congress. *Legislative Studies Quarterly*, 44(3):487–514, 2019. URL https://doi.org/10.1111/lsq.12234.

[15] Christopher T. Kenny, Cory McCartan, Tyler Simko, Shiro Kuriwaki, and Kosuke Imai. Widespread Partisan Gerrymandering Mostly Cancels Nationally, but Reduces Electoral Competition. *Proceedings of the National Academy of Sciences*, 120(25):e2217322120, 2023. URL https://doi.org/10.1073/pnas.2217322120.

[16] Edward R. Tufte. The Relationship between Seats and Votes in Two-Party Systems. *The American Political Science Review*, 67(2):540–554, 1973. URL https://doi.org/10.2307/1958782.

[17] Michael Lyons and Peter F. Galderisi. Incumbency, Reapportionment, and U.S. House Redistricting. *Political Research Quarterly*, 48(4):857–871, 1995. URL https://doi.org/10.2307/448978.

[18] Jamie L. Carson, Michael H. Crespin, Charles J. Finocchiaro, and David W. Rohde. Redistricting and Party Polarization in the U.S. House of Representatives. *American Politics Research*, 35(6):878–904, 2007. URL https://doi.org/10.1177/1532673X07304263.

[19] Corbett A. Grainger. Redistricting and Polarization: Who Draws the Lines in California? *The Journal of Law & Economics*, 53(3):545–567, 2010. URL https://doi.org/10.1086/605724.

[20] Nolan McCarty, Jonathan Rodden, Boris Shor, Chris Tausanovitch, and Christopher Warshaw. Geography, Uncertainty, and Polarization. *Political Science Research and Methods*, 7(4):775–794, 2019. URL https://doi.org/10.1017/psrm.2018.12.

[21] Danny Hayes and Seth C. McKee. The Participatory Effects of Redistricting. *American Journal of Political Science*, 53(4):1006–1023, 2009. URL https://www.jstor.org/stable/20647963.

[22] Danny Hayes and Seth C. McKee. The Intersection of Redistricting, Race, and Participation. *American Journal of Political Science*, 56(1):115–130, 2012. URL https://www.jstor.org/stable/23075147.

[23] Bernard L. Fraga. Redistricting and the Causal Impact of Race on Voter Turnout. *The Journal of Politics*, 78(1):19–34, 2016. URL https://doi.org/10.1086/683601.

[24] Charles R. Hunt. When Does Redistricting Matter? Changing Conditions and Their Effects on Voter Turnout. *Electoral Studies*, 54:128–138, 2018. URL https://doi.org/10.1016/j.electstud.2018.05.007.

[25] Daniel Jones, Neil Silveus, and Carly Urban. Partisan Gerrymandering and Turnout. *The Journal of Law Economics*, 66(3):557–579, 2023. URL https://doi.org/10.1086/725767.

[26] Richard Barnes and Justin Solomon. Gerrymandering and Compactness: Implementation Flexibility and Abuse. *Political Analysis*, 29(4):448–466, 2021. URL https://doi.org/10.1017/pan.2020.36.

[27] Lee Drutman. What We Know About Redistricting and Redistricting Reform, 2022. URL https://www.newamerica.org/political-reform/reports/what-we-know-about-redistricting-and-redistricting-reform/.

[28] Matthew Nelson. Independent Redistricting Commissions Are Associated with More Competitive Elections. *PS: Political Science Politics*, 56(2):207–212, 2023. URL https://doi.org/10.1017/S104909652200124X.

[29] Michael. Li. What Went Wrong with New York's Redistricting, Jun 2022. URL https://www.brennancenter.org/our-work/research-reports/what-went-wrong-new-yorks-redistricting.

[30] Richard. Briffault. Epic Fail: Harkenrider v. Hochul and New York's 2022 Misadventure in "Independent" Redistricting. *Fordham Law Voting Rights and*

Democracy Forum, 1, May 2023. URL https://scholarship.law.columbia.edu/faculty_scholarship/3942.

[31] Otis Dudley Duncan and Beverly Duncan. A Methodological Analysis of Segregation Indexes. *American Sociological Review*, 20(2):210–217, 1955. URL https://doi.org/10.2307/2088328.

[32] James A. Kushner. Apartheid in America: an Historical and Legal Analysis of Contemporary Racial Residential Segregation in the United States. *Howard Law Journal*, 22(4):547–685, 1979. URL https://repository.law.umich.edu/mlr/vol79/iss4/32.

[33] W. A. V. Clark. Residential Segregation in American Cities: A Review and Interpretation. *Population Research and Policy Review*, 5(2):95–127, 1986. URL https://doi.org/10.1007/BF00137176.

[34] George Galster. Residential Segregation in American Cities: A Contrary Review. *Population research and policy review*, 7(2):93–112, 1988. URL https://www.jstor.org/stable/40229955.

[35] Douglas S. Massey. American Apartheid: Segregation and the Making of the Underclass. *The American journal of sociology*, 96(2):329–357, 1990. URL https://www.jstor.org/stable/2781105.

[36] Douglas S. Massey. Getting Away with Murder: Segregation and Violent Crime in Urban America. *University of Pennsylvania Law Review*, 143(5):1203–1232, 1995. URL https://doi.org/10.2307/3312474.

[37] David R. Williams and Chiquita Collins. Racial Residential Segregation: A Fundamental Cause of Racial Disparities in Health. *Public Health Reports (1974)*, 116 (5):404–416, 2001. URL https://doi.org/10.1093/phr/116.5.404.

[38] John Iceland. Beyond Black and White: Metropolitan residential segregation in multi-ethnic America. *Social Science Research*, 33(2):248–271, 2004. URL https://doi.org/10.1016/S0049-089X(03)00056-5.

[39] Jacob S. Rugh and Douglas S. Massey. Segregation in Post-Civil Rights America: Stalled Integration or End of the Segregated Century? *Du Bois Review*, 11(2): 205–232, 2014. URL https://doi.org/10.1017/S1742058X13000180.

[40] Paul A. Jargowsky. Take the Money and Run: Economic Segregation in U.S. Metropolitan Areas. *American Sociological Review*, 61(6):984–998, 1996. URL https://doi.org/10.2307/2096304.

[41] Tara Watson. Inequality and the Measurement of Residential Segregation by Income in American Neighborhoods. *The Review of Income and Wealth*, 55(3): 820–844, 2009. URL https://doi.org/10.1111/j.1475-4991.2009.00346.x.

[42] Jonathan J. B. Mijs and Elizabeth L. Roe. Is America Coming Apart? Socioeconomic Segregation in Neighborhoods, Schools, Workplaces, and Social Networks, 1970–2020. *Sociology Compass*, 15(6), 2021. URL https://doi.org/10.1111/soc4.12884.

[43] Emily Badger. Political Migration: A New Business of Moving Out to Fit In, Aug 2017. URL https://www.nytimes.com/2017/08/16/upshot/political-migration-a-new-business-of-moving-out-to-fit-in.html.

[44] John. Burnett. Americans Are Fleeing to Places Where Political Views Match Their Own, Feb 2022. URL https://www.npr.org/2022/02/18/1081295373/the-big-sort-americans-move-to-areas-political-alignment.

[45] Margaret Talev and David Nather. Two Americans Index: Why People Move to Red and Blue States, Aug 2022. URL https://www.axios.com/2022/08/08/two-americas-poll-red-blue-states.

[46] Dora Mekouar. Are Americans Purposely Moving Next to People Who Share Their Politics?, May 2022. URL https://www.voanews.com/a/are-americans-purposely-moving-next-to-people-who-share-their-politics-/6577320.html.

[47] Chris Schlak. Do We Live in 2 Americas? Voters Reward GOP for Economics, but Culture Wars Pull Us Apart., Oct 2022. URL https://www.usatoday.com/story/opinion/2022/10/14/america-political-divide-geographical-future-conservatism/8027048001/.

[48] Nicholas Riccardi. Conservatives Go to Red States and Liberals Go to Blue as the Country Grows More Polarized, Jul 2023. URL https://apnews.com/article/polarization-republicans-democrats-abortion-gender-colorado-idaho-406b5a841d4d47

[49] Marin Cogan. The Dream — and Reality — of Moving to Florida, Sep 2023. URL https://www.vox.com/cities-and-urbanism/23853800/florida-population-growth-newcomers-migration.

[50] Trip Gabriel. Two Families Got Fed Up With Their States' Politics. So They Moved Out., Oct 2023. URL https://www.nytimes.com/2023/10/07/us/politics/politics-states-moving.html.

[51] Suzanne Blake. Political Tensions Lead Some Americans to Move to Other States, Feb 2024. URL https://www.newsweek.com/americans-moving-relocating-political-reasons-1867856.

[52] Bill Bishop and Robert G. Cushing. *The Big Sort: Why the Clustering of Like-Minded America is Tearing Us Apart*. Tantor Audio, 2017. URL https://dl.acm.org/doi/10.5555/3164899.

[53] Samuel J. Abrams and Morris P. Fiorina. "The Big Sort" That Wasn't: A Skeptical Reexamination. *PS: Political Science Politics*, 45(2):203–210, 2012. URL https://doi.org/10.1017/S1049096512000017.

[54] Jesse Sussell. New Support for the Big Sort Hypothesis: An Assessment of Partisan Geographic Sorting in California, 1992–2010. *PS: Political Science Politics*, 46 (4):768–773, 2013. URL https://doi.org/10.1017/S1049096513001042.

[55] Ron Johnston, David Manley, and Kelvyn Jones. Spatial Polarization of Presidential Voting in the United States, 1992-2012: The "Big Sort" Revisited. *Annals of the American Association of Geographers*, 106(5):1047–1062, 2016. URL https://www.jstor.org/stable/45387658.

[56] Corey Lang and Shanna Pearson-Merkowitz. Partisan Sorting in the United States, 1972–2012: New Evidence from a Dynamic Analysis. *Political Geography*, 48:119–129, 2015. URL https://doi.org/10.1016/j.polgeo.2014.09.015.

[57] Jacob R. Brown and Ryan D. Enos. The Measurement of Partisan Sorting for 180 Million Voters. *Nature Human Behaviour*, 5(8):998–1008, 2021. URL https://doi.org/10.1038/s41562-021-01066-z.

[58] Joseph A. Aistrup, Binita Mahato, and John C. Morris. The 1990s Party Realignment of U.S. Presidential Elections: Geographic Sorting of Counties by Blue or Red. *Social Science Quarterly*, 104(4):636–668, 2023. URL https://doi.org/10.1111/ssqu.13288.

[59] Philip A. Klinkner. Red and Blue Scare: The Continuing Diversity of the American Electoral Landscape. *The Forum*, 2(2), 2004. URL https://doi.org/10.2202/1540-8884.1035.

[60] Edward L. Glaeser and Bryce A. Ward. *Myths and Realities of American Political Geography*. NBER working paper series no. w11857. National Bureau of Economic Research, Cambridge, Mass, 2005. URL https://www.jstor.org/stable/30033653.

[61] Jonathan Mummolo and Clayton Nall. Why Partisans Do Not Sort: The Constraints on Political Segregation. *The Journal of Politics*, 79(1):45–59, 2017. URL https://doi.org/10.1086/687569.

[62] Gregory J. Martin and Steven W. Webster. Does Residential Sorting Explain Geographic Polarization? *Political Science Research and Methods*, 8(2):215–231, 2020. URL https://doi.org/10.1017/psrm.2018.44.

[63] Matt Motyl, Ravi Iyer, Shigehiro Oishi, Sophie Trawalter, and Brian A. Nosek. How Ideological Migration Geographically Segregates Groups. *Journal of Experimental Social Psychology*, 51:1–14, 2014. URL https://doi.org/10.1016/j.jesp.2013.10.010.

[64] James G. Gimpel and Iris Hui. Inadvertent and Intentional Partisan Residential Sorting. *The Annals of Regional Science*, 58(3):441–468, 2017. URL https://doi.org/10.1007/s00168-016-0802-5.

[65] Jowei Chen and Jonathan Rodden. Unintentional Gerrymandering: Political Geography and Electoral Bias in Legislatures. *Quarterly Journal of Political Science*, 8(3):239–269, 2013. URL http://dx.doi.org/10.1561/100.00012033.

[66] Dylan Matthews. How 2 Academics Got the Supreme Court to Reexamine Gerrymandering, Oct 2017. URL https://www.vox.com/policy-and-politics/2017/6/19/15831640/supreme-court-gerrymandering-wisconsin.

[67] Nate Cohn and Quoctrung Bui. How the New Math of Gerrymandering Works, Oct 2017. URL https://www.nytimes.com/interactive/2017/10/03/upshot/how-the-new-math-of-gerrymandering-works-supreme-court.html.

[68] Gowri Ramachandran and Dara Gold. Using Outlier Analysis to Detect Partisan Gerrymanders: A Survey of Current Approaches and Future Directions. *Election Law Journal: Rules, Politics, and Policy*, 17(4):286–301, 2018. URL https://doi.org/10.1089/elj.2018.0503.

[69] Mark Monmonier. *Bushmanders and Bullwinkles: How Politicians Manipulate Electronic Maps and Census Data to Win Elections*. University of Chicago Press, 2001. URL https://doi.org/10.1080/00344890308523238.

[70] William Vickrey. On the Prevention of Gerrymandering. *Political Science Quarterly*, 76(1):105–110, 1961. URL https://doi.org/10.2307/2145973.

[71] James B. Weaver and Sidney W. Hess. A Procedure for Nonpartisan Districting: Development of Computer Techniques. *The Yale Law Journal*, 73(2):288–308, 1963. URL https://doi.org/10.2307/794769.

[72] S. W. Hess, J. B. Weaver, H. J. Siegfeldt, J. N. Whelan, and P. A. Zitlau. Nonpartisan Political Redistricting by Computer. *Operations Research*, 13(6):998–1006, 1965. URL https://www.jstor.org/stable/167658.

[73] Stuart S. Nagel. Simplified Bipartisan Computer Redistricting. *Stanford Law Review*, 17(5):863–899, 1965. URL https://doi.org/10.2307/1226994.

[74] Micah Altman. The Computational Complexity of Automated Redistricing: Is Automation the Answer? *Rutgers Computer Technology Law Journal*, 23(1): 81–142, 1997. URL https://thesis.library.caltech.edu/1871/6/5chapter_5.pdf.

[75] Carmen Cirincione, Thomas A. Darling, and Timothy G. O'Rourke. Assessing South Carolina's 1990s Congressional Districting. *Political Geography*, 19(2):189–211, 2000. URL https://doi.org/10.1016/S0962-6298(99)00047-5.

[76] Nolan McCarty, Keith T. Poole, and Howard Rosenthal. Does Gerrymandering Cause Polarization? *American Journal of Political Science*, 53(3):666–680, 2009. URL https://www.jstor.org/stable/25548144.

[77] Wendy K. Tam Cho and Yan Y. Liu. Toward a Talismanic Redistricting Tool: A Computational Method for Identifying Extreme Redistricting Plans. *Election Law Journal*, 15(4):351–366, 2016. URL https://doi.org/10.1089/elj.2016.0384.

[78] Daniel B. Magleby and Daniel B. Mosesson. A New Approach for Developing Neutral Redistricting Plans. *Political Analysis*, 26(2):147–167, 2018. URL https://doi.org/10.1017/pan.2017.37.

[79] Jowei Chen and Jonathan Rodden. Cutting Through the Thicket: Redistricting Simulations and the Detection of Partisan Gerrymanders. *Election Law Journal*, 14(4):331–345, 2015. URL https://doi.org/10.1089/elj.2015.0317.

[80] Jowei Chen and David Cottrell. Evaluating Partisan Gains from Congressional Gerrymandering: Using Computer Simulations to Estimate the Effect of Gerrymandering in the U.S. House. *Electoral Studies*, 44:329–340, 2016. URL https://doi.org/10.1016/j.electstud.2016.06.014.

[81] Jowei Chen. The Impact of Political Geography on Wisconsin Redistricting: An Analysis of Wisconsin's Act 43 Assembly Districting Plan. *Election Law Journal*, 16(4):443–452, 2017. URL https://doi.org/10.1089/elj.2017.0455.

[82] Gregory Herschlag, Robert Ravier, and Jonathan C Mattingly. Evaluating Partisan Gerrymandering in Wisconsin. 2017. URL https://doi.org/10.48550/arXiv.1709.01596.

[83] Daryl DeFord, Moon Duchin, and Justin Solomon. A Computational Approach to Measuring Vote Elasticity and Competitiveness. *Statistics and Public Policy*, 7 (1):69–86, 2020. URL https://doi.org/10.1080/2330443X.2020.1777915f.

[84] Gregory Herschlag, Han Sung Kang, Justin Luo, Christy Vaughn Graves, Sachet Bangia, Robert Ravier, and Jonathan C. Mattingly. Quantifying Gerrymandering in North Carolina. *Statistics and Public Policy*, 7(1):30–38, 2020. URL https://doi.org/10.48550/arXiv.1801.03783.

[85] Annika King, Jacob Murri, Jake Callahan, Adrienne Russell, and Tyler J. Jarvis. Mathematical Analysis of Redistricting in Utah. *Statistics and Public Policy*, 9 (1):136–148, 2022. URL https://doi.org/10.48550/arXiv.2107.05515.

[86] Jeanne Clelland, Haley Colgate, Daryl DeFord, Beth Malmskog, and Flavia Sancier-Barbosa. Colorado in Context: Congressional Redistricting and Competing Fairness Criteria in Colorado. *Journal of Computational Social Science*, 5 (1):189–226, 2022. URL https://doi.org/10.48550/arXiv.2011.06049.

[87] Thomas P. Towzey. Unintentional Gerrymandering: Why Location Matters in Politics. *USF St. Petersburg campus Honors Program Theses (Undergraduate).*, 2014. URL https://digitalcommons.usf.edu/honorstheses/159/.

[88] Hannah Sharp. The Unintentional Gerrymandering of America: How Population Shifts in Congressional Districts Contribute to the Wasting of Votes, as Measured by the Efficiency Gap. *Boise State University Theses and Dissertations*, 2020. URL https://scholarworks.boisestate.edu/td/1641/.

[89] Richard J. Powell, Jesse T. Clark, and Matthew P. Dube. Partisan Gerrymandering, Clustering, or Both? A New Approach to a Persistent Question. *Election Law Journal*, 19(1):79–100, 2020. URL https://doi.org/10.1089/elj.2019.0605.

[90] Daryl R. DeFord and Moon Duchin. Redistricting Reform in Virginia: Districting Criteria in Context. *Virginia Policy Review*, 12(2):120–146, 2019. URL https://mggg.org/VA-criteria.pdf.

[91] Ruth C. Silva. Reapportionment and Redistricting. *Scientific American*, 213(5): 20–27, 1965. URL https://www.jstor.org/stable/24931179.

[92] Michael S. Kang. Hyperpartisan Gerrymandering. *Boston College Law Review*, 61 (4):1379–1445, 2020. URL https://ssrn.com/abstract=3396178.

[93] Bernard Grofman, Lisa Handley, and Richard G. Niemi. *Minority Representation and the Quest for Voting Equality*. Cambridge University Press, 1992. URL https://doi.org/10.1017/CBO9780511664090.

[94] Alex Keena, Michael Latner, Anthony J. McGann, and Charles Anthony Smith. Common Forms of Gerrymandering in the United States. *Decyzje*, (32):41–61, 2019. URL https://journals.kozminski.edu.pl/system/files/Keena%20et%20al.pdf.

[95] Olga Pierce and Lois Beckett. Redistricting, a Devil's Dictionary, Nov 2011. URL https://www.propublica.org/article/redistricting-a-devils-dictionary.

[96] Ben Philpott. Hispanics at Heart of Redistricting Debate, Apr 2011. URL https://www.texastribune.org/2011/04/08/hispanics-at-heart-of-texas-redistricting-debate/.

[97] Lee Nichols. The Shape of Things to Come, Apr 2011. URL https://www.austinchronicle.com/news/2011-04-15/the-shape-of-things-to-come/.

[98] John Archibald. Segregated Now, Segregated Tomorrow, Segregated Forever?, Feb 2011. URL https://www.al.com/archiblog/2012/02/segregated_now_segregated_tomo.html.

[99] J. David Gopoian and Darrell M. West. Trading Security for Seats: Strategic Considerations in the Redistricting Process. *The Journal of Politics*, 46(4):1080–1096, 1984. URL https://doi.org/10.2307/2131243.

[100] Amihai Glazer, Bernard Grofman, and Marc Robbins. Partisan and Incumbency Effects of 1970s Congressional Redistricting. *American Journal of Political Science*, 31(3):680–707, 1987. URL https://doi.org/10.2307/2111288.

[101] Andrew Gelman and Gary King. Enhancing Democracy Through Legislative Redistricting. *The American Political Science Review*, 88(3):541–559, 1994. URL https://doi.org/10.2307/2944794.

[102] Richard Forgette, Andrew Garner, and John Winkle. Do Redistricting Principles and Practices Affect U.S. State Legislative Electoral Competition? *State Politics Policy Quarterly*, 9(2):151–175, 2009. URL https://www.jstor.org/stable/40421634.

[103] Seth E. Masket, Jonathan Winburn, and Gerald C. Wright. The Gerrymanderers Are Coming! Legislative Redistricting Won't Affect Competition or Polarization Much, No Matter Who Does It. *PS: Political Science Politics*, 45(1):39–43, 2012. URL https://www.jstor.org/stable/41412719.

[104] Benjamin Fifield, Kosuke Imai, Jun Kawahara, and Christopher T. Kenny. The Essential Role of Empirical Validation in Legislative Redistricting Simulation.

Statistics and Public Policy, 7(1):52–68, 2020. URL https://doi.org/10.1080/2330443X.2020.1791773.

[105] Cory McCartan and Kosuke Imai. Sequential Monte Carlo for Sampling Balanced and Compact Redistricting Plans. 2020. URL https://doi.org/10.48550/arXiv.2008.06131.

[106] Daniel D. Polsby and Robert D. Popper. The Third Criterion: Compactness as a Procedural Safeguard Against Partisan Gerrymandering. *Yale Law & Policy Review*, 9:301, 1991. URL https://www.jstor.org/stable/40239359.

[107] Micah Altman. Modeling the Effect of Mandatory District Compactness on Partisan Gerrymanders. *Political Geography*, 17(8):989–1012, 1998. URL https://doi.org/10.1016/S0962-6298(98)00015-8.

[108] Bernard. Grofman. *Race and Redistricting in the 1990s*. Agathon Series on Representation. Agathon Press, New York, 1998.

[109] Joseph E. Schwartzberg. Reapportionment, Gerrymanders, and the Notion of "Compactness". *Minnesota Law Review*, 50:443–452, 1965. URL https://scholarship.law.umn.edu/mlr/1701.

[110] Ernest C. Reock. A Note: Measuring Compactness as a Requirement of Legislative Apportionment. *Midwest Journal of Political Science*, 5(1):70–74, 1961. URL https://doi.org/10.2307/2109043.

[111] Richard G. Niemi, Bernard Grofman, Carl Carlucci, and Thomas Hofeller. Measuring Compactness and the Role of a Compactness Standard in a Test for Partisan and Racial Gerrymandering. *The Journal of Politics*, 52(4):1155–1181, 1990. URL https://doi.org/10.2307/2131686.

[112] Aaron R. Kaufman, Gary King, and Mayya Komisarchik. How to Measure Legislative District Compactness If You Only Know It When You See It. *American Journal of Political Science*, 65(3):533–550, 2021. URL https://www.jstor.org/stable/45415627.

[113] H. P. Young. Measuring the Compactness of Legislative Districts. *Legislative Studies Quarterly*, 13(1):105–115, 1988. URL https://doi.org/10.2307/439947.

[114] Maria Chikina, Alan Frieze, and Wesley Pegden. Assessing Significance in a Markov Chain Without Mixing. *Proceedings of the National Academy of Sciences*, 114(11):2860–2864, 2017. URL https://doi.org/10.48550/arXiv.1608.02014.

[115] Bernard Grofman and Gary King. The Future of Partisan Symmetry as a Judicial Test for Partisan Gerrymandering after LULAC v. Perry. *Election Law Journal*, 6(1):2–35, 2007. URL https://doi.org/10.1089/elj.2006.6002.

[116] Nicholas O. Stephanopoulos and Eric M. McGhee. The Measure of a Metric: The Debate Over Quantifying Partisan Gerrymandering. *Stanford Law Review*, 70(5): 1503–1568, 2018. URL https://ssrn.com/abstract=3077766.

[117] Robert X. Browning and Gary King. Seats, Votes, and Gerrymandering: Estimating Representation and Bias in State Legislative Redistricting. *Law Policy*, 9(3): 305–322, 1987. URL https://doi.org/10.1111/j.1467-9930.1987.tb00413.x.

[118] Benjamin Plener Cover. Quantifying Partisan Gerrymandering: An Evaluation of the Efficiency Gap Proposal. *Stanford Law Review*, 70(4):1131–1233, 2018. URL https://law.yale.edu/sites/default/files/area/center/liman/document/ssrn-id3019540.pdf.

[119] John F. Nagle. How Competitive Should a Fair Single Member Districting Plan Be? *Election Law Journal*, 16(1):196–209, 2017. URL https://lipid.phys.cmu.edu/nagle/Publications/2017NagleELJCompetitiveness.pdf.

[120] Jonathan Krasno, Daniel B. Magleby, Michael D. McDonald, Shawn Donahue, and Robin E. Best. Can Gerrymanders Be Detected? An Examination of Wisconsin's State Assembly. *American Politics Research*, 47(5):1162–1201, 2019. URL https://doi.org/10.1177/1532673X18767890.

[121] Michael D. McDonald and Robin E. Best. Unfair Partisan Gerrymanders in Politics and Law: A Diagnostic Applied to Six Cases. *Election Law Journal*, 14(4):312–330, 2015. URL https://doi.org/10.1089/elj.2015.0358.

[122] Mira Bernstein and Moon Duchin. A Formula Goes to Court: Partisan Gerrymandering and the Efficiency Gap. *Notices of the American Mathematical Society*, 64 (9):1020–1024, 2017. URL https://doi.org/10.48550/arXiv.1705.10812.

[123] Gregory S. Warrington. Quantifying Gerrymandering Using the Vote Distribution. *Election Law Journal*, 17(1):39–57, 2018. URL https://doi.org/10.48550/arXiv.1705.09393.

[124] Gregory S Warrington. Introduction to the Declination Function for Gerrymanders. 2018. URL https://doi.org/10.48550/arXiv.1803.04799.

[125] Kristopher Tapp. Measuring Political Gerrymandering. *The American Mathematical Monthly*, 126(7):593–609, 2019. URL https://www.jstor.org/stable/48662153.

[126] Daryl R. DeFord, Nicholas Eubank, and Jonathan Rodden. Partisan Dislocation: A Precinct-Level Measure of Representation and Gerrymandering. *Political Analysis*, 30(3):403–425, 2022. URL https://doi.org/10.1017/pan.2021.13.

[127] Micah Altman, Karin MacDonald, and Michael McDonald. From Crayons to Computers: The Evolution of Computer Use in Redistricting. *Social Science Computer Review*, 23(3):334–346, 2005. URL https://doi.org/10.1177/0894439305275855.

[128] Curtis C. Harris Jr. A Scientific Method of Districting. *Behavioral Science*, 9(3): 219–225, 1964. URL https://doi.org/10.1002/bs.3830090303.

[129] Daryl DeFord, Moon Duchin, and Justin Solomon. Recombination: A Family of Markov Chains for Redistricting. *Harvard Data Science Review*, 2021. URL https://doi.org/10.48550/arXiv.1911.05725.

[130] Myung Jin Kim. Optimization Approaches to Political Redistricting Problems. *PhD thesis, The Ohio State University*, 2011. URL https://etd.ohiolink.edu/acprod/odb_etd/etd/r/1501/10?clear=10&p10_accession_num=osu1306896676.

[131] Hai Jin. Spatial Optimization Methods and System for Redistricting Problems. *University of South Carolina (Doctoral dissertation)*, 2017. URL https://scholarcommons.sc.edu/etd/4544.

[132] Roland G. Fryer and Richard Holden. *Measuring the Compactness of Political Districting Plans*, volume 54. [The University of Chicago Press, The Booth School of Business, University of Chicago, The University of Chicago Law School], 2011. URL https://doi.org/10.1086/661511.

[133] Vincent Cohen-Addad, Philip N. Klein, and Neal E. Young. Balanced Power Diagrams for Redistricting. 2017. URL https://doi.org/10.48550/arXiv.1710.03358.

[134] Vincent Cohen-Addad, Philip N. Klein, and Neal E. Young. Balanced Centroidal Power Diagrams for Redistricting. 2018. URL https://doi.org/10.1145/3274895.3274979.

[135] Harry Levin and Sorelle Friedler. Automated Congressional Redistricting. *The ACM Journal of Experimental Algorithmics*, 24(1):1–24, 2019. URL https://doi.org/10.1145/3316513.

[136] Olivia Guest, Frank J. Kanayet, and Bradley C. Love. Gerrymandering and Computational Redistricting. *Journal of Computational Social Science*, 2(2):119–131, 2019. URL https://doi.org/10.1007/s42001-019-00053-9.

[137] Matt Jacobs and Olivia Walch. A Partial Differential Equations Approach to Defeating Partisan Gerrymandering. 2018. URL https://doi.org/10.48550/arXiv.1806.07725.

[138] Hamidreza Validi, Austin Buchanan, and Eugene Lykhovyd. Imposing Contiguity Constraints in Political Districting Models. *Operations Research*, 70(2):867–892, 2022. URL https://doi.org/10.1287/opre.2021.2141.

[139] Jowei Chen and Jonathan Rodden. The Loser's Bonus: Political Geography and Minority Party Representation. 2016. URL https://cpd.berkeley.edu/wp-content/uploads/2016/04/ucb.pdf.

[140] Jonathan C. Mattingly and Christy Vaughn. Redistricting and the Will of the People. 2014. URL https://doi.org/10.48550/arXiv.1410.8796.

[141] Maria Chikina, Alan Frieze, Jonathan C. Mattingly, and Wesley Pegden. Practical Tests for Significance in Markov Chains. 2019. URL https://hdl.handle.net/10161/19299.

[142] Benjamin Fifield, Michael Higgins, Kosuke Imai, and Alexander Tarr. Automated Redistricting Simulation Using Markov Chain Monte Carlo. *Journal of Computational and Graphical Statistics*, 29(4):715–728, 2020. URL https://doi.org/10.1080/10618600.2020.1739532.

[143] Yan Y. Liu, Wendy K. Tam Cho, and Shaowen Wang. PEAR: a Massively Parallel Evolutionary Computation Approach for Political Redistricting Optimization and Analysis. *Swarm and Evolutionary Computation*, 30:78–92, 2016. URL https://doi.org/10.1016/j.swevo.2016.04.004.

[144] Micah Altman and Michael P. McDonald. BARD: Better Automated Redistricting. *Journal of Statistical Software*, 42(4):1–28, 2011. URL https://doi.org/10.18637/jss.v042.i04.

[145] Metric Geometry and Gerrymandering Group. *GerryChain*, 2018. URL https://github.com/mggg/gerrychain. Python Library.

[146] Christopher T. Kenny, Cory McCartan, Ben Fifield, and Kosuke Imai. *redist: Simulation Methods for Legislative Redistricting*, 2022. URL https://alarm-redist.org/redist/. R package.

[147] Cory McCartan, Christopher T. Kenny, Tyler Simko, George Garcia, Kevin Wang, Melissa Wu, Shiro Kuriwaki, and Kosuke Imai. Simulated Redistricting Plans for the Analysis and Evaluation of Redistricting in the United States. *Scientific Data*, 9(1):689–689, 2022. URL https://doi.org/10.1038/s41597-022-01808-2.

[148] Matthew Levendusky. *The Partisan Sort: How Liberals Became Democrats and Conservatives Became Republicans*. University of Chicago Press, Chicago, 2009. URL https://doi.org/10.7208/chicago/9780226473673.001.0001.

[149] Ian McDonald. Migration and Sorting in the American Electorate: Evidence From the 2006 Cooperative Congressional Election Study. *American Politics Research*, 39(3):512–533, 2011. URL https://doi.org/10.1177/1532673X10396303.

[150] Bill Bishop and Robert Cushing. Response to Philip A. Klinkner's "Red and Blue Scare: The Continuing Diversity of the American Electoral Landscape.". *The Forum*, 2(2), 2004. URL https://doi.org/10.2202/1540-8884.1038.

[151] P. A. P. Moran. The Interpretation of Statistical Maps. *Journal of the Royal Statistical Society. Series B (Methodological)*, 10(2):243–251, 1948. URL https://www.jstor.org/stable/2983777.

[152] Luc Anselin. Local Indicators of Spatial Association—LISA. *Geographical Analysis*, 27(2):93–115, 1995. URL https://doi.org/10.1111/j.1538-4632.1995.tb00338.x.

[153] Volker Grimm, Uta Berger, Finn Bastiansen, Sigrunn Eliassen, Vincent Ginot, Jarl Giske, John Goss-Custard, Tamara Grand, Simone K. Heinz, Geir Huse, Andreas Huth, Jane U. Jepsen, Christian Jørgensen, Wolf M. Mooij, Birgit Müller, Guy Pe'er, Cyril Piou, Steven F. Railsback, Andrew M. Robbins, Martha M. Robbins, Eva Rossmanith, Nadja Rüger, Espen Strand, Sami Souissi, Richard A. Stillman, Rune Vabø, Ute Visser, and Donald L. DeAngelis. A Standard Protocol for Describing Individual-Based and Agent-Based Models. *Ecological Modelling*, 198(1):115–126, 2006. URL https://doi.org/10.1016/j.ecolmodel.2006.04.023.

[154] Volker Grimm, Uta Berger, Donald L. DeAngelis, J. Gary Polhill, Jarl Giske, and Steven F. Railsback. The ODD Protocol: A Review and First Update. *Ecological Modelling*, 221(23):2760–2768, 2010. URL https://doi.org/10.1016/j.ecolmodel.2010.08.019.

[155] Birgit Müller, Friedrich Bohn, Gunnar Dreßler, Jürgen Groeneveld, Christian Klassert, Romina Martin, Maja Schlüter, Jule Schulze, Hanna Weise, and Nina Schwarz. Describing Human Decisions in Agent-Based Models – ODD+D, an Extension of the ODD Protocol. *Environmental Modelling Software : with Environment Data News*, 48:37–48, 2013. URL https://doi.org/10.1016/j.envsoft.2013.06.003.

[156] Ballotpedia. United States House of Representatives , 2025. URL https://ballotpedia.org/United_States_House_of_Representatives.

[157] Ballotpedia. Partisan Composition of State Legislatures, 2025. URL https://ballotpedia.org/Partisan_composition_of_state_legislatures.

[158] Ballotpedia. Election Results, 2020: State Legislatures, 2020. URL https://ballotpedia.org/Election_results,_2020:_State_legislatures.

[159] Ballotpedia. Election Results, 2022: State Legislatures, 2022. URL https://ballotpedia.org/Election_results,_2022:_State_legislatures.

[160] Sarah Cannon, Ari Goldbloom-Helzner, Varun Gupta, JN Matthews, and Bhushan Suwal. Voting Rights, Markov Chains, and Optimization by Short Bursts. *Methodology and Computing in Applied Probability*, 25(1):36, 2023. URL https://doi.org/10.48550/arXiv.2011.02288.

[161] Eric Dignum, Efi Athieniti, Willem Boterman, Andreas Flache, and Michael Lees. Mechanisms for Increased School Segregation Relative to Residential Segregation: a Model-based Analysis. *Computers, Environment and Urban Systems*, 93:101772, 2022. URL https://doi.org/10.1016/j.compenvurbsys.2022.101772.

[162] Henri Bal, Dick Epema, Cees de Laat, Rob van Nieuwpoort, John Romein, Frank Seinstra, Cees Snoek, and Harry Wijshoff. A Medium-Scale Distributed System for Computer Science Research: Infrastructure for the Long Term. *Computer*, 49 (5):54–63, 2016. URL https://doi.org/10.1109/MC.2016.127.

[163] I.M Sobol. Global Sensitivity Indices for Nonlinear Mathematical Models and their Monte Carlo Estimates. *Mathematics and Computers in Simulation*, 55(1): 271–280, 2001. URL https://doi.org/10.1016/S0378-4754(00)00270-6.

[164] Ratto M. Andres T. Campolongo F. Cariboni J. Gatelli D. Saisana M. Saltelli, A. and S. Tarantola. *Global Sensitivity Analysis. The Primer.* John Wiley Sons, Ltd, 2007. URL https://doi.org/10.1002/9780470725184.ch4.

[165] Alexander Kraskov, Harald Stögbauer, and Peter Grassberger. Estimating Mutual Information. *Physical Review E*, 69(6):066138, 2004. URL https://doi.org/10.48550/arXiv.cond-mat/0305641.

[166] Gábor J. Székely, Maria L. Rizzo, and Nail K. Bakirov. Measuring and Testing Dependence by Correlation of Distances. *The Annals of Statistics*, 35(6):2769–2794, 2007. URL http://www.jstor.org/stable/25464608.

[167] Arthur Gretton, Olivier Bousquet, Alex Smola, and Bernhard Schölkopf. Measuring Statistical Dependence with Hilbert-Schmidt Norms. In Sanjay Jain, Hans Ulrich Simon, and Etsuji Tomita, editors, *Algorithmic Learning Theory*, pages 63–77, Berlin, Heidelberg, 2005. Springer Berlin, Heidelberg. URL https://doi.org/10.1007/978-3-642-24412-4.

[168] John F. Nagle. What Criteria Should Be Used for Redistricting Reform? *Election Law Journal*, 18(1):63–77, 2019. URL https://doi.org/10.1089/elj.2018.0514.

[169] Joseph Cerrone. Research brief: Why are most congressional elections uncompetitive?, 2019. URL https://www.uniteamerica.org/articles/research-brief-why-are-most-congressional-elections-uncompetitive-2.